UC Berkeley
UC Berkeley Electronic Theses and Dissertations

Title
Synthesis and Characterization of Metallocorrole Complexes

Permalink
https://escholarship.org/uc/item/7jj519jb

Author
Buckley, Heather Louisa

Publication Date
2014

Peer reviewed|Thesis/dissertation

eScholarship.org Powered by the California Digital Library
University of California

Synthesis and Characterization of Metallocorrole Complexes

By

Heather Louisa Buckley

A dissertation submitted in partial satisfaction of the

requirements for the degree of

Doctor of Philosophy

in

Chemistry

in the

Graduate Division

of the

University of California, Berkeley

Committee in charge:

Professor John Arnold, Chair
Professor Kenneth Raymond
Professor Ronald Gronsky

Fall 2014

Synthesis and Characterization of Metallocorrole Complexes

Copyright © 2014

By

Heather Louisa Buckley

Abstract

Synthesis and Characterization of Metallocorrole Complexes

By

Heather Louisa Buckley

Doctor of Philosophy in Chemistry
University of California Berkeley
Professor John Arnold, Chair

Chapter 1: Recent Developments in Out-of-Plane Metallocorrole Chemistry Across the Periodic Table

A brief review of recent developments in metallocorrole chemistry, with a focus on species with significant displacement of the metal from the N_4 plane of the corrole ring. Comparisons based on X-ray crystallographic data are made between a range of heavier transition metal, lanthanide, actinide, and main group metallocorrole species.

Chapter 2: Synthesis of Lithium Corrole and its Use as a Reagent for the Preparation of Cyclopentadienyl Zirconium and Titanium Corrole Complexes

The unprecedented lithium corrole complex (Mes_2(*p*-OMePh)corrole)Li_3·6THF (**2-1·6THF**), prepared via deprotonation of the free-base corrole with lithium amide, acts as precursor for the preparation of cyclopentadienyl zirconium(IV) corrole (**2-2**) and pentamethylcyclopentadienyl titanium(IV) corrole (**2-3**).

Chapter 3: Lanthanide Corroles: A New Class of Macrocyclic Lanthanide Complexes

The first examples of lanthanide corroles are prepared by two synthetic routes. (Mes_2(*p*-OMePh)corrole)La·4.5DME (**3-1·4.5DME**) and (Mes_2(*p*-OMePh)corrole)Tb·4DME (**3-2·4DME**) are prepared from the free base corrole and $Ln((NSiMe_3)_2)_3$, while (Mes_2(*p*-OMePh)corrole)Gd·TACNMe_3 (**3-3·TACNMe_3**) is prepared by metathesis of the recently reported Li_3corrole and $GdCl_3$

Chapter 4: Corroles that "Click": Modular Synthesis of Azido- and Propargyl-Functionalized Metallocorrole Complexes and Convergent Synthesis of a Bis-Corrole Scaffold

Bis-corroles have been prepared through a convergent synthesis using a copper-catalyzed azide-alkyne cycloaddition. Synthesis of the final homo- and heterobimetallic complexes has been achieved in 3-4 steps from commercially available materials in good overall yield. *Meso*-substituted corroles functionalized with a single azido or propargyl group were used as key starting materials. ($(C_6F_5)_2$(*p*-O(CH_2CCH)Ph)corroleH_3) (**4-1**) and

((C$_6$F$_5$)$_2$(*m*-CH$_2$N$_3$)Ph)corroleH$_3$) (**4-3**) were metallated with copper or iron, and attached by Huisgen azide-alkyne cycloaddition ("click" reaction) first to small substrates and then to each other, demonstrating a convergent synthesis of bimetallic bis-corrole molecules.

For Nanna and Grandma

who helped build a world where anything is possible

and

For my sister Hilary

for always reminding me that I am someone worth being like when I grow up

Table of Contents

Preface on Corroles: "If You Like It Put a Nineteen Membered Ring on It!"

I have had amazing support from my friends and family over the past five years at Berkeley, for which I am particularly grateful because many of you don't know a whole lot about what I do. I have given many of you brief explanations from time to time, but these don't often do justice to the question of what could possibly take so many years. The next few pages are an attempt to give a sense of the context of my thesis, without requiring that everyone who reads them go through a PhD in chemistry.

There is a molecular structure found in both plants and animals that, for how little of it there is, makes a surprisingly large contribution to the colours we associate with life, and to the chemistry that keeps life going. We find this structure in blood in the form of hemoglobin, and in plants in the form of chlorophyll. In blood, hemoglobin provides the red colour, and it serves the essential purpose of carrying oxygen from our lungs to all of the cells in our body. Chlorophyll is what makes plants green, and it captures light that is used to make food and building materials for plants.

The structure that makes all of this possible is called porphyrin. Porphyrin is a ring-shaped molecule made out of twenty carbon atoms (grey in the adjacent picture) and four nitrogen atoms (blue in the adjacent picture), arranged so that they all sit in the same plane – you can rest a model of it flat on a table. This is somewhat unusual for chemical models, which tend to extend in three dimensions.

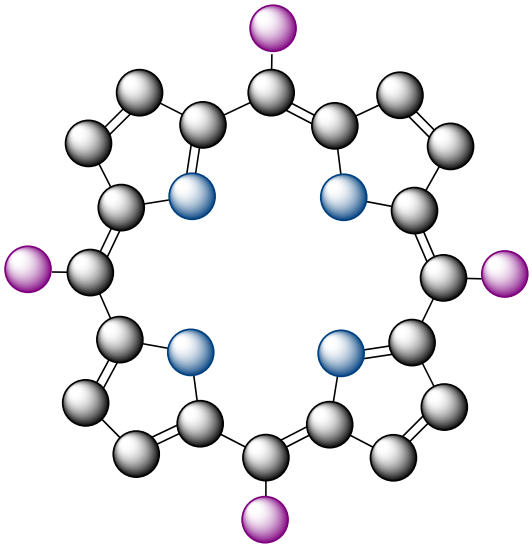

The bright colours of porphyrin molecules are a direct result of the fact that they lie in a plane because electrons in the molecule are able to run all over the flat surface of the molecule. Imagine dropping a marble into a shallow dish filled with water – the electrons bounce around the porphyrin the way that waves will bounce around in the dish. When the molecule is hit with light, the ripples change just as they would if you shook the table on which your dish was standing. What is happening is that the electrons absorb some of the energy from incoming light (scientists refer to this as the electrons becoming "excited" – really!), and in their case the electrons are absorbing particular colours of visible light, which results in them looking colourful. Because of these colours, chemists have prepared many different porphyrins and have used them as dyes and for imaging in medical applications such as Magnetic Resonance Imaging (MRI).

In addition to having bright colours, porphyrins have the ability to hold nearly any atom in the periodic table in the middle of their ring. They do so using extra electrons on those four nitrogen atoms to form bonds; a chemical bond is formed any time that electrons are shared between two atoms. It is particularly common in this sort of molecule for the nitrogen atoms to form bonds

with metals because the nitrogen atoms have too many electrons and the metals do not have enough.

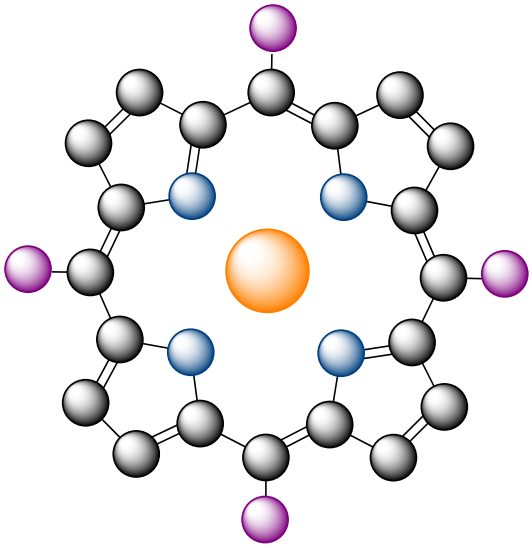

Once a metal is attached into the middle of a porphyrin, it can be involved in many interesting chemical reactions. One of the reasons that this works so well is because of the whole molecule sitting in a plane as I mentioned before. In hemoglobin, there is an iron atom in the middle of the ring, and it is to this iron atom that oxygen from the air gets attached. Most other molecules that include iron would not be able to do this, but because there is a big open space on the top (and bottom) of the molecule, there is a side of the iron atom where oxygen can be attached.

There are many other examples of metals and porphyrins attached to each other, and these have been well studied. Some of these have been used as catalysts in major industrial processes like making plastics, and others have been shown to be potentially useful for replacing platinum in fuel cells – I will come back to this idea later. Many of the more unusual ones were first prepared by my research advisor, Professor Arnold and by PhD students in his research group back in the early 1990s. This has been an advantage in my project because the "collective memory" of my elders is available to me.

However, by the nature of a PhD project, my goal was not to study something that had been done before, but to build on it and to find some new and exciting chemistry. I have not actually worked with the porphyrin molecules I discussed in the previous pages, but I have worked with a variant of them. "Corrole" is the name of my molecule, and it has not been studied nearly as extensively as porphyrin because it is not known in nature, and good methods to make it in a chemistry laboratory have been available for less than a decade. In fact, my six-week visit to Poland in 2012 was spent training under the woman who, for her PhD work, developed the way that we now make corrole molecules.

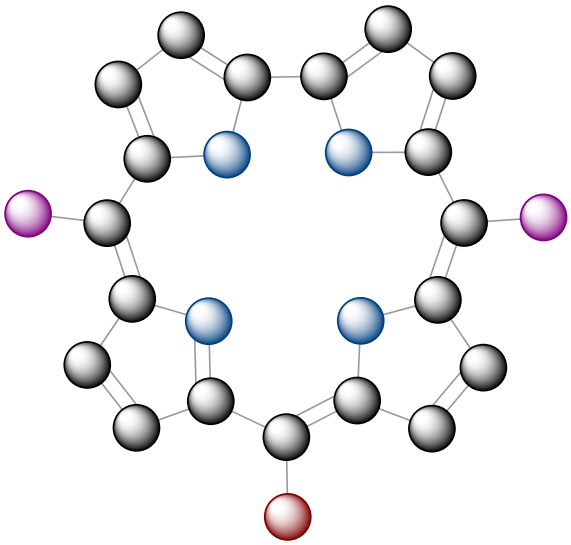

There are a few things that are different about corroles as compared to porphyrins that make them interesting to study. One is the fact that corroles are made with nineteen carbon atoms instead of twenty (hence the title of this section). This is important because it means the ring has slightly less space in the middle of it, and because it results in a ring with more extra electrons in it, which in turn holds more tightly to a metal and is attracted to a metal that is missing a lot of

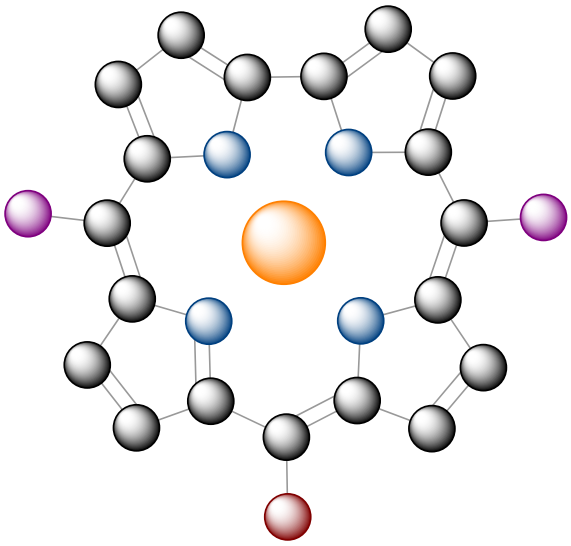

electrons. The other is the fact that the symmetry of the molecule is lower – if you look at the picture of porphyrin you can see lots of ways to divide it in half and have both sides identical, but with the corrole there is only one way to do this. This means that we can make corrole with one side different from all the other sides (represented by the red sphere), whereas in porphyrin all four sides are often the same (represented by magenta spheres).

Overall, my PhD thesis can be divided into two major parts. Each one draws some component from research that has been done before, and combines it with my own ideas to make something entirely new.

In the first idea, I have used a version of the corrole molecule that was prepared in Poland and I have attached a long list of elements to it. These metals include lithium, sodium, potassium, titanium, zirconium, hafnium, vanadium, niobium, tantalum, lanthanum, cerium, gadolinium, terbium. With collaborators I have also studied attaching sulphur, arsenic, selenium, tellurium, phosphorus, thorium, and uranium to the corrole ring.

Part of the motivation behind making these molecules is the technical challenge – some of these molecules are so sensitive to air, water, and light that very few research laboratories in the world would be able to prepare them. While we can make guesses, we often don't know how sensitive they will be until we have made them.

The other reason for making these compounds is that they may be useful. We know that porphyrins have many uses, and it is reasonable to predict that a similar but not identical molecule might do the same job, and might do it better. One particular example of this is the molecule where gadolinium is combined with corrole. Gadolinium is widely used in medical imaging (such as tumor detection) because it is fluorescent, but in order to fluoresce it first has to absorb light. While gadolinium does not do this very well, porphyrin has been shown to work as an "antenna" and to absorb light and then transmit the energy to the gadolinium. In some situations, corrole is an even better antenna than porphyrin because it absorbs a higher percentage of the light. We do not yet know if corrole will be better than porphyrin in this case, but if it is then it could be used to detect smaller tumors or using less intense radiation.

In a further extension of the possibility that my chemistry might be useful, there is a belief that is best expressed by a quote from Albert Einstein. He says: "we cannot solve our problems with the same level of thinking that created them." My interpretation of this is that we need to explore new frontiers and to gain new knowledge simply to advance human understanding of the universe. The knowledge from my PhD research may have no practical application today, but may lead to advances that help us solve problems that we have not yet identified.

The second idea I have worked with involved changing the corrole molecule itself. This was inspired by the fact that corrole molecules with iron in them, similar to porphyrin molecules with iron in them, can potentially be used as catalysts to replace platinum in fuel cells. Platinum is expensive and mining it is ethically questionable both in terms of treatment of the human workforce and environmental damage. Other research groups have studied corrole molecules with iron and cobalt in them, and they have observed that these molecules can be catalysts for the reaction that converts two molecules of hydrogen and one molecule of oxygen into two molecules of water.

A catalyst is useful for this reaction because it decreases the amount of energy needed to get the reaction to start. The reaction is similar to the one that occurs in a combustion engine, where a spark is used to convert the fuel (gasoline, or hydrogen in my case) and air (which includes oxygen) into energy, with water and carbon dioxide as byproducts. In our case we are trying to get electricity instead of heat out of the reaction. This is because in theory, we can get over 95 % efficiency by extracting electrical energy, but in a combustion engine the maximum amount of energy we can get in theory is only 23 %.

Even though other researchers have shown that corrole molecules can be good catalysts for the conversion of oxygen and hydrogen to water, this is not enough information to take all of the platinum out of fuel cells and to replace it with corrole molecules. This is because of a number of engineering challenges. I do not have the ability to solve all of those, but one of the major challenges that I can solve is that the corrole molecules need to be strongly attached to a surface to use them. This is because in order to generate electricity the corrole molecules need to be able to receive and transmit electrons, and so they need to be touching an electrode.

In preliminary tests, corrole molecules have been put on electrode surfaces by dissolving them in a solvent, putting a drop of that solvent on the electrode, and then letting the solvent evaporate. This is the same way that a Sharpie marker works – the dye molecules in ink are dissolved in toluene, and when you write with them the toluene quickly evaporates and leaves colour. The smell of Sharpie markers is toluene evaporating. However, just like Sharpie ink, which can be rubbed off of surfaces like glass even after it has dried, corrole molecules can be rubbed off electrode surfaces fairly easily. Finding a way to attach corroles so that they don't rub off is a challenge.

I have found one solution to this challenge using a reaction called "click" chemistry. Some chemists won the Nobel Prize for this reaction in 2001 because it has a lot of uses. The "click" reaction allows you to attach two molecules, or a molecule and a surface, together as easily as putting together two Lego blocks. However, it forms a strong chemical bond, and so if you try to pull them apart again it is as if those two Lego blocks had fast-drying superglue on them. In order to do the "click" reaction, your molecule has to have a certain sequence of carbon or nitrogen atoms sticking off the side of it. In the case of corrole molecules, putting those atoms there meant re-designing the molecule; by analogy, this special sequence changed the foundation of the molecular "building" and so all of the steps of construction had to be changed to account for this. The final result is best described as a "corrole that clicks".

I have done a few different things with my "corroles that click". In keeping with the original purpose, I have attached them to an electrode surface and seen that this works fairly well – because the molecules are big, they get in each others' way and so it is more like adding Lego pieces to the inside of my Lego space-shuttle model than just putting together two blocks. This part still needs work before the engineering challenge is completely solved, and I am working with some scientists who are experts with surfaces on the next step of this project.

In addition, I have attached two corroles to each other using the "click" reaction. There are no practical applications of this right now, but there are a number of uses for pairs of the porphyrin molecules I mentioned earlier, and so it is likely that corroles could be used in similar ways. While I have been working on corrole molecules for fuel cells, a group of scientists in Israel have published several papers showing that corrole molecules can be used to prevent heart disease, lower cholesterol, and detect tumors. All of these uses face a similar challenge to corrole molecules in fuel cells: getting the corrole molecules to go where you want them to go, and then getting them to stay there. I have proposed that "corroles that click" could be attached to antibodies that would carry them to the right place in the human body.

In many ways my research has gone full circle. I started with inspiration from colourful molecules in biology like hemoglobin and chlorophyll, used these ideas to make completely new corrole molecules using many elements from all over the periodic table, and ended up back at the beginning with an idea that will help biology, either through improving human health or through making alternative energy technologies like fuel cells and batteries more sustainable. The next step is not yet certain, but I am sure it will be an adventure!

Experimental Details

All of the chapters of my thesis, except for the introduction, have a section that explains how I actually did what I did. The idea of this section is to make it possible for another person with general chemistry training to be able to repeat my experiments. This is important because reproducibility, the idea that if you do the same thing again you will get the same results, is central to science. It is also important because if somebody else has an idea that builds on my science, they should be able to copy what I have done and then go from there without having to "reinvent the wheel".

In this section I will not go into all of the details of all of my molecules, but I will explain a bit about how we know we have made what we think we have made, and how we can predict what these molecules are likely to do in other reactions. This is important because we cannot see the molecules with the naked eye, but over the last two centuries scientists have developed many ways to "see" molecules, and either to get a snapshot of exactly what they look like, or to say that the molecules are similar enough before and after a chemical reaction that the only thing that changed is what we expected to change. Learning how to use all of these tools to understand chemistry has been a critical and fascinating part of my PhD.

Method 1: Ultraviolet (UV) visible absorption spectrum. All of the corrole molecules I have made are strongly coloured, and those colours are very characteristic. However many of them are similar in colour, so to simply say a molecule is "green" or "purple" isn't enough information to identify it. Instead we like to know what wavelength of light (measured in nanometers, where red light is about 650 nm, violet light is about 400 nm, and sunlight contains light of all wavelengths between about 300 and 800 nm) is most strongly absorbed by the corrole molecule. To do this, I dissolve a bunch of corrole molecules in a solvent and put that solution in a tube made of quartz that is called a cuvette. I also put some solvent without any corrole molecule in it into an identical cuvette. Then I shine each wavelength of light (300 nm, 301 nm, 302 nm…etc.) through the two cuvettes and compare what intensity of the light gets through the one with corrole molecule in it as compared to the one with no corrole molecule. I can draw a graph of these percentages versus wavelength, and the wavelength that has the lowest percentage of light allowed through is the "absorption maximum". The absorption maximum does not by itself tell us which molecule we have, but it is a very easy experiment to do and can be used as a "fingerprint" when the experiment is repeated, as an early test to make sure nothing went wrong.

Method 2: Nuclear Magnetic Resonance, or NMR spectrum. This method is very similar to a well-known medical process called MRI, or magnetic resonance imaging. Both of these methods rely on an interesting property of hydrogen atoms: there is only one proton in their nucleus and it behaves like a miniature bar magnet. In normal situations, all of the hydrogen-atom bar magnets are pointed in random directions, similar to if you were to sprinkle a bunch of iron filings onto a piece of paper. However, if you put a big magnet nearby then you see all of the iron filings form a particular pattern – each one is a small magnet and it points in a particular direction.

In NMR and MRI, a giant electromagnet is placed around a solution containing many molecules of the corrole (or around a person) and when the magnet is turned on, all the hydrogen atoms in the corrole molecules have their nuclei pointed in a certain direction. It is important to note that this does not cause the molecules to move – if it did then MRI on living humans would not be possible. After all of the nuclei have been pointed in one direction by the magnetic field, the magnetic field is turned off. Over the seconds that follow, the nuclei "relax" back to their original positions. Energy went into the nuclei to get them all to point one way, and that energy is released as they relax (return to random orientations). We can observe this relaxation, and this is the part where MRI and NMR are slightly different. In MRI, we take a picture of *where* the nuclei are relaxing, and this gives us a very detailed look at the human body because the number of hydrogen atoms is different in bone and in soft tissue and around the edge of scars and damaged tissue. Radiologists know what each of these environments looks like because millions of MRIs have been taken over the years. In NMR, I look at *how long* the nuclei take to relax, and what energy of magnetic field affects them the most. I use this information to tell me what other atoms are around the hydrogen atoms in my molecule; I can figure this out because all of the other atoms have electrons, and their electric fields interact with the magnetic fields. Similarly to MRI, chemists have a large database of millions of compounds that I can compare my compound to. Even though my corrole molecules are new, they have many parts that are the same as molecules that other chemists have published and the same as each other.

Method 3: Mass Spectrometry. If I were in charge of the world, I would make an amusement park ride based on mass spectrometry. In this method, yet another solution containing a bunch of

corrole molecules is injected into a machine where it is heated up to a very high temperature very quickly and bombarded with electrons. The result of this is that each corrole molecule ends up carrying an extra electron, so it has a negative charge. The space that all of these charged corrole molecules are in then has a voltage applied to it, so that all of the corrole molecules travel toward the positive end. The trick is that there is a hole in the positive end, and so when the charged corrole molecules get there they go flying through at top speed. Outside of that hole, there is a magnetic field that bends the path of the charged corrole molecules (again, the electric and magnetic fields are interacting). The amount of bending of that path depends on the ratio of charge to mass, with heavier molecules turning the corner less tightly because they have more momentum. As the particles round the corner they run into a detector that can identify exactly how heavy they are based on the speed they were going, the strength of the magnetic field, and where they landed on the detector. Knowing the exact mass to four or five decimal places allows us to have a very good guess of what atoms are in the molecule because every atom has a different mass and so every combination is unique. It does not tell us how those atoms are arranged, but as before it can be combined with the other methods to get a complete picture.

Method 4: Cyclic voltammetry. When studying molecules, understanding how easy it is to add or remove one electron from the molecule can provide a lot of information about the structure of a molecule and what reactions it might be able to do. I have done some of this work myself, but a lot of it has been done by my collaborators Leah and Brendon. To find out how much energy is needed to add electrons or take them out of one of my corrole molecules, we make yet another solution containing a bunch of corrole molecules, and then we put two electrodes into this solution and plug them in to an instrument that can change the voltage difference between the two electrodes. This is similar to attaching the solution to one flashlight battery, then two, then three, except that the changes in voltage are much smaller (0.001 Volts at a time, vs. 1.5 Volts at a time if you added batteries one by one). When the voltage difference between the two electrodes is small, there is no current through the solution because there is not enough energy to add or remove electrons from the corrole molecules. However, when the voltage difference reaches a certain threshold, which is different for each molecule, electrons will “hop” between the electrode and the corrole molecules in the solution and we will record an electrical current. From this information we can determine how easily the corrole molecules will react with other chemicals. How easily a reaction happens can be useful or problematic depending on the situation – too easy a reaction and the molecule falls apart, too difficult a reaction and we can’t do any fun chemistry with it. The important thing in this case is that we know what sort of reactivity to expect and so we can make decisions about what kinds of chemical reactions to try next.

Method 5: X-ray crystallography. X-ray crystallography is the most powerful tool in my toolkit for determining what I have made, but it is also the most difficult to use because in order to use it, I have to grow perfect crystals of my molecules. Doing this is similar to growing crystals of table salt by dissolving as much salt as possible in boiling water, and then allowing it to cool down until solid starts to appear. It is possible to do this with nearly any molecule that is a solid at room temperature, however to get crystals to grow so that they are not touching any other crystals, and so that they are big enough (approximately 0.1 mm in each dimension) takes skill, patience, and a bit of luck.

Once I have grown perfect crystals of my molecules, I put them in the beam of an X-ray source. The results are similar to what you would see with the crystal that hangs in the window of my bedroom window, which makes rainbows on the walls in sunlight, if you were to shine only red light on the crystal. Instead of seeing rainbows, you would see red spots all over the walls of my room. Using some interesting math (which involves taking the inverse of space – a long explanation that I won't get into here because it took months before I could think about it without my brain exploding) you could use the positions of the spots to calculate the shape of the crystal, even if it was too small for you to see it. In a similar way, I shine X-rays of a single wavelength on a crystal of one of the corrole molecules and take a picture of the spots that result on a wall behind it. By rotating the crystal and doing this hundreds of times, I can get a map that shows me the positions of all of the atoms in the molecules in the crystal. This gives me a three-dimensional rendering that looks rather like the models I would make with a molecular model kit, only it is a real image based on data rather than just a prediction. The moments in my PhD where I was able to complete (with the help of a computer) all of the mathematical operations necessary to show one of these three dimensional maps were all very exciting moments because of the amount of certainty they gave me that what I was trying to do was working.

By using UV-visible spectroscopy, nuclear magnetic resonance spectroscopy, mass spectrometry, cyclic voltammetry, and X-ray crystallography, I can get complete pictures of my molecules that allow me to confirm that I have made all of these new molecules, and to know something about how their properties compare to other existing molecules. This helps me to decide what to do next with these molecules, either starting to study other reactions they can do or considering how to start using them in new applications.

Acknowledgements

Many times in the course of my PhD, I have been convinced that I would never be in the position to write a long-winded list of thank you's to open my thesis, because I often wasn't sure there would be enough success to have a thesis to write. But here I am, five years later, with a stack of paper that says I get a degree! (Mom and Dad, I promise this is the last one, at least for a good long while…). There are so many people who have made this possible, and I am sure I will miss some here, but in a couple of pages I will try, inadequately, to sum up the appreciation I have of all of your contributions to my life.

At Berkeley, I could not have asked for a better mentor than Prof. John Arnold. John, you accepted me into your lab solely on the basis of the fact that I was really excited about a crazy idea; you gave me space to try, to fail, and then helped me pick the pieces back up and reframe them into what has been a reasonably successful PhD. Thank you to Sergio and Pete for helping me get started here, and to Ashleigh, Dan, and Thomas for going through all the painful steps together. Thank you to Ben, Alison, Bernie, Nick, Trevor, Clément, Andreas, and a handful of other postdocs and visiting students for making the Arnold lab a fun place to do chemistry, and especially to Leah for being my constant confidante and sharer of both sarcasm and giggles in the safe space that is 516 Latimer, and Brendon and Kat for making sure we are up to date on modern music and celebrity gossip. Thank you to everyone who helped me with instrumentation and data analysis along the way: Chris and Olivia in NMR, Zhongrui in MS, Antonio in X-ray, and others. To the members of OTTERS, thank you for making my PhD special and unique by having a project that took me out of my comfort zone and kept me excited to learn new things. Thank you also to the many people who keep things running behind the scenes: Rain, Lynn, Adele, Roger, Ira, Doty, Aileen, Rebecca in the international office, and Sean and Brad in the stockroom, to name just a few.

Collaborations have been central to my work in the latter parts of my PhD. Mitch, Wayne, Penny, Jerzy, Neil, and Stefanie, thank you for visiting and working with me, and in many cases hosting me in your home labs as well. A huge thank you to everyone in Poland for hosting me: Daniel, Beata, Mariusz, Mikołaj, Aga, Jasek, and the rest of the Gryko groups in lab, Ashka, Rafael, and Max as climbing partners, and most especially Janic, who shared not only half of his fumehood, but also weekend cycling adventures, stories, and philosophical debates.

Being a Fulbright fellow truly touched my life, from the financial freedom it gave me for international travel, but more importantly due to the many friends I now have all over the world. I have been honoured by the time so many people have taken to share their lives with me, and the open invitations to visit Chile, Argentina, Namibia, Bangladesh, and myriad other countries. Thank you especially to Vijay, Joel, John, Atif, Sarah, Vince, Eduardo, Robbie, Fariah, Mike, Emily, Jessica, and Gabriel for being a part of my story.

Thank you to the many teachers, faculty and instructors who have mentored me at home in Canada: to Mrs. James, who in Grade 4 insisted that I could do better work, to Mr. McManus and Mrs. Datta for inspiring me to love chemistry, to Stephan Bonfield for feeding my thirst for broader social context, to everyone I worked with at the Glenmore Sailing School for helping me to break out of my introverted shell, and to M. Marran and Mme. Bergerman for having my back

when I took a big risk and decided to pursue parts of my high school education in French. Bilingualism has broken down so many barriers and given me the courage to travel. Thank you to the Science One program faculty at the University of British Columbia for encouraging me to question everything, to Warren Piers for letting me follow my own path, to Laurel Schafer, for asking tough questions and giving me a second chance, and especially to Jen Love for tirelessly supporting me through the many twists and turns that have led to my PhD.

While the distance is small, moving to the United States from Canada was a terrifying affair. A number of people made this big scary country seem small, friendly and amazing. Thank you to Mark and Jeanette for being such phenomenal roommates for the entire five years, and to Luca, Olesya, and Hannah for filling our house with fun, laughter, and people who would share my love of cookies. Thank you to Olivia for being my very first friend in Berkeley, and sticking with me through our entire PhDs in the dual role as friend and goddess of both the NMR and porphyrin synthesis. Thank you to the climbing crew as well for welcoming me into their fold: Lea, Julian, Kristen, Lee Huang, Marc, Will, Jonah and many other who have joined us over the years. Thank you to Stephen and Jonathan for adopting me like a sister. Thank you also to the athletes, parents, and coaches of Berkeley High Coup Ultimate: Jordan, Kyle, James, Jake, Lindy, Chloe, Rio, Jamie, Bettina and Hans, Liane and Paul, Larry and Marice, Wiz and Donald, Tom and Martha, Yattiel and Micah, the girls of California Roll, and so many more parents and athletes who make our team the most spirited family in California.

To my many friends at the Cal Sailing Club, I wouldn't have survived these five years without your friendship, support, patient teaching, delicious (if occasionally questionable) food, and perpetual silliness. Peter, Peter, and Peter, Stella, Rob, Mark, Sophie, Sofien, Brad, Bryce, Damus, Diane, Cindoll, Trilbus, Mankey, Roberto, Ilya, Sepideh, Onur, Ming, Lon, Paco, Joolz, Brandon, Dewey, a gaggle of great dayleaders, and many others: I am both a better windsurfer and a better person because of your support. Moving beyond Berkeley as I keep growing as a windsurfer, I owe so much of my happiness to the travelling circus that is Team Puppies: Carl, Chris, Russell, and Michael.

Knowing that I have the unconditional love and support of so many friends at home in both Vancouver and Calgary has given me the confidence to keep plugging, even when all I wanted to do was hop on a plane and fly back to Canada. I have slept on so many of your couches, shared so many cups of tea, meals and cycling adventures on my trips home. Pam and Jason, both on our epic bike trip and beyond, you have been both amazing friends and role models for me on how to be a grownup in all the right ways. Doug, Sam, Zev, and Aidan you have been partners in fun adventures and infinite nerdiness; I value having friends who are more excited about the process of figuring out how something works than the end result. Colin, the fact that we still finish each other's sentences sometimes after 5 years in different cities is a little bit creepy. Yuen Ying, you paved the way for how to finish a PhD and follow a new path. Kim, your perseverance inspires me. Shirley and Stan, having an extra set of parents in Vancouver has kept me grounded – thank you for making sure my parents don't need to worry about me. Nicola, the fact that every time I come home, you always find time for tea and bike rides reminds me that I am special – I feel so very lucky that we found each other at UBC more than a decade ago.

Ted and Doreen, I am truly blessed to have grown up with such loving neighbours who always have space in their hearts and homes for an extra grandchild or two. Aunt Val, you are the best ally a girl could ever ask for both personally and professionally; I value both your love and your mentorship. Greg and Shirl, I appreciate the balance that you bring to my intellectual world; I am lucky to have smart, funny, good people like both of you looking out for me. Also you have read more of my papers than most of my friends who have PhDs, for which I am grateful. Deborah, who would have thought a locker partner could be so well chosen? You, Mike, and Hugo are a bubble of happiness where I always feel at home, and a model of balancing life with an interesting career. Debbie and Mike, I am so lucky to have grown up as a part of your family; the nicest thing anyone has ever said about me was the first time you introduced me to a friend as your other daughter. Lindsay, thank you for being both a big sister and a best friend – you did everything first and so I always knew it was possible. It has been amazing growing together from little girls watching *Heidi* to university roommates and beyond; now I am following you again out of school and into the real world.

Papa, thank you for being a model of hard work, honesty, dedication, and how to be just the best of what a person can be. I am so grateful for how you have supported me down this long path of school, even though it is so very different from your own path. Thank you for teasing me just enough to help me grow a thick skin, but never so much that I doubted myself. The love that you and Nanna shared with us growing up gave me a space to grow, learn and build; I am happy that you and Joyce have built a second life together and appreciate that I get to be a part of it, and that you have continued to adapt in a world where you can talk to your kids thousands of miles away.

Michael, thank you for being my partner in crime, in cookies, in windsurfing, in bike rides, and in other adventures for the past four years. Thank you for being the balance to my stress, for making me smile, and for knowing when I need hugs, and when I need burritos. More than once you have been a reason to stick out the PhD process for another day.

Hilary, thank you for being the most inspiring of little sisters. I know I wasn't the easiest big sister to grow up with, but I am so proud of the separate path you have struck out on, of your intelligence and wit, of your ability to succeed in the face of adversity, and your bravery in identifying when it is time to choose a new path. Your growth into a real person who is different from everyone else we both know has given me the confidence to grow in my own directions as well.

And finally, Mom and Dad. Thank you for being my biggest cheerleaders, my harshest constructive critics and my unconditional support network. From the very beginning, you have encouraged me to be curious, to read and explore and invent and imagine and play, and to ask millions of questions. You have driven me to field hockey practice, to band rehearsal in the dead of winter, to Vancouver to go to university, and to the airport for 6 am flights. You have taught me sewing and sailing and long division and atomic theory and how to drive and maintain a car (maybe so you didn't have to drive me so many places?); from those foundational skills I have had the confidence to learn so much more and assimilate it into the framework of knowledge and curiosity you instilled in me. More importantly, you have taught me the value of time shared with building family and community projects like sports and science fairs; how to identify my gifts and how to share them with those around me. In all of my spectacular failures, you have

never once said “I told you so”, but have always asked “so what can we do to help you with what comes next?” Between you, you have edited nearly everything I have ever written (including this thesis), regardless of whether it was written in plain English, in Chemistry, or in French. You have celebrated my successes, found the bright side of struggles, and always sounded happy to hear my voice, even on a crackly line from India at 3 am. You have believed in me, in my capacity to change and adapt and work hard and be smart enough, and that confidence has helped me to see the brighter side of myself during the hardest parts of my PhD. I can truly say that I wouldn’t be who I am today without the steadfast positive influence you have both been on my life.

Berkeley, California, United States of America
July 2014

Chapter 1: Recent Developments in Out-of-Plane Metallocorrole Chemistry Across the Periodic Table

Introduction

The field of corrole chemistry is rapidly growing, with new corrole ligands, new metallocorrole complexes, and new synthetic methodologies surrounding corroles appearing in the chemical literature on a frequent basis. For a molecule that has been synthetically readily accessible for only fifteen years, the breadth of chemistry now demonstrated is remarkable. This is well demonstrated by the changes in corrole chemistry discussed in *The Porphyrin Handbook* in 2000[1,2] as compared to the much more extensive chemistry discussed in the 2010 edition of the *Handbook of Porphyrin Science*.[3,4]

The original preparation[5–9] and structural characterization[10] of corrole in the 1960s and 1970s was inspired at least in part by the structural similarity of corrole to the naturally occurring corrin ring in vitamin B12. Subsequent study was hampered by synthetic inaccessibility of corroles until 1999, when two new routes to the preparation of free base corrole were published by Paolesse[11] and Gross.[12,13] Over the next decade, a wealth of synthetic methodologies and variants were developed for synthesis of corroles,[14] with meso-substituents,[15–21] various beta-substituents,[22–26] and eventually including both charged[27,28] and chiral[29] free-base corroles. The development of these organic syntheses is beyond the scope of this review, but the range of properties imparted by these synthetic options has greatly broadened the scope of applications of corroles.

Given that it was a biological metallomacrocycle that first inspired the preparation of corrole, it is unsurprising that much of the interest in corroles lies in the preparation and application of metallocorrole complexes. Several review articles have appeared in the last five years outlining the inorganic chemistry of corroles. In particular, a 2009 review by Aviv-Harel and Gross[30] outlined some exceptional properties of corroles that led to early applications of their complexes, and a 2012 review by Palmer[31] outlined the use of many first row transition metal corrole complexes as oxo, imido, and nitrido transfer agents. The latter review also discussed in great detail the noninnocence of the corrole ligand in formally high-valent metal complexes. This topic is also discussed in the latest edition of the Handbook of Porphyrin Science,[3] and has great relevance to the applications of structurally modified species such as hangman porphyrins and pacman porphyrin-corrole dyads, which have seen application in oxygen reduction and water oxidation.[4] A review of main group corrole chemistry has also highlighted advances and applications in this field.[32] The contents of these aforementioned reviews will not be repeated here, except insofar as they serve for comparison to new corrole chemistry.

Much of the most recent progress in corrole chemistry has been towards the preparation of more air-sensitive complexes. As a result, several unexplored regions of the periodic table have recently become subjects of great interest. Alkali metals, early transition metals, lanthanides, and actinides were unknown in the corrole literature until 2012, and heavy elements including third row transition metals and heavy main group species had very limited representation. Figure 1.1 shows a depiction of the periodic table with those elements that have been coordinated to corrole ligand highlighted. The preparation, structural characteristics, and preliminary reactivity of these corrole complexes will be the focus of this review.

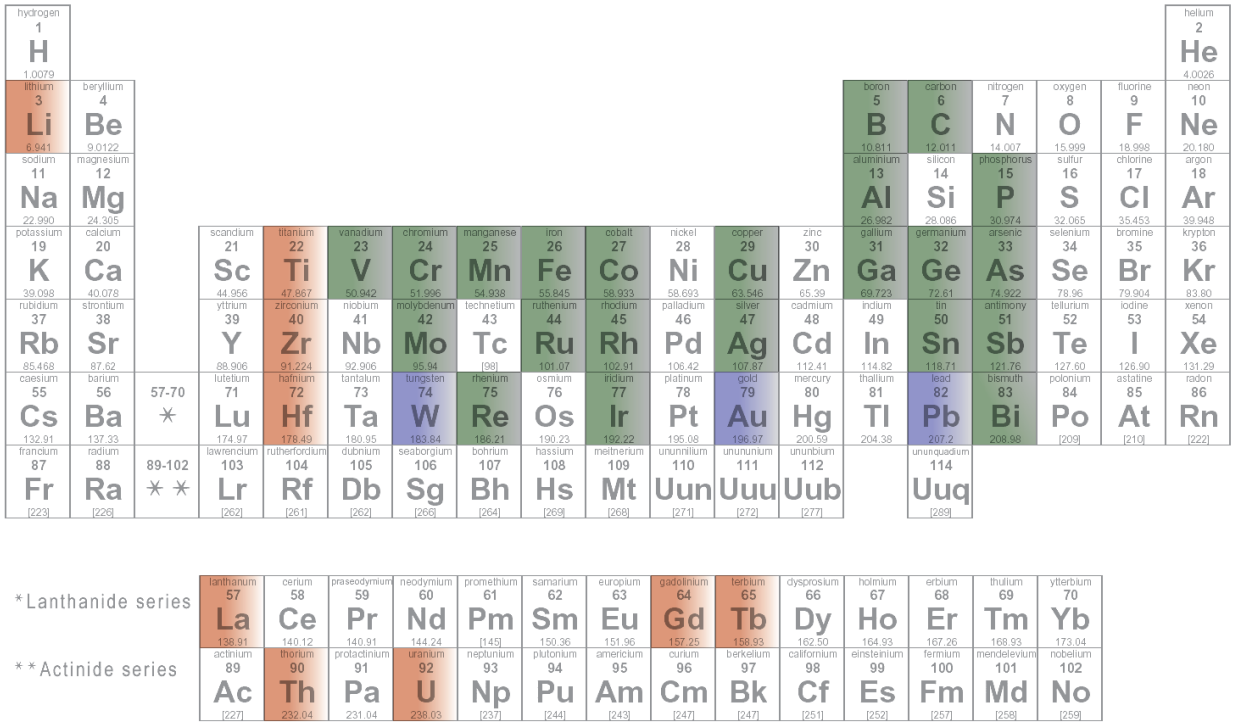

Figure 1.1. Periodic Table of Corroles. Green denotes metals with some corrole species known as of 2009. Blue denotes three new metals coordinated to corrole by other scientists: tungsten,[33] gold,[34] and lead.[35] Red denotes metals coordinated to corrole as a result of recent work in the Arnold group.

The development of metallocorrole chemistry closely mirrors that of metalloporphyrins. Much of the early work on metallocorroles focused on Mn, Fe, Co, and Cu due to their synthetic accessibility and biological significance. Corrole complexes are often prepared by similar methods to their porphyrin analogues,[36] by combining the free-base ligand in solution or suspension with a simple metal halide or acetate salt, with or without heating. The complex is then typically isolated by column chromatography.

The relatively late development of early transition metal, lanthanide, and actinide chemistry in both fields is largely due to the limitations of these methods in the face of air sensitive compounds. The sensitivity of these molecules is twofold. For one, the early transition metals, lanthanides, and actinides are all strongly oxophilic. Compounding this is the fact that, due to their larger radii as compared to their late transition metal counterparts, all of these metals are forced to sit significantly out of the plane of the macrocycle ring. This leaves the metal more sterically exposed, and strains the metal-nitrogen bonds, making these bonds more prone to hydrolysis to reform the free-base ligand. The oxophilicity may serve to explain why many of the species reviewed here and many examples of heavier metal porphyrin complexes are metal-oxo compounds.

To prepare and isolate air-sensitive metalloporphyin complexes, a new set of methodologies was developed.[37,38] The first involves reacting the free base porphyrin with a metal alkyl or silyl amide complex to generate the metal complex. (Scheme 1.1a). This reaction is driven thermodynamically by the formation of a strong C-H or C-N bond to produce metal porphyrins such as (OEP)Y[$CH(SiMe_3)_2$] (OEP = β-octaethylporphyrin).[39,40]

The second method for the preparation of air sensitive metalloporphyrin complexes was made possible by the isolation of alkali metal porphyrins, Li_2(porphyrin), Na_2(porphyrin) and K_2(porphyrin).[41–44] Salt metathesis of one of these with a metal halide X_2MR_n leads to the formation of R_nM(porphyrin) complexes (Scheme 1b). Examples include (OEP)$ZrCl_2$,[45] (OEP)ScCl,[46,47] (OEP)$ZrCl_2$ and (OEP)$Zr(CH_2SiMe_3)_2$,[45,48] (TPP)$SnPh_2$,[49] and the sandwich complexes $[Ta(OEP)_2][TaCl_6]$,[50] $Zr(OEP)_2$ and $Hf(OEP)_2$.[51] Beyond the initial preparation of these complexes, several formally lower valent species were synthesized, facilitated by the redox active nature of the porphyrin ligand.[52,53] This type of reactivity has not yet been achieved with early transition metal corrole chemistry. However, the similar redox-active nature of corrole, as demonstrated by catalytic multi-electron chemistry with first row transition metal complexes,[4,54] suggests that reduction chemistry of some of the complexes presented here should be possible.

Just as the two major synthetic routes discussed above led to the development of a wide range of previously inaccessible porphyrin compounds, so have analogous developments facilitated the preparation of new classes of metallocorrole complexes. In the sections that follow, these recent developments of alkali metal, early transition metal, lanthanide, actinide, and heavy transition metal and main-group corrole complexes are highlighted. The review then concludes with a comparison of some basic structural properties of known metallocorrole species, and a prospectus on the next frontiers of air-sensitive chemistry of metal corrole complexes.

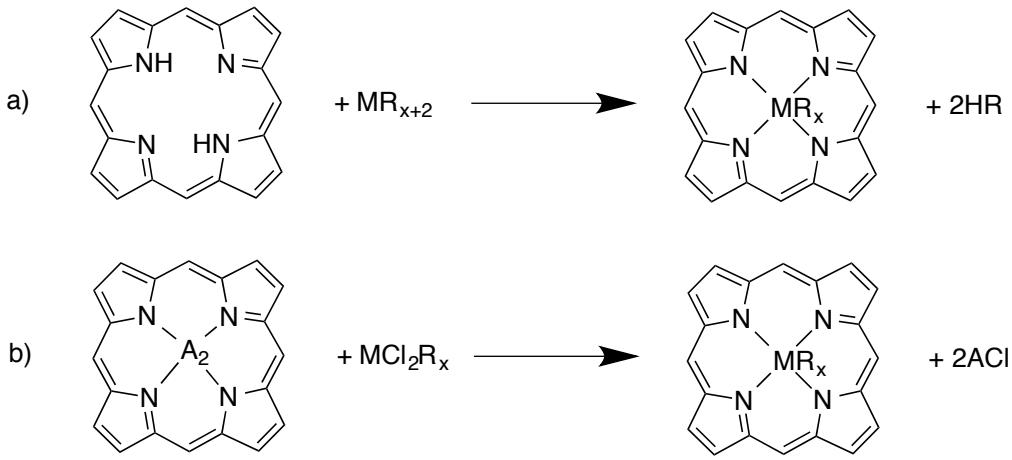

Scheme 1.1. General scheme for preparation of early transition metal porphyrin complexes by a) C-H bond formation and b) salt metathesis. (M = metal, R = alkyl substituent, x = any integer, A = alkali metal). Substituents on porphyrins are not shown.

Alkali Metal Corroles

While metalloporphyrin salts of Li, Na, and K have all been isolated and fully structurally characterized,[42] alkali metal corrole complexes have proven considerably more elusive. The only structurally characterized compound in this group is a lithium corrole, Mes_2(p-OMePh)corroleLi$_3$·6THF reported by our group in 2012.[55] This complex was structurally characterized as the $[Li(DME)_{2.5}]^+[Mes_2(p\text{-}OMePh)corroleLi_2(DME)_{1.5}]^-$ salt (See Chapter 2, Figure 2.1) with one lithium coordinated by solvent and two lithiums coordinated by all four nitrogen atoms of the corrole, sitting above and below the plane of the ring. This is different from both reported lithium porphyrin species: dilithium octaethylporphyrin and dilithium mesotetrakis(3,4,5-tri-methoxypheny1)porphyrin (Li_2(OEP) and Li_2(TMPP)) both are observed as ion pairs with a single lithium in the plane of the porphyrin ring and the second lithium coordinated only by solvent.[42] This structure more closely resembles that of sodium and potassium porphyrinates, in which one metal ion is coordinated above and the other below the plane of the porphyrin.[42] However, the single lithium peak observed in the ^{7}Li NMR spectrum of the lithium corrole suggests rapid exchange between the lithium atoms, and unpublished data from our group suggest that the solution-phase coordination environment of lithium in this species may be solvent-dependent.

The only other mention of lithium corroles in the literature is a metal organic framework (MOF) impregnated with corrole and doped with lithium.[56] The locations of the lithium atoms are determined computationally and are not consistent with what those of the structurally characterized lithium salt.

Group 4 and 5 Metallocorroles

The first group 4 and 5 corrole complexes to be isolated were oxotitanium(IV) and oxovandium(IV) species identified spectroscopically by Licoccia et al in 1995.[57] These compounds are both reported as doubly deprotonated [MO(corroleH)] species, and ^{1}H NMR spectroscopy and IR spectroscopy of the Ti complex appear to confirm the characterization of the extra proton as being associated with the corrole, rather than a more typical configuration with corrole as a trianionic ligand and a terminal hydroxo. The vanadium complex is believed not to form a metal(V) species due to the small ionic radius of high-valent vanadium.

More recently, a number of group 4 corrole complexes have been isolated and structurally characterized using the salt metathesis methodology outlined above (Scheme 1.2). Titanium(IV) and zirconium(IV) cyclopentadienyl species were prepared from metal trichloride cyclopentadienyl starting materials, providing lopsided "sandwich" complexes of the two metals.[55] Subsequent to this, reactions of titanium, zirconium, and hafnium tetrachloride with Mes_2(p-OMePh)corroleLi$_3$·6THF provided the metal(IV) chloride corrole complexes of all three group 4 metals.[58] Interestingly, the Zr and Hf corrole chlorides exist as dimers both in solution and in solid-state structure, but the Ti corrole chloride exists as a monomer. The preference of the Ti corrole complex for a monomeric structure may be attributed to the smaller ionic radius of Ti as compared to its heavier congeners. Reactions of the Ti corrole chloride have been performed with both NaCp* and Me_3SiCH_2MgCl to produce the corresponding organometallic species in a preliminary demonstration of possible reactivity of these systems.

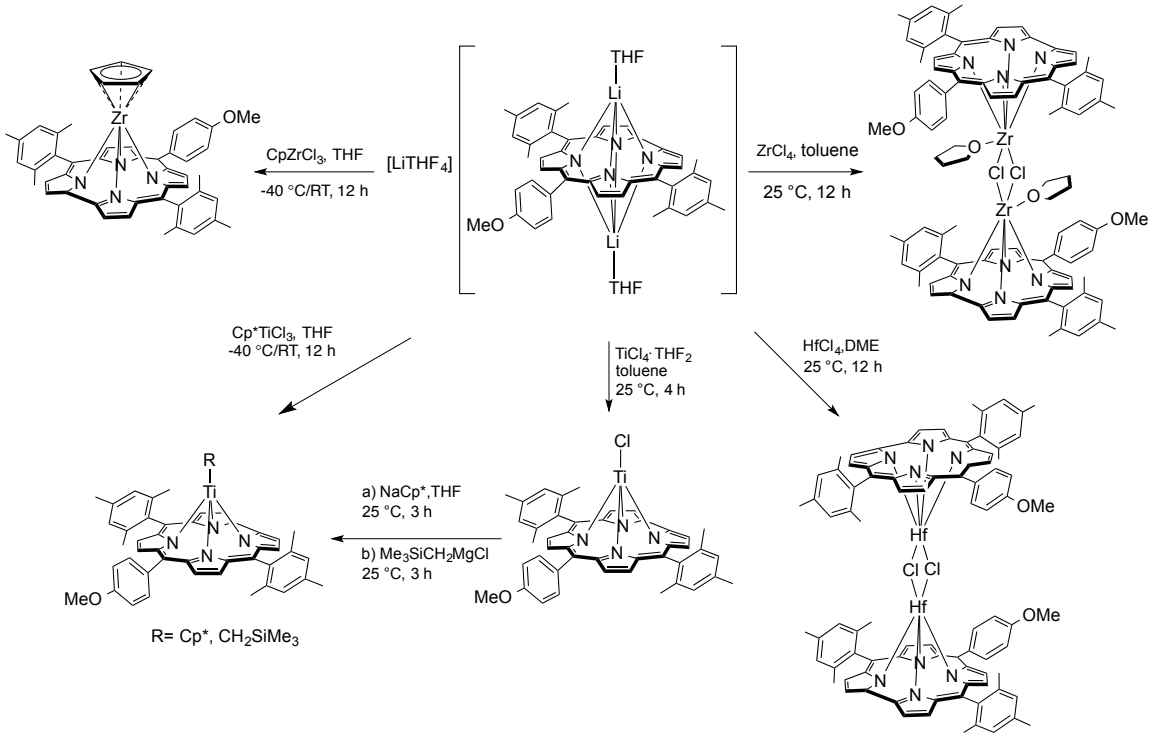

Scheme 1.2. Preparation of group 4 corrole complexes from lithium corrole.

Group 6 Metallocorroles

High valent chromium[59] and molybdenum[60] oxo corrole complexes have been known for over 30 years, and their chemistry is extensively covered in the aforementioned review by Palmer.[31] Lower valent corrole complexes are considerably less common in general and in the early metals in particular, although an interesting $[((C_6F_5)_3corroleMo)O]_2Mg(THF)_4$ species, initially formed with adventitious magnesium residual from starting material synthesis, was recently reported and is an example of a structurally characterized molybdenum(IV) corrole.[61] This structural characterization supports the spectroscopic identification of two other related molybdenum(IV) corrole species.

The first example of a tungsten corrole species, and indeed the first 5d early transition metal corrole complex, was also reported recently.[33] The compound is binuclear, with two tungsten(VI) corrole units bridged by three oxygen atoms. This structure is similar to those known for a number of early transition metal porphyrins, with hafnium[62–64] being one of the closest in structural analogy both to this species and to the chloride-bridged hafnium corrole mentioned above. Similar to other heavy metal-macrocycle complexes, the tungsten is large enough that it sits considerably out of the plane of the corrole despite its high valency.

Lanthanide and Actinide Metallocorroles

Interest in the use of conjugated macrocycles as "antennae" for luminescence sensitization of lanthanides led to the preparation some years ago of lanthanide porphyrin complexes.[65] However, the preparation of corrole complexes to the same end has been achieved only recently. In early 2013, Gross and coworkers published molecules dubbed lanthanide-corrole conjugates, where the periphery of the corrole molecule was extended to include chelating groups that supported Nd, Er, Yb, and Lu ions.[66] These metals were not directly coordinated by the corrole, but luminescence transfer between the corrole and metal was demonstrated.

Later that same year, the first examples of corroles directly coordinating to lanthanides were published by our group.[67] These were prepared by the two methodologies described above for the preparation of air-sensitive metallocorroles: the lanthanum and terbium complexes by salt metathesis and the gadolinium through the reaction of free base corrole with gadolinium(III) silyl amide (Scheme 1.3).

The only two actinide corrole complexes reported in the literature[68] are bridged chloride species which very closely resemble the zirconium and hafnium(IV) corrole chlorides.[58] Differences between the cyclic voltammetry of the uranium(IV) and the thorium(IV) species indicate that the uranium(IV) centre is likely involved in the redox activity of this species.

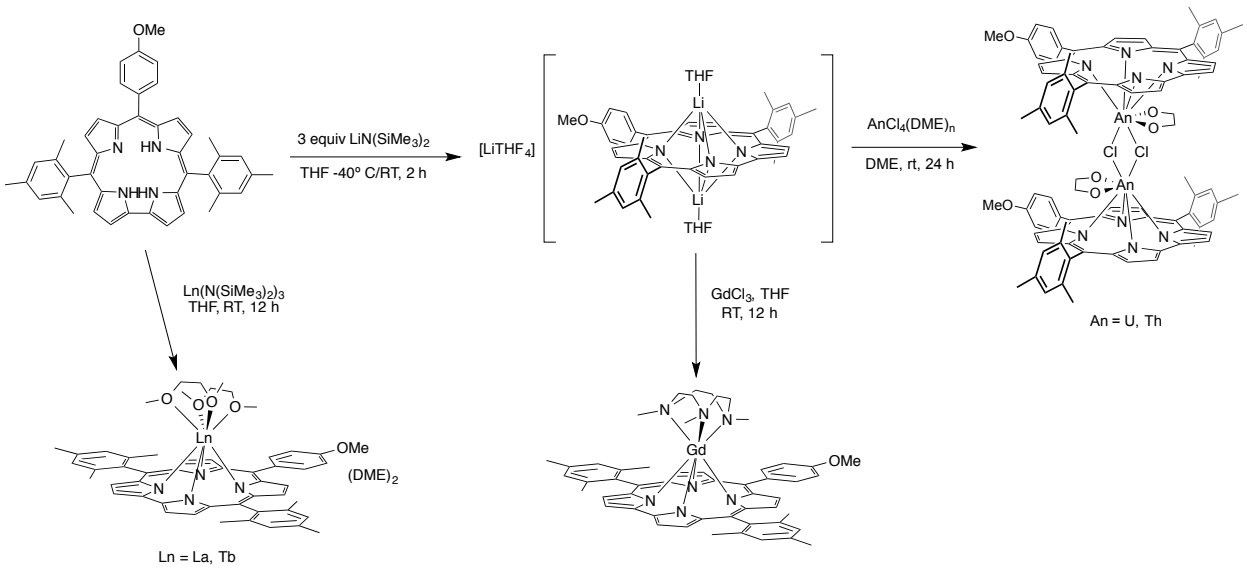

Scheme 1.3. Preparation of lanthanide and actinide corrole complexes.

Comparison of Structurally Characterized Corrole Complexes of Large Metals

Metals with a range of ionic radii are accommodated by macrocycles in a number of ways. Porphyrins have the ability to ruffle slightly to contract their ring size for small metals, and to expand the N_4 core slightly for metals with ionic radii slightly larger than the optimal 0.65 Å.[38] Corroles are more rigid; it has been demonstrated computationally that they cannot ruffle,[69] and the slightly contracted ring as compared to porphyrin has even less space to accommodate early transition metals and heavy metals within the plane of the ring.

A useful metric for comparing metallocorrole structures is the distance from the N_4 plane to the metal. While the dataset is still too small to make broad comparisons, this information may be used to anticipate metal displacement from corrole rings in future work, which in turn should be a predictive tool for the preparation of bis-corrole or other metal sandwich complexes based on predictions of ligand-based steric interactions.

Several points of interest can be taken from Table 1.1. The first is in comparing three titanium corrole species, where the M-N_4 distance is considerably longer for the Cp* species than for either the chloride or alkyl species. This is consistent with steric interactions between the Cp* ligand and the mesityl substituents on the corrole ring. Similar steric congestion between the THF ligands and the corrole substituents may account for the fact that the M-N_4 distance on the zirconium μ-Cl dimer is substantially longer than for that on the equivalent hafnium species.

This extent of variation in metal corrole distances with other changes to the ligand environment suggests that great care must be taken when drawing any comparisons between corrole species. Lanthanum(III) corrole currently holds the record for the greatest distance of a metal out of an N_4 conjugated macrocycle plane at 1.469 Å. This seems consistent with its lower valency than the actinide(IV) corroles reported and larger ionic radius than later lanthanides. However, it is clear that many factors contribute to metal-ligand interaction in corrole species, and a larger set of structurally characterized corroles will be needed before these trends can be fully elaborated.

Conclusions and Future Work

While coverage of the "periodic table of corroles" has increased substantially in recent years, the future of this field still poses many challenges and opportunities. Isolation of heavier alkali metal corrole salts will no doubt lead to further synthetic opportunities, as well as presenting interesting structural information themselves. While lanthanide complexes are close analogues, the smaller members of Group 3 have not yet been characterized in corrole complexes – chemistry at these valency-saturated but sterically accessible metals could be of great interest.

Across the periodic table, there is still a dearth of lower-valent metal complexes of corroles. The reactivity of such compounds could present new opportunities in small molecule activation and catalysis, particularly as the non-innocent nature of corrole as a ligand comes to be better understood.

Table 1.1. Metrical Parameters of Selected Crystallographically Characterized Metallocorrole Complexes

Metal	***Meso*-Corrole**	**Other Ligand**	**M-N_4 Plane Distance (Å)**	**M-L Distance (Range) (Å)**	**M-$N_{corrole}$ Distance Range (Å)**	**Reference**
Li	Mes_2(p-OMePh)	DME	1.030	1.934(5)-1.988(5)	2.061(5)-2.214(5)	[55]
Ti	Mes_2(p-OMePh)	Cp*	0.820	2.3764(19)-2.4159(18)	2.0389(15)-2.0562(14)	[55]
Ti	Mes_2(p-OMePh)	Cl	0.667	2.220(6)	1.985(2)-1.996(2)	[58]
Ti	Mes_2(p-OMePh)	CH_2SiMe_3	0.656	2.031(2)	1.978(2)-2.009(2)	[58]
Zr	Mes_2(p-OMePh)	Cp	0.914	2.451(3)-2.493(3)	2.094(2)-2.174(2)	[55]
Zr	Mes_2(p-OMePh)	μ-Cl THF	1.355	2.6852(12)-2.6897(11)	2.161(3)-2.166(3)	[58]
Hf	Mes_2(p-OMePh)	μ-Cl	1.184	2.121(3)-2.296(4)	2.142(4)-2.157(4)	[58]
Mo	$(C_6F_5)_3$	=O	0.729	1.684(2)	2.033(2)-2.039(2)	[70]
W	$(C_6F_5)_3$	μ-O	0.961	1.804(6)-2.217(6)	2.058(7)-2.124(7)	[33]
La	Mes_2(p-OMePh)	$(DME)_2$	1.469	2.661(6)-2.746(6)	2.426(6)-2.447(6)	[67]
Gd	Mes_2(p-OMePh)	$TACNMe_3$	1.262	2.668(5)-2.688(5)	2.294(5)-2.350(4)	[67]
Tb	Mes_2(p-OMePh)	$(DME)_2$	1.272	2.540(6)-2.719(8)	2.310(5)-2.325(6)	[67]
Th	Mes_2(p-OMePh)	μ-Cl	1.409	2.886(1)-2.932(2)	2.356(4)-2.413(7)	[68]
U	Mes_2(p-OMePh)	μ-Cl	1.392	2.840(1)-2.873(2)	2.293(6)-2.357(7)	[68]
Bi	$(C_6F_5)_3$	(none)	1.15	(N/A)	2.23(1)-2.28(1)	[71]

References

(1) Paolesse, R. In *The Porphyrin Handbook, Volume 2 Chapter 11*; 2000; pp. 201–232.
(2) Erben, C.; Will, S.; Kadish, K. M. In *The Porphyrin Handbook, Volume 2, Chapter 12*; 2000; pp. 233–300.
(3) McGown, A. J.; Badiei, Y. M.; Leeladee, P.; Prokop, K. A.; DeBeer, S.; Goldberg, D. P. In *Handbook of Porphyrin Science, Volume 14, Chapter 66*; 2010; pp. 525–599.
(4) Lemon, C. M.; Dogutan, D. K.; Nocera, D. G. In *Handbook of Porphyrin Science, Volume 25, Chapter 99*; 2010; pp. 1–143.
(5) Johnson, A. W.; Price, R. *J. Chem. Soc.* **1960**, 1649–1653.
(6) Johnson, A. W.; Kay, I. T. *Proc. Chem. Soc. London* **1961**, 168–169.
(7) Johnson, A. W.; Kay, I. T. *Proc. Chem. Soc.* **1964**, 89–90.
(8) Johnson, A. W.; Kay, I. T. *J. Chem. Soc.* **1965**, 1620–1629.
(9) Johnson, A. W.; Kay, I. T. *Proc. R. Soc. London Ser. A* **1965**, *288*, 334.
(10) Harrison, H. R.; Hodder, O. J. R.; Hodgkin, D. C. *J. Chem. Soc. B.* **1971**, 640–645.
(11) Paolesse, R.; Mini, S.; Sagone, F.; Boschi, T.; Jaquinod, L.; Nurco, D. J.; Smith, K. M. *Chem. Commun.* **1999**, *2*, 1307–1308.
(12) Gross, Z.; Galili, N.; Saltsman, I. *Angew. Chem. Int. Ed.* **1999**, *38*, 1427–1429.
(13) Gross, Z.; Galili, N.; Simkhovich, L.; Saltsman, I.; Botoshsnsky, M.; Blaser, D.; Boese, R.; Goldberg, I. *Org. Lett.* **1999**, *1*, 599–602.
(14) Gryko, D. T. *J. Porphyrins Phthalocyanines* **2008**, *12*, 906–917.
(15) Koszarna, B.; Gryko, D. T. *J. Org. Chem.* **2006**, *71*, 3707–3717.
(16) Gryko, D. T.; Koszarna, B. *Org. Biomol. Chem.* **2003**, *1*, 350–357.
(17) Gryko, D. T.; Jadach, K. *J. Org. Chem.* **2001**, *66*, 4267–4275.
(18) Gryko, D. T.; Piechota, K. E. *J. Porphyrins Phthalocyanines* **2002**, *6*, 81–97.
(19) Paolesse, R.; Nardis, S.; Sagone, F.; Khoury, R. G. *J. Org. Chem.* **2001**, *66*, 550–556.
(20) Decréau, R. A.; Collman, J. P. *Tetrahedron Lett.* **2003**, *44*, 3323–3327.
(21) Pomarico, G.; Vecchi, A.; Mandoj, F.; Bortolini, O.; Cicero, D. O.; Galloni, P.; Paolesse, R. *Chem. Commun.* **2014**, *50*, 4076–4078.
(22) Thomas, K. E.; Wasbotten, I. H.; Ghosh, A. *Inorg. Chem.* **2008**, *47*, 10469–10478.
(23) Mahammed, A.; Botoshansky, M.; Gross, Z. *Dalt. Trans.* **2012**, *41*, 10938–10940.
(24) Pomarico, G.; Nardis, S.; Paolesse, R.; Ongayi, O. C.; Courtney, B. H.; Fronczek, F. R.; Vicente, M. G. H. *J. Org. Chem.* **2011**, *76*, 3765–3773.
(25) Gao, D.; Canard, G.; Giorgi, M.; Balaban, T. S. *Eur. J. Inorg. Chem.* **2012**, *2012*, 5915–5920.
(26) Blumenfeld, C. M.; Grubbs, R. H.; Moats, R. A.; Gray, H. B.; Sorasaenee, K. *Inorg. Chem.* **2013**, *52*, 4774–4776.
(27) Fu, B.; Huang, J.; Ren, L.; Weng, X.; Zhou, Y.; Du, Y.; Wu, X.; Zhou, X.; Yang, G. *Chem. Commun.* **2007**, 3264–3266.
(28) Gershman, Z.; Goldberg, I.; Gross, Z. *Angew. Chem. Int. Ed.* **2007**, *46*, 4320–4324.
(29) Guilard, R.; Gryko, D. T.; Canard, G.; Barbe, J. M.; Koszarna, B.; Brandès, S.; Taisor, M. *Org. Lett.* **2002**, *4*, 4491–4494.
(30) Aviv-Harel, I.; Gross, Z. *Chem. Eur. J.* **2009**, *15*, 8382–8394.
(31) Palmer, J. H. *Struct. Bond.* **2012**, *142*, 49–90.
(32) Aviv-Harel, I.; Gross, Z. *Coord. Chem. Rev.* **2010**, *255*, 717–736.
(33) Nigel-Etinger, I.; Goldberg, I.; Gross, Z. *Inorg. Chem.* **2012**, *51*, 1983–1985.

(34) Rabinovich, E.; Goldberg, I.; Gross, Z. *Chem. Eur. J.* **2011**, *17*, 12294–12301.
(35) Schöfberger, W.; Lengwin, F.; Reith, L. M.; List, M.; Knör, G. *Inorg. Chem. Commun.* **2010**, *13*, 1187–1190.
(36) Buchler, J. W. In *The Porphyrins*; 1978; p. 389.
(37) Arnold, J. In *The Porphyrin Handbook, Volume 3 Chapter 17*; Kadish, K. M.; Smith, K. M.; Guilard, R., Eds.; Academic Press: New York, 1999; pp. 113–128.
(38) Brand, H.; Arnold, J. *Coord. Chem. Rev.* **1995**, *140*, 137–168.
(39) Schaverien, C. J. *J. Chem. Soc., Chem. Commun.* **1991**, 458–460.
(40) Schaverien, C. J.; Orpen, A. G. *Inorg. Chem.* **1991**, *30*, 4968–4978.
(41) Arnold, J. *J. Chem. Soc., Chem. Commun.* **1990**, *1990*, 976–978.
(42) Arnold, J.; Dawson, D. Y.; Hoffman, C. G. *J. Am. Chem. Soc.* **1993**, *115*, 2707–2713.
(43) Brand, H.; Capriotti, J. A.; Arnold, J. *Inorg. Chem.* **1994**, *33*, 4334–4337.
(44) Dawson, D. Y.; Arnold, J. *J. Porphyrins Phthalocyanines* **1997**, *1*, 121–124.
(45) Brand, H.; Arnold, J. *Organometallics* **1993**, *12*, 3655–3665.
(46) Arnold, J.; Hoffman, C. G. *J. Am. Chem. Soc.* **1990**, *81*, 8620–8621.
(47) Arnold, J.; Hoffman, C. G.; Dawson, D. Y.; Hollander, F. J. *Organometallics* **1993**, *12*, 3645–3654.
(48) Brand, H.; Arnold, J. *J. Am. Chem. Soc.* **1992**, *114*, 2266–2267.
(49) Dawson, D. Y.; Sangalang, J. C.; Arnold, J. *J. Am. Chem. Soc.* **1996**, *118*, 6082–6083.
(50) Dawson, D. Y.; Brand, H.; Arnold, J. *J. Am. Chem. Soc.* **1994**, *116*, 9797–9798.
(51) Martin, P. C.; Arnold, J.; Bocian, D. F. *J. Phys. Chem.* **1993**, *97*, 1332–1338.
(52) Gebauer, A.; Dawson, D. Y.; Arnold, J. *J. Chem. Soc., Dalt. Trans.* **2000**, 111–112.
(53) Brand, H.; Arnold, J. *Angew. Chem. Int. Ed. Engl.* **1994**, *33*, 95–97.
(54) Stefanelli, M.; Nardis, S.; Tortora, L.; Fronczek, F. R.; Smith, K. M.; Licoccia, S.; Paolesse, R. *Chem. Commun.* **2011**, *47*, 4255–4257.
(55) Buckley, H. L.; Chomitz, W. A.; Koszarna, B.; Tasior, M.; Gryko, D. T.; Brothers, P. J.; Arnold, J. *Chem. Commun.* **2012**, *48*, 10766–10768.
(56) Stergiannakos, T.; Tylianakis, E.; Klontzas, E.; Trikalitis, P. N.; Froudakis, G. E. *J. Phys. Chem. C* **2012**, *116*, 8359–8363.
(57) Licoccia, S.; Paolesse, R.; Tassoni, E.; Poliziob, F. *J. Chem. Soc., Dalt. Trans.* **1995**, 3617–3621.
(58) Padilla, R.; Buckley, H. L.; Ward, A. L.; Arnold, J. *Chem. Commun.* **2014**, *50*, 2922–2924.
(59) Matsuda, Y.; Yamada, S.; Murakami, Y. *Inorg. Chim. Acta* **1980**, *44*, 309–311.
(60) Murakami, Y.; Matsuda, Y.; Yamada, S. *Chem. Lett.* **1977**, *6*, 689–692.
(61) Nigel-Etinger, I.; Goldberg, I.; Gross, Z. *Inorg. Chem.* **2013**, *52*, 3381–3387.
(62) Huhmann, J. L.; Corey, J. Y.; Rath, N. P.; Campana, C. F. *J. Organomet. Chem.* **1996**, *513*, 17–26.
(63) Ryu, S.; Kim, J.; Yeo, H.; Kim, K. *Inorg. Chim. Acta* **1995**, *228*, 233–236.
(64) Falber, A.; L., T.; Goldberg, I.; Favilla, M. V.; Drain, C. M. *Inorg. Chem.* **2008**, *47*, 454–467.
(65) Kachura, T. F.; Sevchenko, A. N.; Solv'ev, K. N.; Tsvirko, M. P. *Dokl. Phys. Chem* **1974**, *217*, 1121–1124.
(66) Semenishyn, N.; Gross, Z. *Dalt. Trans.* **2013**, *42*, 3775–3778.
(67) Buckley, H. L.; Anstey, M. R.; Gryko, D. T.; Arnold, J. *Chem. Commun.* **2013**, *49*, 3104–3106.

(68) Ward, A. L.; Buckley, H. L.; Lukens, W. W.; Arnold, J. *J. Am. Chem. Soc.* **2013**, *135*, 13965–13971.
(69) Thomas, K. E.; Conradie, J.; Hansen, L. K.; Ghosh, A. *Inorg. Chem.* **2011**, 3247–3251.
(70) Luobeznova, I.; Raizman, M.; Goldberg, I.; Gross, Z. *Inorg. Chem.* **2006**, *45*, 386–394.
(71) Reith, L. M.; Stiftinger, M.; Monkowius, U.; Knör, G.; Schoefberger, W. *Inorg. Chem.* **2011**, *50*, 6788–6797.

Chapter 2: Synthesis of Lithium Corrole and its Use as a Reagent for the Preparation of Cyclopentadienyl Zirconium and Titanium Corrole Complexes

Introduction

Complexes of macrocyclic ligands have numerous applications in catalysis and small molecule activation.[1–4] In particular, the relatively rigid conjugated structures of porphyrins and corroles are of interest because the non-innocent nature of the ligand allows for strong coordination of metals and metalloids in a variety of oxidation states.[5,6] These structures have broad applications ranging from light harvesting[7] to non-linear optics.[8]

Recent synthetic advances in the preparation of *meso*-substituted corroles have allowed for the efficient preparation of a range of free-base corroles.[9,10,11] This synthetic breakthrough has facilitated extensive activity in the preparation of metallocorrole complexes, both mid-to-late transition metal complexes and main group species.[12–18] Very recently, iridium,[19] gold,[20–22] lead[23] and bismuth[24] complexes have been synthesized. However, corrole complexes containing alkali metals have not been reported to date. Although spectroscopic evidence of titanium(IV) and vanadium(V) oxo corrole complexes has been reported,[25] no structural reports of early (groups 3-5) transition metal corroles were found in the Cambridge database.

Alkali metal salts of porphyrins were first described spectroscopically in the middle of the previous century.[26–28] Structural characterization was reported in the early 1990s,[29] and the complexes were demonstrated to be useful metathesis reagents in the preparation of early transition metal porphyrin complexes.[30–32] Notably, the larger early transition metals sit outside the plane of the porphyrin ring, and are "capped" by ancillary ligands. This effect is expected to be accentuated in corrole species due to the smaller ring size; some late transition metals sit outside the plane of the corrole ring.[5] The trianionic corrole ligand is non-innocent and forms complexes with metals in high formal oxidation states (such as Fe(IV), Cr(IV, V), Mn(V) etc.);[13] the non-planarity of the metal complexes and availability of high oxidation states has the potential to improve access to the metal centre for reactive small molecule substrates.

Here we present the preparation of the first alkali metal corrole complex and its use as a metathesis reagent in the synthesis of new organometallic group 4 complexes; these include the first example of a zirconium(IV) corrole compound and a structurally characterized titanium(IV) corrole complex.

Results and Discussion

Combination of the free base 10-(4-methoxyphenyl)-5,15-dimesitylcorrole ((Mes$_2$(*p*-OMePh)corrole)H$_3$) with three equivalents of LiN(SiMe$_3$)$_2$ at -40 ºC in THF leads to an immediate colour change from deep purple to a deep green solution. Warming the solution to room temperature, stirring for two hours, and subsequent reduction of the volume and addition of hexanes produces a deep green solid (74 % yield) upon cooling to -40 ºC and subsequent filtration. Complex **2-1·6THF** (Scheme 2.1) has been characterized by ^{1}H NMR, ^{7}Li NMR, and UV-visible spectroscopies, and ESI mass spectrometry. Recrystallization of the solid by vapour diffusion at room temperature (1,2-dimethoxyethane (DME)/hexanes) provided dark green plates suitable for characterization by X-ray crystallography.

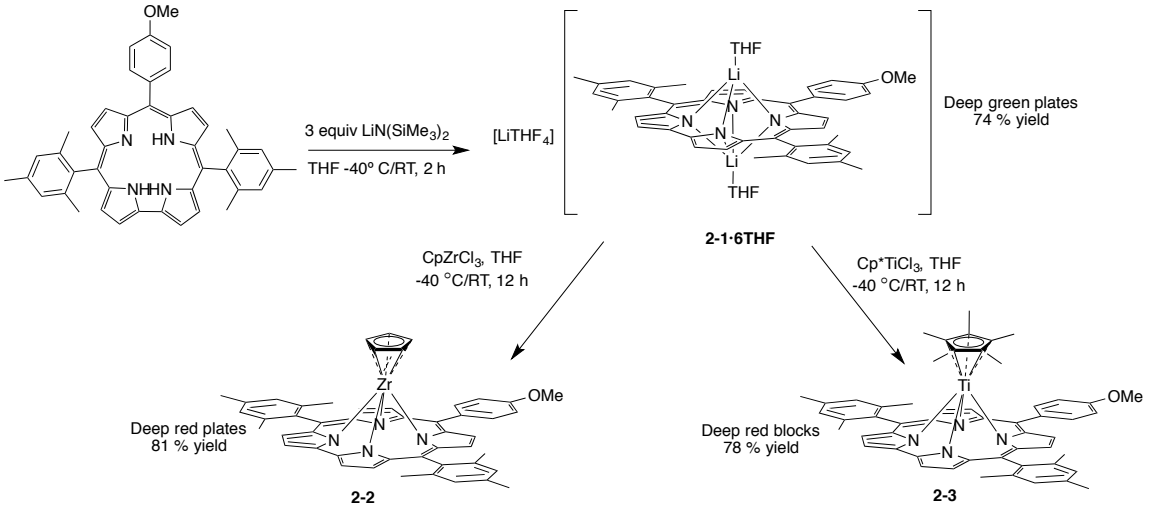

Scheme 2.1. Synthesis of lithium corrole **2-1·6THF**, Cp zirconium(IV) corrole **2-2**, and Cp* titanium(IV) corrole **2-3**.

The crystal structure of the lithium corrole **2-1·4DME** is shown in Figure 2.1. Two of the lithium atoms are located approximately equidistant above and below the N_4 plane of the corrole (1.021 Å and 1.040 Å, respectively), with an average N-Li bond distance of 2.141(14) Å and a Li-Li separation of 2.065(7) Å; each lithium atom is coordinated by one oxygen atom from solvent. The third lithium occurs as a solvated cation coordinated by five oxygens from three DME molecules. A search of the Cambridge database reveals that the metal-to-N_4-plane distances in **2-1·4DME** are exceeded only by a recently reported structure for bismuth(III) corrole,[33] which exhibits a Bi-N_4 distance of 1.144 Å.

The binding of the two lithium atoms above and below the plane of **2-1** differs from the structures observed by X-ray crystallography for dilithium octaethylporphyrin and dilithium mesotetrakis(3,4,5-tri-methoxypheny1)porphyrin (Li_2(OEP) and Li_2(TMPP)); both occurred as ion pairs with a single lithium in the plane of the porphyrin ring and the second lithium coordinated only by solvent.[29] The greater anionic charge of the corrole ring likely accounts for this structure, which resembles the sandwich structures observed for sodium and potassium porphyrinates.[29]

The ^{1}H NMR spectrum (C_6D_6) of (Mes_2(*p*-OMePh)corrole)Li_3·6THF indicates the incorporation of six molecules of THF. The disappearance of the highly shielded, characteristic broad N-H peak at ~ -2.5 ppm found in the spectrum of free-base corrole confirms the complete deprotonation of the corrole ligand. The ^{7}Li NMR spectrum (C_6D_6) shows a single peak at -8.40 ppm, suggesting fast exchange in this solvent environment.

The isolated (Mes_2(*p*-OMePh)corrole)Li_3·6THF has been compared to the free-base corrole by UV-visible absorption spectroscopy. Spectra of both free-base corrole and its lithium complex demonstrate a split Soret band characteristic of sterically hindered *meso*-substituted corroles.[34] Moderate red-shifts of both the Soret bands from 407 and 428 nm to 422 and 446 nm and of the Q-bands from 567, 606, and 639 nm to 587 and 636 nm are consistent with retention of planarity of the corrole chromophore upon lithiation. A substantial hyperchromic effect observed for the lowest energy Q band corresponds with an observed colour change from purple to green. Titration of (Mes_2(*p*-OMePh)corrole)H_3 in THF with $LiN(SiMe_3)_2$ was monitored by UV-visible spectroscopy, which indicates a gradual speciation up to the addition of two equivalents of $LiN(SiMe_3)_2$, at which point the spectrum matches exactly that of the isolated (Mes_2(*p*-OMePh)corrole)Li_3 (Figure 2.2). No further change is observed in the absorption spectrum upon addition of up to 8.5 equivalents of $LiN(SiMe_3)_2$, suggesting that non-coordinated Li ions do not affect the UV-visible spectrum. This is to be expected because they do not interact with the corrole-ring chromophore.

In addition to our structural interest in the trilithio corrole species, we targeted its synthesis in the hope that it might function as a reagent to prepare hitherto unknown metallocorrole complexes, in a manner related to that described for the corresponding porphyrinates but previously untested in corrole chemistry.[2,35] Accordingly, we treated chloride salts of the early transition metals Ti and Zr with the lithiated corrole.

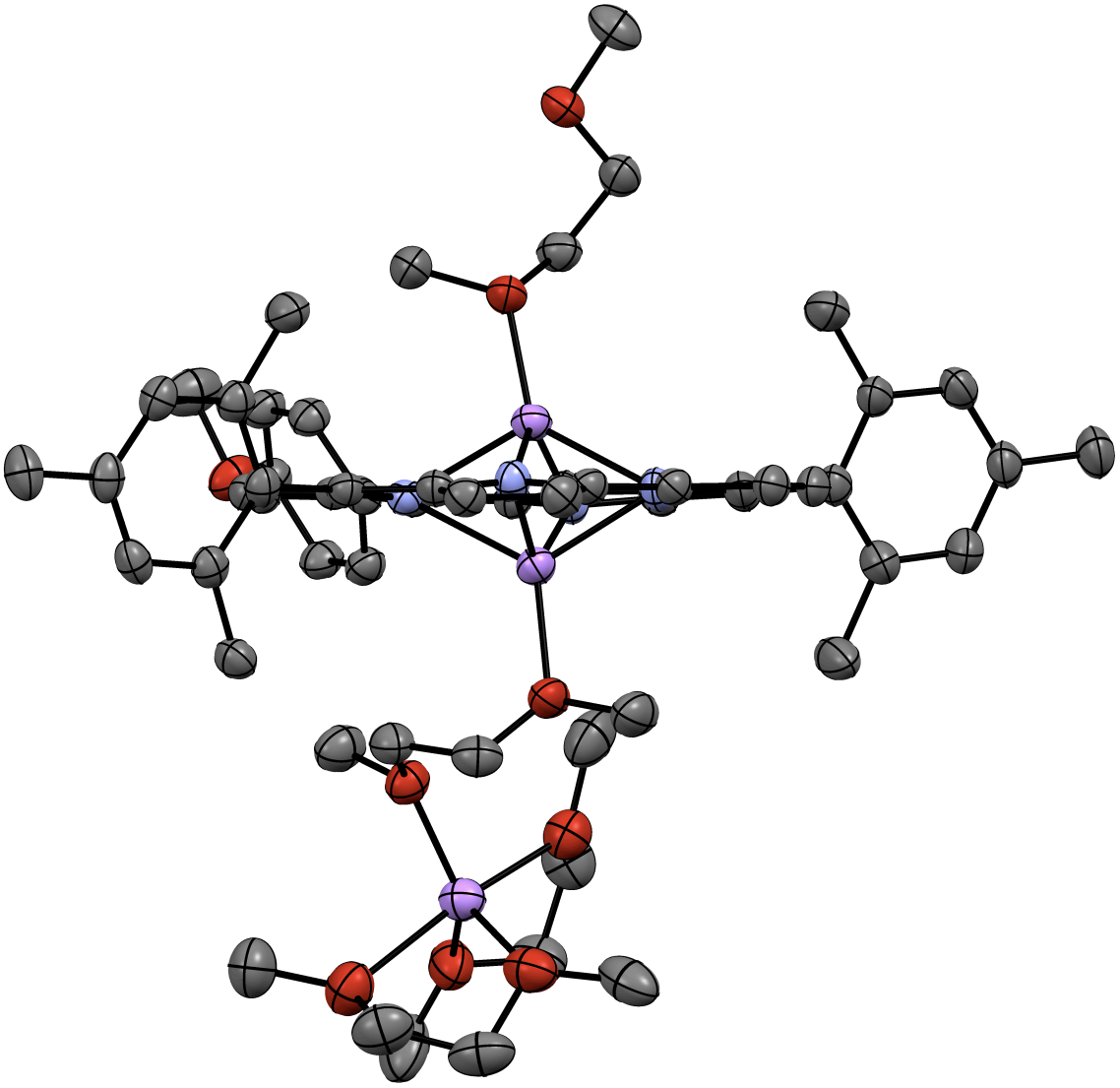

Figure 2.1. Molecular structure of lithium corrole **2-1·4DME**, determined by single-crystal X-ray diffraction. H atoms omitted for clarity; thermal ellipsoids at 50 % probability level.

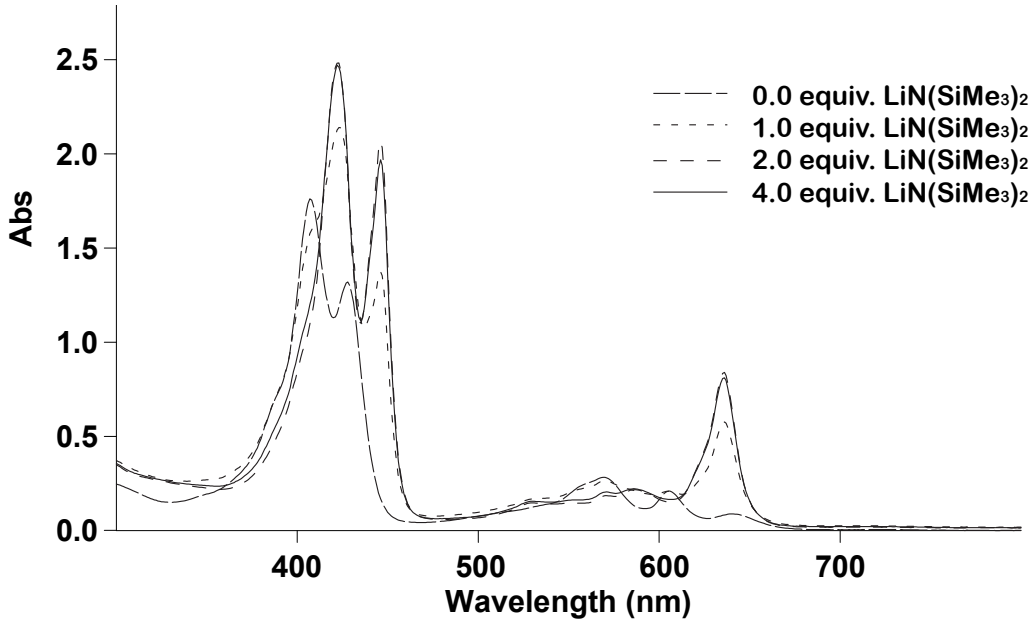

Figure 2.2. Titration of free-base corrole with $LiN(SiMe_3)_2$ as monitored by UV-visible spectroscopy.

The cyclopentadienyl zirconium(IV) corrole complex (Mes_2(*p*-OMePh)corrole)ZrCp (**2-2**) was prepared by the combination in THF at -40 ºC of **2-1·6THF** with 1.1 equivalents of $CpZrCl_3$. Warming this solution to room temperature and stirring overnight results in a dark brown solution. Removal of the solvent under vacuum, washing the solid with hexane and filtering produces a deep red solution from which deep red microcrystals are isolated by cooling to -40 ºC (81 % yield). This species has been characterized by ^{1}H and ^{13}C NMR and UV-visible spectroscopies, and mass spectrometry (see Experimental Details). Crystals suitable for X-ray diffraction were grown by slow evaporation of pentane at -40 ºC (Figure 2.3).

The pentamethylcyclopentadienyl titanium(IV) corrole complex (Mes_2(*p*-OMePh)corrole)TiCp* (**2-3**) was prepared in a similar manner to **2-2**, generating deep red microcrystals in 78 % yield. This species has been characterized by ^{1}H NMR and UV-visible spectroscopies, and mass spectrometry (see Experimental Details). Crystals suitable for X-ray diffraction were grown by vapour diffusion at room temperature (toluene/hexane) (Figure 2.4).

In both **2-2** and **2-3**, the ^{1}H NMR spectra display an upfield shift of the Cp$^{(*)}$ ring that is consistent with the shielding effects of the corrole ring. The C_5H_5 peak in **2-2** is observed at 3.11 ppm, and the $C_5(CH_3)_5$ peak in **2-3** is observed at -0.05 ppm. The loss of mirror symmetry about the plane of the corrole is demonstrated by three distinct singlets in the ^{1}H NMR spectra of both **2-2** and **2-3**, which correspond to the methyl substituents of the mesityl group. In both free base- and lithium corrole the *ortho*-methyl substituents are equivalent by ^{1}H NMR spectroscopy.

As predicted, both the zirconium(IV) and titanium(IV) centres sit well outside the average N_4 plane of the corrole (Zr-N_4 0.914 Å, Ti-N_4 0.820 Å). These displacements are shorter than for the recently reported tungsten(VI) oxo corrole[36] (W-N_4 0.961 Å), but longer than those reported for the corresponding Mo[37] and Cr[38] corroles (Mo-N_4 0.729 Å, Cr-N_4 0.562 Å), as is expected when comparing group 4 to group 6 metal complexes.

The Zr and Ti complexes **2-2** and **2-3** are each capped by a Cp$^{(*)}$ ligand, forming a lopsided "sandwich" complex with the Cp$^{(*)}$ ligands η^5-coordinated to the respective metal centres. Both complexes display broader peaks in the UV-visible spectrum than the free-base corrole and lithium corrole **2-1**; this is consistent with the loss of planarity of the chromophore in the transition metal species.

Conclusion

In summary, unique examples of an alkali metal corrole salt, a zirconium corrole complex and a titanium corrole complex have been prepared and characterized spectroscopically and structurally. Importantly, a new route to metallocorrole complexes through metathesis has been demonstrated; corrole complexes of these metals cannot be synthesized directly from the free-base corrole. Spectroscopic and structural studies are on-going to demonstrate the application of this methodology to the preparation of new metallocorrole complexes.

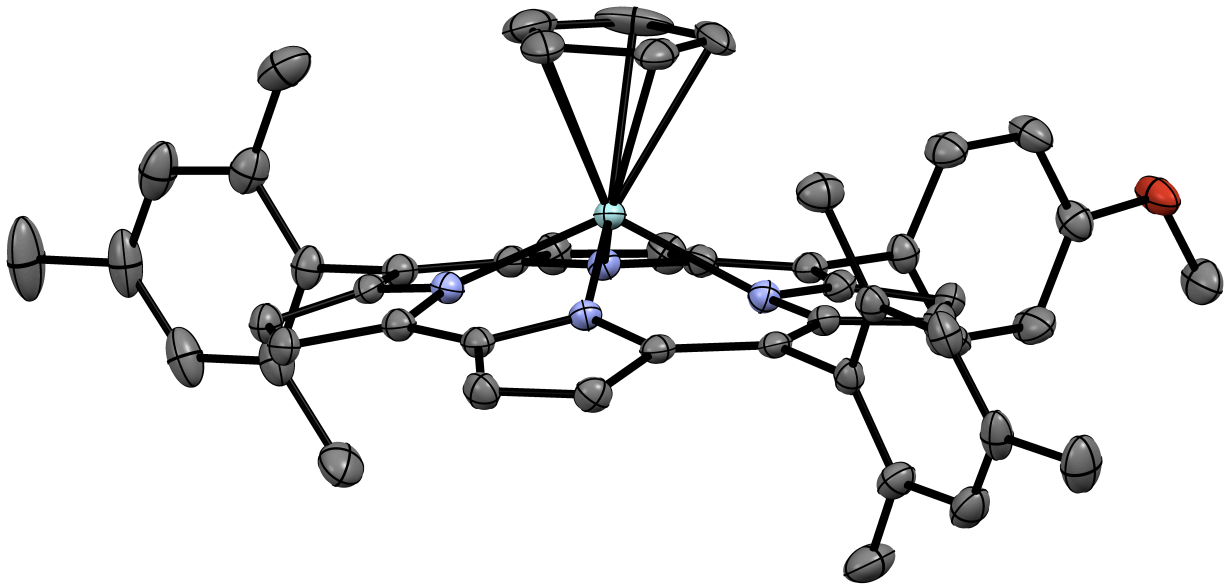

Figure 2.3. Molecular structure of Cp zirconium(IV) corrole **2-2**, determined by single-crystal X-ray diffraction. H atoms omitted for clarity; thermal ellipsoids at 50 % probability level.

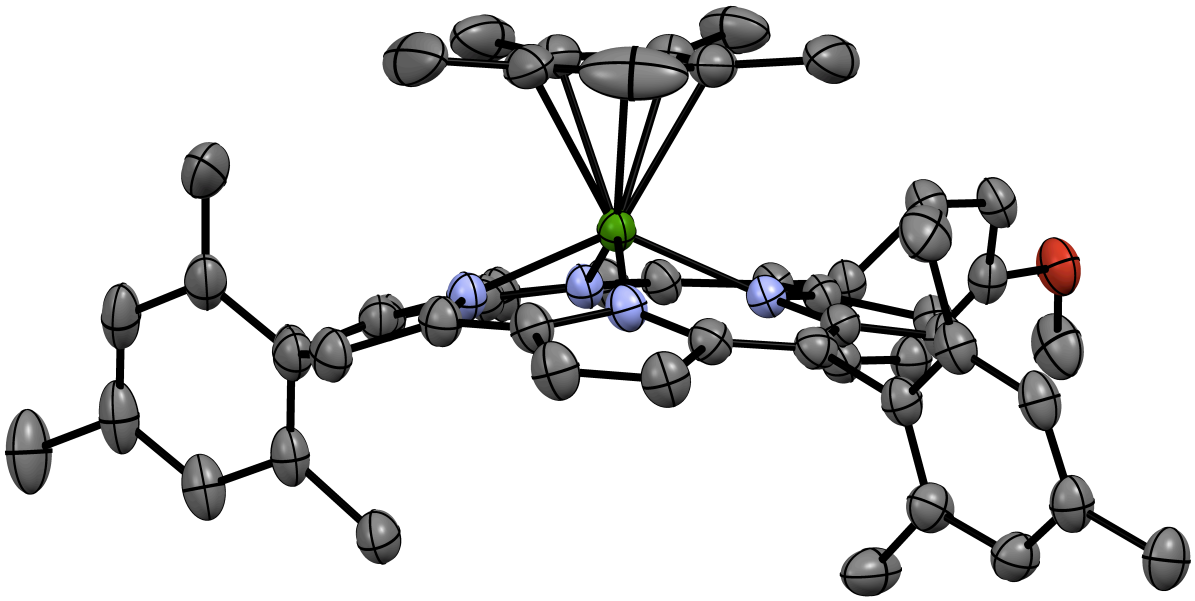

Figure 2.4. Molecular structure of pentamethylcylopentadienyl titanium(IV) corrole **2-3** determined by single-crystal X-ray diffraction. H atoms omitted for clarity; thermal ellipsoids at 50 % probability level.

Experimental Details

General Considerations

Unless otherwise noted, all reactions were performed using standard Schlenk and N_2-atmosphere glovebox techniques. Glassware and cannulae were stored in an oven at *ca.* 180 ºC. Solvents were dried by passing through a column of activated alumina and degassed with nitrogen.[39] C_6D_6 was dried over Na/benzophenone, and vacuum transferred. All NMR spectra were obtained in C_6D_6 at ambient temperature using Bruker AVB-400 or AVQ-400 spectrometers. ^{1}H NMR chemical shifts (δ) were calibrated relative to residual solvent peak. UV-visible spectra were determined with a Varian Cary 50UV-vis spectrophotometer using a 1 mm quartz cell. Mass spectral data (ESI-MS, positive mode) were obtained at the University of California, Berkeley Microanalytical Facility, using vacuum-dried samples dissolved in dry THF. X-ray crystal diffraction analyses were performed at the University of California, Berkeley CHEXRAY facility. Melting points were determined using sealed capillaries prepared under nitrogen and are uncorrected. $LiN(SiMe_3)_2$[40] and 5-(2,4,6-trimethylphenyl)dipyrromethane[41] were prepared according to literature procedures. 4-methoxybenzaldehyde, hydrazine (1.0 M in THF), *p*-chloranil were obtained from Aldrich. Cyclopentadienyl zirconium(IV) trichloride and pentamethylcyclopentadienyl titanium(IV) trichloride were obtained from Strem Chemicals.

Synthesis and characterization of free base corrole and complexes 2-1, 2-2, and 2-3

5,15-bis(2,4,6-trimethylphenyl)-10-(4-methoxyphenyl)corrole (Mes_2(*p*-OMePh)corroleH_3) was prepared according to a modified literature procedure[10] under benchtop conditions with solvents used as received. As much as possible, flasks were covered with aluminum foil to reduce exposure to light. 5-(2,4,6-trimethylphenyl)dipyrromethane (2.64 g, 10 mmol) and 4-methoxybenzaldehyde (612 μL, 5.0 mmol) were dissolved in methanol (1 L). Concentrated hydrochloric acid (36 %, 50 mL) was combined with 500 mL distilled water, and the acid solution was added to the methanol solution with stirring, immediately producing a peach-colored suspension. The mixture was stirred for two hours at room temperature, and then extracted with chloroform (5 x 200 mL, or until the aqueous layer is pale yellow). The organic extracts were combined, dried over sodium sulfate, filtered, and diluted to 1.25 L. *p*-Chloranil (3.69 g, 15 mmol) was added and the reaction was stirred overnight at room temperature. The solution was concentrated to 100 mL by rotary evaporation, then filtered through a silica pad and eluted with methylene chloride. The combined eluents were concentrated to dryness, and dissolved in 25 mL THF. To this solution was added hydrazine solution (1.0 M in THF, 10 mL) and the solution was stirred for 10 minutes. The solution was then concentrated to dryness. Column chromatography on silica (ramped 100 % hexane to 1:1 methylene chloride: hexane, R_f = 0.55 in 1:1 methylene chloride:hexane) provides pure corrole (450 mg, 14 % yield). ^{1}H NMR (600 MHz, $CDCl_3$) δ 8.87 (d, *J* = 4.1 Hz, 2H, β-*H*), 8.49 (d, *J* = 4.6 Hz, 2H, β-*H*), 8.47 (d, *J* = 4.6 Hz, 2H, β-*H*), 8.31 (s, 2H, β-*H*), 8.06, 7.25 (AA'BB', *J* = 8.6 Hz), 7.26 (s(broad), 4H, $C_6H_2(CH_3)_3$), 4.06 (s, 3H, OCH_3), 2.59 (s, 6H, $C_6H_2(CH_3)_2$(*p*-CH_3)), 1.92 (s, 12H, $C_6H_2CH_3$(*o*-$CH3$)$_2$), (-3) – (-1) (s(broad), 3H, N*H*). UV-Vis (CH_2Cl_2, nm) 407, 427, 566, 605, 636. ESI-MS (+) Calcd: 641.3275 for $C_{44}H_{41}N_4O$, observed 641.3304. M.p. > 300 °C.

Note: The major monomeric byproduct of this reaction is Mes_2(p-OMePh)$_2$porphyrin (R_f = 0.5 in 1:1 methylene chloride: hexane, vs. R_f = 0.55 in 1:1 methylene chloride: hexane for the corrole). The porphyrin can generally be removed by careful monitoring of the silica plug eluent before reduction of the product with hydrazine. If these two products fail to separate by column chromatography, the corrole can be suspended in a minimum volume of hot hexane, cooled, and filtered to remove the porphyrin with minimal loss of yield.

Trilithium 5,15-bis(2,4,6-trimethylphenyl)-10-(4-methoxyphenyl)corrole hexakis(tetrahydrofuran) (Mes_2(*p*-OMePh)corroleLi$_3$·6THF) (**2-1·6THF**). Mes_2(*p*-OMePh)corroleH$_3$ (300 mg, 0.47 mmol) and lithium bis-trimethylsilylamide (236 mg, 1.41 mmol) were combined in a Schlenk flask. The flask was cooled to -40 ºC and 15 mL THF was added by cannula. The solution was allowed to warm to room temperature and stirred for two hours. The volume of the solution was reduced to ~7 mL under vacuum, 2-3 mL of hexane was added by cannula, and the solution was cooled to -40 ºC and cannula filtered to generate a deep green solid (380 mg, 74 % yield). Crystals suitable for X-ray diffraction were grown by vapor diffusion of hexane into a concentrated solution of dimethoxyethane at room temperature. ^{1}H NMR (C_6D_6): 8.91 (m, 2H, β-*H*), 8.85 (m, 2H, β-*H*), 8.70 (s(broad), 2H, β-*H*), 8.51 (s(broad), 2H, β-*H*), 8.35 (d, *J* = 7.9 Hz, 2H, C_6H_3*H*-OMe), 7.38 (s, 4H, C_6*H*$_2$Me$_3$), 7.25 (d, *J* = 7.9 Hz, 2H, C_6H_3*H*-OMe), 3.57 (s, 3H, OC*H*$_3$), 2.59 (s, 6H, $C_6H_2Me_2$(p-C*H*$_3$)), 2.40 (m, 24H, THF), 2.31 (s, 12H, C_6H_2Me(o-C*H*$_3$)$_2$), 0.79 (qt, *J* = 11.4, 7.2 Hz, 24H, THF). ^{7}Li NMR (C_6D_6, referenced to LiCl in H_2O): -8.40. UV-vis (nm): 422, 446, 587, 626. ESI-MS (+) Calcd: 644.3122 for $C_{44}H_{37}N_4O_1Li_1$, 651.3282 for $C_{44}H_{37}N_4O_1Li_2$ Observed: 644.3189, 651.3557. Mp: decomposition above 350 ºC.

Cyclopentadienyl zirconium(IV) 5,15-bis(2,4,6-trimethylphenyl)-10-(4-methoxyphenyl) corrole (CpZrMes_2(*p*-OMePh)corrole) (**2-2**). Mes_2(*p*-OMePh)corroleLi$_3$·6THF (100 mg, 0.092 mmol), and cyclopentadienyl zirconium(IV) trichloride (36 mg, 0.10 mmol) were combined in a Schlenk flask. The flask was cooled to -40 ºC and 10 mL THF was added by cannula. The solution was allowed to warm to room temperature and stirred overnight. The solvent was removed under vacuum and the resulting solid was taken up in hexane. The solution was cooled to -40 ºC and cannula filtered to generate deep red microcrystals (59 mg, 81 % yield). Crystals suitable for X-ray diffraction were grown by slow evaporation of pentane at -40 ºC. ^{1}H NMR (400 MHz, C_6D_6): δ 8.88 (d, *J* = 4.0 Hz, 2H, β-*H*), 8.84 (d, *J* = 4.3 Hz, 2H, β-*H*), 8.78 (d, *J* = 4.4 Hz, 2H, β-*H*), 8.70 (d, *J* = 4.0 Hz, 2H, β-*H*), 8.33 (dd, *J* = 8.4, 2.3 Hz, 1H, C_6H_3*H*-OMe), 7.62 (dd, *J* = 8.4, 2.3 Hz, 1H, C_6H_3*H*-OMe), 7.39-7.36 (m, 4H, C_6*H*$_2$Me$_3$), 7.29 (dd, *J* = 8.3, 2.7 Hz, 1H, C_6H_3*H*-OMe), 7.00 (dd, *J* = 8.4, 2.8 Hz, 1H, C_6H_3*H*-OMe), 3.52 (s, 3H, OC*H*$_3$), 3.11 (s, 5H, C_5*H*$_5$), 2.60 (s, 6H, $C_6H_2Me_2$C*H*$_3$), 2.53 (s, 6H, $C_6H_2Me_2$C*H*$_3$), 1.44 (s, 6H, $C_6H_2Me_2$C*H*$_3$).^{13}C NMR (101 MHz, C_6D_6): δ 159.84, 144.11, 142.14, 141.65, 139.97, 139.30 (d, *J* = 4.0 Hz), 137.59 (d, *J* = 15.9 Hz), 135.39, 134.76, 128.77, 128.48 (d, *J* = 12.2 Hz), 126.77 (d, *J* = 12.6 Hz), 124.92, 119.51, 117.16, 113.33, 113.03, 110.30, 101.24, 67.27, 55.03, 22.35, 21.60, 20.52. UV-vis (nm): 421, 583. ESI-MS (+) Calcd: 792.2400 for $C_{49}H_{42}O_1N_4Zr_1$ Observed: 792.2426. Mp: decomposition above 350 ºC.

Pentamethylcyclopentadienyl titanium(IV) 5,15-bis(2,4,6-trimethylphenyl)-10-(4-methoxyphenyl)-corrole. (Cp*TiMes_2(*p*-OMePh)corrole) (**2-3**). Mes_2(*p*-OMePh)corroleLi$_3$·6THF (60 mg, 0.055 mmol), and pentamethylcyclopentadienyl titanium(IV)

trichloride (36 mg, 0.061 mmol) were combined in a vial in the glovebox and 6 mL THF was added. The solution was stirred overnight. The solvent was removed under vacuum and the resulting solid was taken up in hexane. The solution was cooled to -40 ºC and filtered to generate deep red microcrystals (29 mg, 78 % yield). Crystals suitable for X-ray diffraction were grown by vapor diffusion of hexane into a concentrated solution of toluene at room temperature. ^{1}H NMR (C_6D_6): δ 8.80 (d, *J* = 4.2 Hz, 2H, β-*H*), 8.76 (d, *J* = 4.5 Hz, 2H, β-*H*), 8.62, (d, *J* = 4.6 Hz, 2H, β-*H*), 8.55 (d, *J* = 4.2 Hz, 2H, β-*H*), 7.56 (d, *J* =8.4 Hz, 1H, C_6H_3*H*-OMe), 7.42 (s, 2H, C_6*H*$_2Me_3$), 7.33 (dd, *J* = 10.6, 4.1 Hz, 1H, C_6H_3*H*-OMe), 7.13 (d, J = 6.2 Hz, 1H, C_6H_3*H*-OMe), 6.94 (dd, 10.6, 4.1 Hz, 1H, C_6H_3*H*-OMe), 6.88 (s, 2H, C_6*H*$_2Me_3$), 3.54 (s, 3H, OC*H*$_3$) 3.26 (s, 6H, $C_6H_2Me_2$C*H*$_3$), 2.44 (s, 6H, $C_6H_2Me_2$C*H*$_3$), 0.45 (s, 6H, $C_6H_2Me_2$C*H*$_3$), -0.05 (s, 15H, C_5(C*H*$_3$)$_5$).UV-vis (nm): 425, 573. ESI-MS (+) Calcd: 820.3615 for $C_{54}H_{52}O_1N_4Ti_1$ Observed: 820.3641. Mp: decomposition above 350 ºC.

Titration of free base corrole with LiN(SiMe$_3$)$_2$

In the glovebox, a 2.0 mM solution of free base corrole (Solution A) was prepared by dissolving 12.8 mg corrole in 10 mL THF. A 30 mM solution of LiN(SiMe$_3$)$_2$ (Solution B) was prepared by dissolving 10.0 mg LiN(SiMe$_3$)$_2$ in 2 mL THF. 0.05 mL A, 0.95 mL THF were measured into a 1 mm quartz Schlenk cuvette and the UV-visible spectrum of the free-base corrole was recorded at 0.1 mM concentration. 3 mL A (0.006 mmol) and 3 mL THF were measured into a vial, and 0.2 mL (0.006 mmol, 1 equiv) B was added. 0.155 mL (0.00015 mmol) of the solution was removed and diluted to 1.5 mL with THF to produce a 0.1 mM solution; the UV-visible spectrum of this solution was recorded. This procedure was repeated in such a manner as to ensure that 1.0 equiv. of LiN(SiMe$_3$)$_2$ was added to the actual amount of corrole remaining in the reaction vial, and that all UV-visible spectra were obtained at 0.1 mM concentration.

Determination of molecular structure by single-crystal X-ray diffraction

X-ray structural determinations were performed on a Bruker MicroSTAR-H APEX II or Bruker APEX II Quazar diffractometer. Both are Kappa Geometry with DX. Both are 3-circle diffractometers that couple a CCD detector[42] with a sealed-tube source of monochromated Cu-Kα (MicroSTAR) or Mo Kα radiation (Quazar). A crystal of appropriate size was coated in Paratone-N oil and mounted on a Kaptan® loop. The loop was transfered to the diffractometer, centered in the beam, and cooled by a nitrogen flow low- temperature apparatus that had been previously calibrated by a thermocouple placed at the same position as the crystal. Preliminary orientation matrices and cell constants were determined by collection of 60 10 s frames, followed by spot integration and least-squares refinement. The reported cell dimensions were calculated from all reflections with $I > 10\ \sigma$. The data were corrected for Lorentz and polarization effects; no correction for crystal decay was applied. An empirical absorption correction based on comparison of redundant and equivalent reflections was applied using SADABS.[43] All software used for diffraction data processing and crystal-structure solution and refinement are contained in the APEX2 program suite (Bruker AXS, Madison, WI).[44] Thermal parameters for all non-hydrogen atoms were refined anisotropically. For all structures, $R_1 = \Sigma(|F_o| - |F_c|)/\Sigma(|F_o|)$; $wR_2 = [\Sigma\{w(F_o^2 - F_c^2)^2\}/\Sigma\{w(F_o^2)^2\}]^{1/2}$. ORTEP diagrams were created using the ORTEP-3 software package and POV-ray.[45]

Table 2.1 shows crystallographic data for corrole complexes **2-1**, **2-2**, and **2-3**.

Table 2.1. Crystallographic data for **2-1·4DME**, **2-2**, and **2-3**.

Compound	**2-1**	**2-2**	**2-3**
Formula	$C_{60}H_{77}Li_3N_4O_9$	$C_{49}H_{42}N_4OZr$	$C_{54}H_{52}N_4OTi$
Form. wt. (amu)	1019.08	794.09	820.90
Wavelength (Å)	1.54178	0.71073	1.54178
Space Group	$P2_1/n$	Pbca	P-1
a (Å)	14.9866(8)	19.2272(9)	10.8502(10)
b (Å)	23.6356(12)	19.8419(10)	14.0504(13)
c (Å)	16.4784(9)	20.2471(9)	14.6264(13)
α (º)	90	90	96.477(4)
β (º)	101.871(4)	90	93.780(4)
γ (º)	90	90	104.095(4)
V (Å^3)	5712.1(5)	7724.4(6)	2138.7(3)
Z	4	8	2
ρ_{calcd} (g/cm^3)	1.185	1.366	1.275
F_{000}	2184	3296	868
μ (mm^{-1})	0.623	0.328	2.037
$\theta_{min}/\theta_{max}$	3.32/67.77	1.79/26.18	3.06/68.13
Refl'ns collected	55039	127751	34085
Indep. refl'ns	10121	7116	7564
R_{int}	0.0391	0.0784	0.0255
R_1, wR_2	0.0693/0.1905	0.0354/0.0781	0.0418/0.1153
R_1, (all data)	0.0879	0.0598	0.0435
GoF	1.036	1.044	1.043
Res. peak/hole (e$^-$/ Å^3)	0.688/-0.363	0.345/-0.560	0.282/-0.333

References

(1) *The Porphyrin Handbook*; Kadish, K. M.; Smith, K. M.; Guilard, R., Eds.; Academic Press: New York, 2004.
(2) Brand, H.; Arnold, J. *Coord. Chem. Rev.* **1995**, *140*, 137–168.
(3) Saveant, J. M. *Chem. Rev.* **2008**, *108*, 2348–2378.
(4) Zagal, J. H.; Griveau, S.; Silva, J.; Nyokong, T.; Bedioui, F. *Coord. Chem. Rev.* **2010**, *254*, 2755–2791.
(5) Stefanelli, M.; Nardis, S.; Tortora, L.; Fronczek, F. R.; Smith, K. M.; Licoccia, S.; Paolesse, R. *Chem. Commun.* **2011**, *47*, 4255–4257.
(6) Pierloot, K.; Zhao, H.; Vancoillie, S. *Inorg. Chem.* **2010**, *49*, 10316–10329.
(7) Prathapan, S.; Johnson, T. E.; Lindsey, J. S. *J. Am. Chem. Soc.* **1993**, *115*, 7519–7520.
(8) Keinan, S.; Therien, M. J.; Beratan, D. N.; Yang, W. *J. Phys. Chem. A* **2008**, *112*, 12203–12207.
(9) Paolesse, R.; Mini, S.; Sagone, F.; Boschi, T.; Jaquinod, L.; Nurco, D. J.; Smith, K. M. *Chem. Commun.* **1999**, *2*, 1307–1308.
(10) Koszarna, B.; Gryko, D. T. *J. Org. Chem.* **2006**, *71*, 3707–3717.
(11) Gross, Z.; Galili, N.; Saltsman, I. *Angew. Chem. Int. Ed.* **1999**, *38*, 1427–1429.
(12) Aviv-Harel, I.; Gross, Z. *Coord. Chem. Rev.* **2010**, *255*, 717–736.
(13) Simkhovich, L.; Galili, N.; Saltsman, I.; Goldberg, I.; Gross, Z. *Inorg. Chem.* **2000**, *39*, 2704–2705.
(14) Luobeznova, I.; Simkhovich, L.; Goldberg, I.; Gross, Z. *Eur. J. Inorg. Chem.* **2004**, 1724–1732.
(15) Thomas, K. E.; Wasbotten, I. H.; Ghosh, A. *Inorg. Chem.* **2008**, *47*, 10469–10478.
(16) Aviv-Harel, I.; Gross, Z. *Chem. Eur. J.* **2009**, *15*, 8382–8394.
(17) Palmer, J. H. *Struct. Bond.* **2012**, *142*, 49–90.
(18) Thomas, K. E.; Alemayehu, A. B.; Conradie, J.; Beavers, C. M.; Ghosh, A. *Acc. Chem. Res.* **2012**, *45*.
(19) Palmer, J. H.; Durrell, A. C.; Gross, Z.; Winkler, J. R.; Gray, H. B. *J. Am. Chem. Soc.* **2010**, *132*, 9230–9231.
(20) Alemayehu, A. B.; Ghosh, A. *J. Porphyrins Phthalocyanines* **2011**, *15*, 106–110.
(21) Rabinovich, E.; Goldberg, I.; Gross, Z. *Chem. Eur. J.* **2011**, *17*, 12294–12301.
(22) Thomas, K. E.; Alemayehu, A. B.; Conradie, J.; Beavers, C.; Ghosh, A. *Inorg. Chem.* **2011**, *50*, 12844–12851.
(23) Schöfberger, W.; Lengwin, F.; Reith, L. M.; List, M.; Knör, G. *Inorg. Chem. Commun.* **2010**, *13*, 1187–1190.
(24) Reith, L. M.; Himmelsbach, M.; Schoefberger, W.; Knör, G. *J. Photochem. Photobiol., A* **2011**, *218*, 247–253.
(25) Licoccia, S.; Paolesse, R.; Tassoni, E.; Poliziob, F. *J. Chem. Soc., Dalt. Trans.* **1995**, 3617–3621.
(26) Rothemund, P.; Menotti, A. M. *J. Am. Chem. Soc.* **1948**, *70*, 1808.
(27) Dorough, G. D.; Miller, J. R.; Huennekens, F. M. *J. Am. Chem. Soc.* **1951**, *73*, 4315.
(28) Allison, J. B.; Becker, R. S. *J. Phys. Chem.* **1963**, *67*, 2675.
(29) Arnold, J.; Dawson, D. Y.; Hoffman, C. G. *J. Am. Chem. Soc.* **1993**, *115*, 2707–2713.
(30) Brand, H.; Arnold, J. *Organometallics* **1993**, *12*, 3655–3665.
(31) Brand, H.; Capriotti, J. A.; Arnold, J. *Organometallics* **1994**, *13*, 4469–4473.

(32) Brand, H.; Arnold, J. *Angew. Chem. Int. Ed. Engl.* **1994**, *33*, 95–97.
(33) Reith, L. M.; Stiftinger, M.; Monkowius, U.; Knör, G.; Schoefberger, W. *Inorg. Chem.* **2011**, *50*, 6788–6797.
(34) Gryko, D. T.; Piechota, K. E. *J. Porphyrins Phthalocyanines* **2002**, *6*, 81–97.
(35) Arnold, J. In *The Porphyrin Handbook*; Kadish, K. M.; Smith, K. M.; Guilard, R., Eds.; Academic Press: New York, 1999; pp. 113–128.
(36) Nigel-Etinger, I.; Goldberg, I.; Gross, Z. *Inorg. Chem.* **2012**, *51*, 1983–1985.
(37) Luobeznova, I.; Raizman, M.; Goldberg, I.; Gross, Z. *Inorg. Chem.* **2006**, *45*, 386–394.
(38) Meier-Callahan, A. E.; Gray, H. B.; Gross, Z. *Inorg. Chem.* **2000**, *39*, 3605–3607.
(39) Alaimo, P. J.; Peters, D. W.; Arnold, J.; Bergman, R. G. *J. Chem. Ed.* **2001**, *78*, 64.
(40) Amonoo-Neizer, E. H.; Shaw, R. A.; Skovlin, D. O.; Smith, B. C.; Rosenthal, J. W.; Jolly, W. L. *Inorg. Synth.* **1966**, *8*, 19–22.
(41) Laha, J. K.; Dhanalekshmi, S.; Taniguchi, M.; Ambroise, A.; Lindsey, J. S. *Org. Proc. Res. Dev.* **2003**, *7*, 799–812.
(42) SMART: Area Detector Software Package Bruker Analytic X-ray Systems I. Madison WI. SMART: Area Detector Software Package, Bruker Analytic X-ray Systems I. Madison, WI, 2003.
(43) SADABS: Bruker-Nonius Area Detector Scaling and Absorption V2.05 Bruker Analytical X-ray System, I. Madison, WI, 2003.
(44) Sheldrick, G. M. *Acta. Crystallogr. A*. **2008**, *64*, 112.
(45) Farrugia, L. J. *Appl. Crystallogr.* **1997**, *30*, 565.

Chapter 3: Lanthanide Corroles: A New Class of Macrocyclic Lanthanide Complexes

Introduction

Lanthanide complexes and nanomaterials are used extensively in biological imaging and analyses due to the confluence in these metals of low toxicity and interesting photophysical properties. Chelating organic ligands often serve as vehicles for lanthanides in imaging agents because they can serve as the chromophore while maintaining solution stability and preventing coordination of quenching moieties (e.g., water).[1–6] For these reasons, strongly absorbing ligand scaffolds such as conjugated macrocycles are of great interest for lanthanide complex construction.[3,7–9]

Extensive work has been done in the preparation and characterization of lanthanide porphyrin complexes,[10,11] which were first synthesized in the 1970s for use as NMR shift reagents.[8] Single porphyrin, double-decker porphyrin, and supramolecular complexes are known.[10,12–16]

In contrast to lanthanide porphyrins, there have been no examples of lanthanide corroles reported to-date. This is unsurprising given that good methods for the preparation of free-base corroles have existed for just over a decade;[17,18,19] this breakthrough has led to a flurry of activity in which late transition metal, main group, [20–26] and, recently, alkali metal as well as early transition metal corroles have been isolated and characterized.[27] The relatively small size of the corrole cavity forces larger metals to sit quite far (up to 1.144 Å) out of the N_4 plane; this is exemplified in recent examples of iridium,[28] gold,[29–31] lead[32] and bismuth[33] complexes.

Here we present two methods for the preparation of lanthanide corroles. The first is from free-base corrole and lanthanide silyl amides, and the second is by metathesis of the recently reported lithium corrole[27] and the metal chloride.

Results and Discussion

Combination of the free base 10-(4-methoxyphenyl)-5,15-dimesitylcorrole ((Mes$_2$(*p*-OMePh)corrole)H$_3$) with 1.1 equivalents of La(N(SiMe$_3$)$_2$)$_3$[34] at room temperature in THF leads to an immediate colour change from deep purple to a deep green solution. Stirring of this solution overnight, removal of the solvent under vacuum and recrystallization of the solid by vapour diffusion at room temperature (1,2-dimethoxyethane (DME)/hexanes) provided dark purple plates from a dark green solution that were suitable for characterization by X-ray crystallography (58 % yield). Complex (**3-1·4.5DME**) (Scheme 3.1a) has been characterized by ^{1}H NMR and UV-visible spectroscopies and ESI mass spectrometry (See Experimental Details).

The crystal structure of lanthanum corrole **3-1·4.5DME** is shown in Figure 3.1. The lanthanum atom is located 1.469 Å outside of the N_4 plane of the corrole with an average N-La bond distance of 2.438(6) Å. This is the largest metal-N_4 plane separation recorded for a corrole complex to-date, with the previous record held by a recently reported bismuth(III) corrole structure at 1.144 Å.[35] This separation is also consistent with the κ^2-coordination of the La atom by two molecules of DME; excepting cases with η^5-Cp$^{(*)}$ as a capping ligand, there are no examples of metallocorrole complexes where the coordination number at the metal exceeds six.[24]

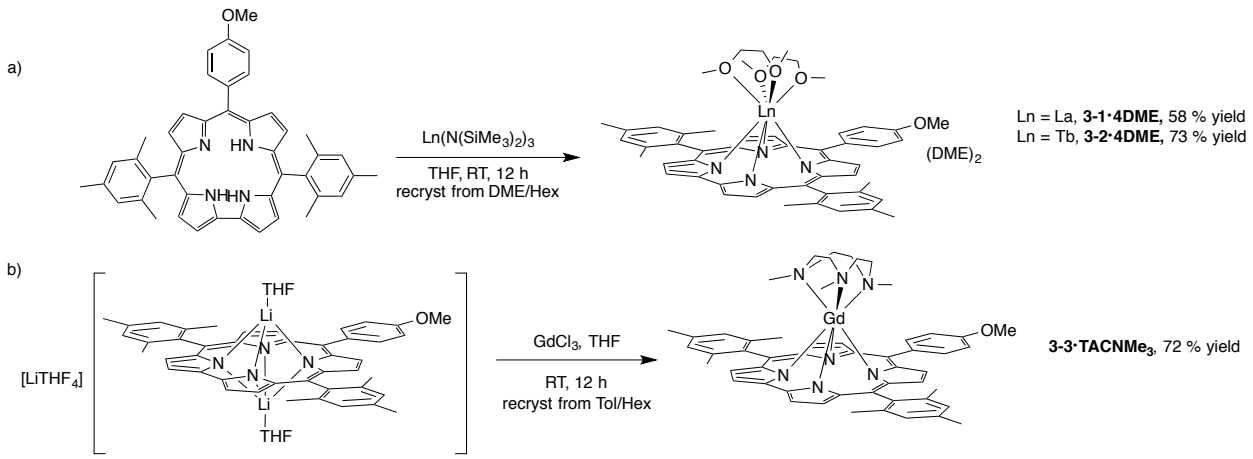

Scheme 3.1 Synthesis of a) lanthanum(III) corrole **3-1·4.5DME** and terbium(III) corrole **3-2·4DME** b) gadolinium(III) corrole **3-3·TACNMe$_3$**.

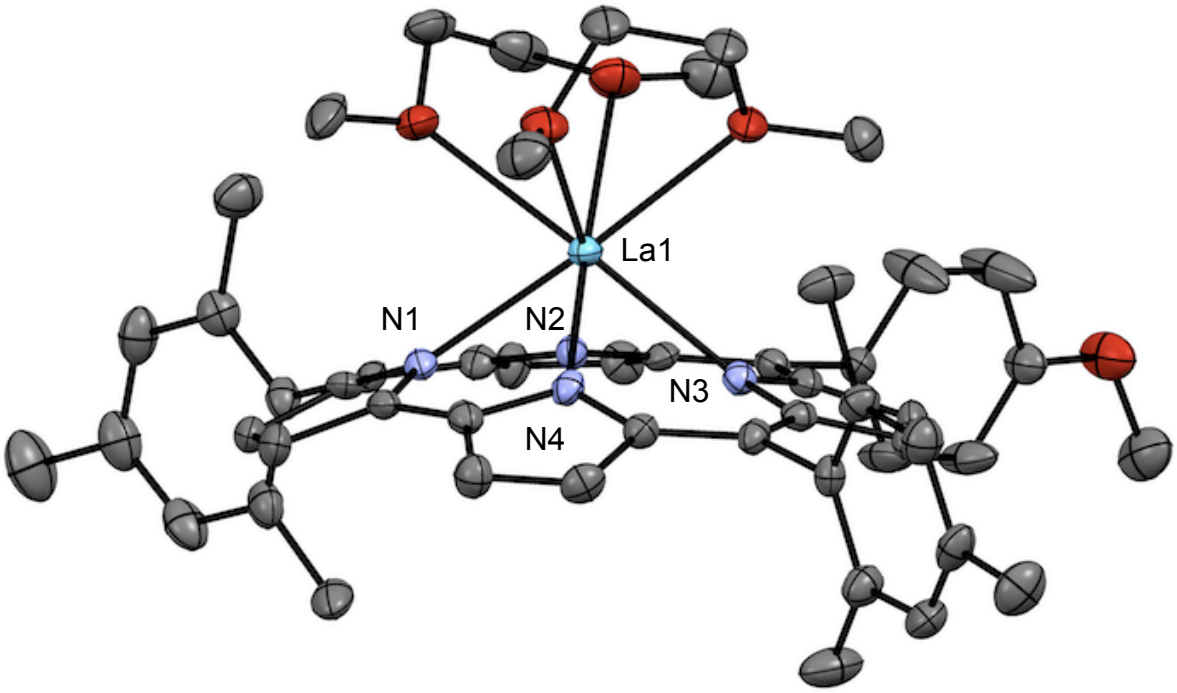

Figure 3.1 Molecular structure of lanthanum corrole **3-1·4.5DME**, determined by single-crystal X-ray diffraction. H atoms and non-coordinated solvent omitted for clarity; thermal ellipsoids at 50 % probability level.

The terbium(III) corrole complex (Mes_2(*p*-OMePh)corrole)Tb·4DME (**3-2·4DME**) was prepared in a manner analogous to **3-1·4.5DME** in 72 % yield. The complex has been characterized by UV-visible spectroscopy, ESI mass spectrometry, and X-ray crystallography (See Experimental Details). ESI MS shows peaks consistent with the incorporation of two atoms of oxygen (corroleTbO_2H^+, calculated 829.2192, observed 829.2198) as well as the coordination one and two molecules of THF to this species, consistent with the availability of adventitious oxygen in the spectrometer and the use of THF to prepare solutions for ESI MS. The crystal structure of **3-2·4DME** is shown in Figure 3.2 and shows a Tb-N_4 plane distance of 1.272 Å, consistent with the smaller ionic radius of Tb(III) as compared to La(III). The two DME molecules coordinated to the Tb are disordered and are modeled isotropically.

The gadolinium(III) corrole complex (Mes_2(*p*-OMePh)corrole)Gd·$TACNMe_3$ (**3-3·TACNMe$_3$**) was prepared by the combination in THF at room temperature of (Mes_2(*p*-OMePh)corrole)Li_3·6THF with 1.1 equivalents of $GdCl_3$ and 1.0 equivalents of 1,4,7-trimethyl-1,4,7-triazacyclononane ($TACNMe_3$) (Scheme 3.1b). Stirring overnight results in a dark green solution. Removal of the solvent and recrystallization of the solid by vapour diffusion at room temperature (toluene/hexane) yields crystals suitable for X-ray diffraction (73 % yield). This species has been characterized by UV-visible spectroscopy and ESI MS (see Experimental Details). The crystal structure of **3-3·TACNMe$_3$** is shown in Figure 3.3 and shows a Gd-N_4 plane distance of 1.262 Å. The structure shows seven-fold coordination of the Gd, which like the La complex is a higher coordination number than previously observed for corroles, but consistent with other lanthanide complexes and with the distance of the metal centre from the N_4 plane.

In addition to the three isolated lanthanide(III) corrole complexes, the three analogues with complementary ligands were prepared *in situ* for comparison by UV-visible spectroscopy. Thus, UV-visible spectra of **3-1·4.5DME**, **3-1·TACNMe$_3$**, **3-2·4DME**, **3-2·TACNMe$_3$**, **3-3·nTHF**, and **3-3·TACNMe$_3$** were obtained in THF (THF likely undergoes rapid exchange with DME, thus the spectra are of THF rather than DME adducts). The spectra for **3-2·4DME** and **3-2·TACNMe$_3$** are unremarkable; both Tb(III) complexes display identical spectra with a single Soret peak at 433 nm and three Q-peaks at 541, 580, and 611 nm. A single Soret band is consistent with the spectra of other metallocorroles with the metal sitting outside of the plane, including Al,[36] Ga,[37,38] and Zr.[27] However, the spectra for the La and Gd complexes are more interesting; both display a single Soret peak in the presence of only DME/THF as ancilliary ligands, but display two Soret peaks in the presence of $TACNMe_3$ and a spectrum essentially identical to that of (Mes_2(*p*-OMePh)corrole)Li_3·6THF. The latter situation is also consistent with sterically hindered (i.e. mesityl-susbsituted) free-base corroles[39] that have retained planarity in solution; this data suggests that the corrole rings in **3-1·TACNMe$_3$** and **3-3·TACNMe$_3$** may be roughly planar in solution.

The ^{1}H NMR spectrum of **3-1·4.5DME** was obtained in d_8-toluene at room temperature, and it was found that all corrole peaks at this temperature are broad and the number of peaks exceeds the number anticipated. This is attributed largely to rapid exchange of the DME ligands. Variable temperature (VT) NMR was used to determine that the broadening is exacerbated in the case of the aromatic protons of the *p*-methoxyphenyl ring at the 10-position of the corrole; the barrier to rotation of this ring relative to the corrole is low but significant at room temperature. At lower temperatures (263 K) some sharpening of the peaks is observed and it is possible to see doublets

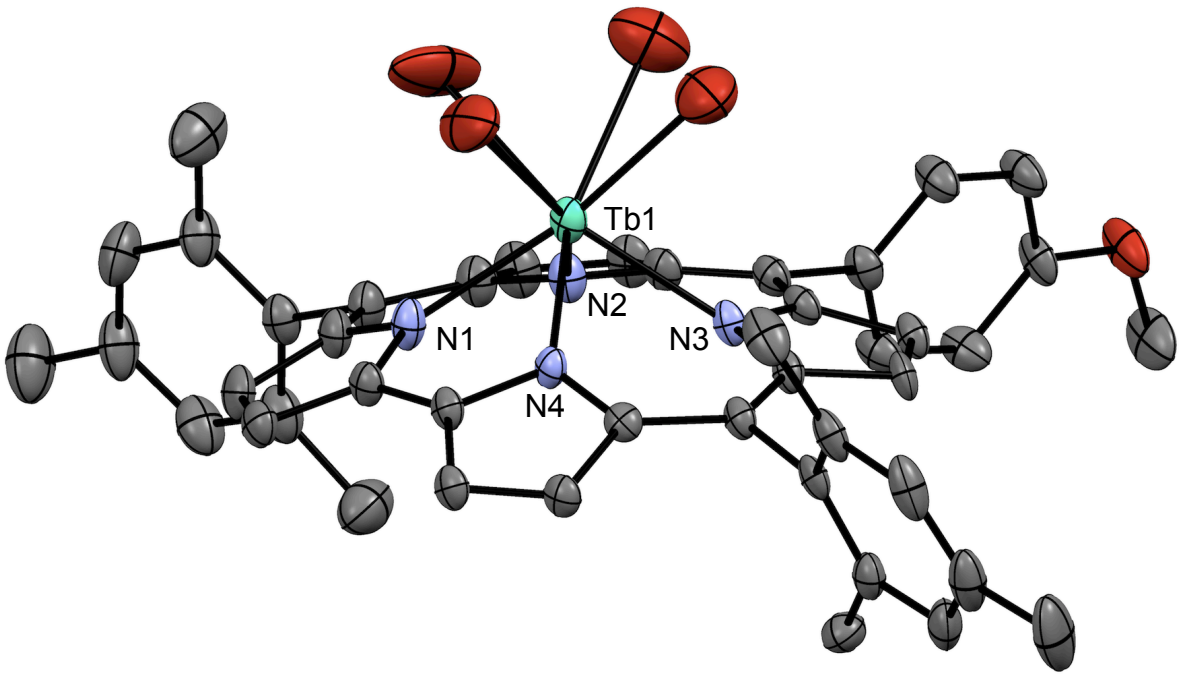

Figure 3.2. Molecular structure of terbium(III) corrole **2·4DME** determined by single-crystal X-ray diffraction. H atoms and solvent molecules except for coordinated O atoms have been omitted for clarity; thermal ellipsoids at 50 % probability level.

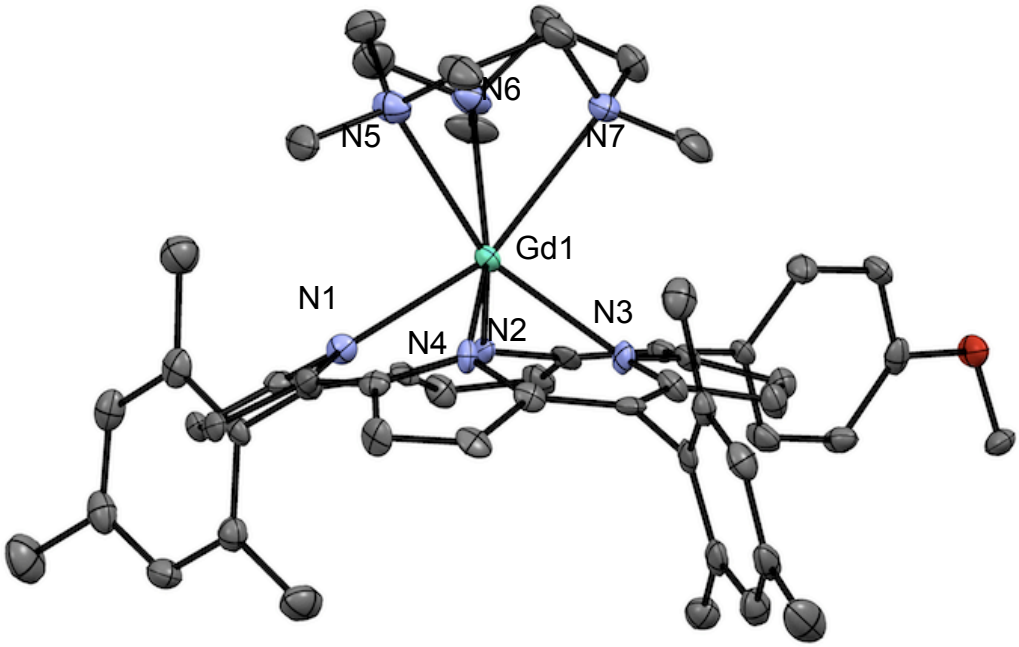

Figure 3.3. Molecular structure of gadolinium corrole **3-3·TACNMe$_3$**, determined by single-crystal X-ray diffraction. H atoms and non-coordinated solvent omitted for clarity; thermal ellipsoids at 50 % probability level.

partially resolved for the β-*H*s, as well as sharpening of some of the aromatic *p*-methoxyphenyl peaks as non-equivalent peaks with an integration of 1 H each. The symmetric inequivalence of these peaks is consistent with the structure observed by X-ray crystallography, where the aryl rings clearly sit out of the plane of the corrole. At high temperatures, all peaks become too broad to provide any useful data. Figure 3.4 shows VT NMR spectra for **3-1·4DME**.

To complement the variable temperature NMR spectroscopy performed on **3-1·4.5DME** and to confirm that a single species has in fact been isolated, a slight excess of $TACNMe_3$ was added to an NMR tube containing **3-1·4.5DME**. At room temperature, the main result of the addition was a considerable sharpening of the peaks in the aromatic region and the clear emergence of only four β-*H* doublets and two aromatic singlets from the mesityl groups at room temperature. At 323 K, both the ortho- and meta- protons of the *p*-methoxyphenyl ring were observed to coalesce into doublets, confirming that their apparent absence at room temperature was indeed due to the moderate barrier to rotation of that ring. Figure 3.5 shows VT NMR spectra for **3-1·TACNMe$_3$** and the peaks at room temperature are reported in the Experimental Details.

Conclusion

In summary, the first examples of lanthanide corrole complexes (of La, Gd, and Tb) have been prepared by two routes and have been characterized spectroscopically and structurally. In addition to salt-metathesis chemistry, the amine-elimination route shown here provides a further attractive avenue to prepare new metallocorrole complexes. Given the large molar absorption coefficient of corrole ligand and the possibility to use various excitation wavelengths, this strategy has the potential to be used for sensitization of NIR-emitting lanthanide cations. Efforts are underway to extend this methodology across the lanthanide series and to explore the use of these materials as fluorescence imaging agents.

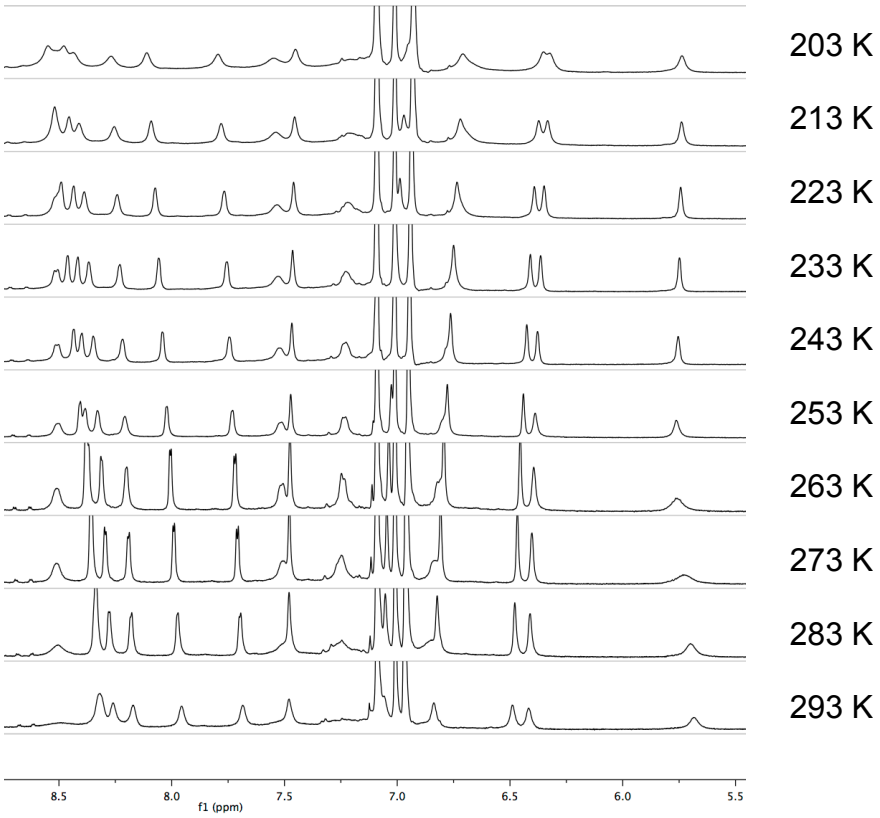

Figure 3.4. ^{1}H NMR spectra of **3-1·4.5DME** in d_8-toluene at variable temperatures.

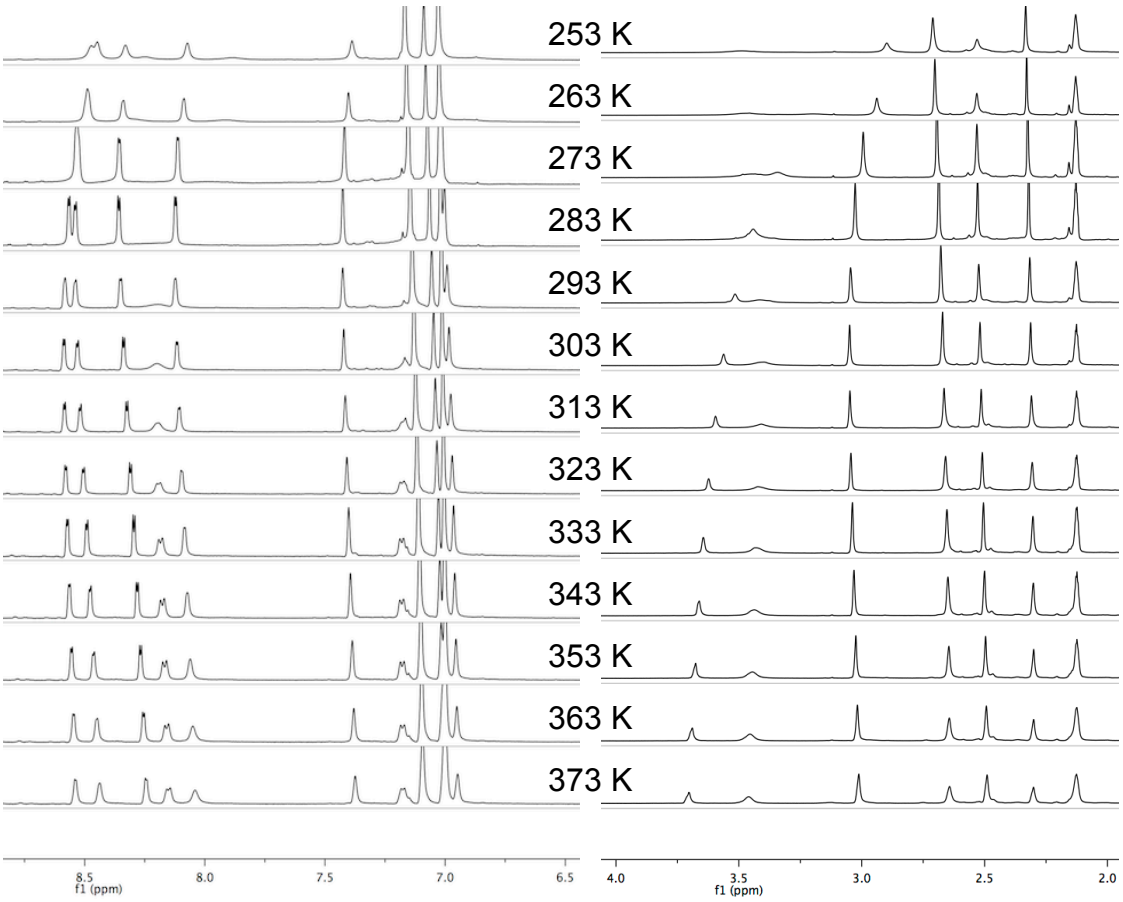

Figure 3.5. ^{1}H NMR spectra of **3-1·TACNMe$_3$** in d_8-toluene at variable temperatures (left and right spectra at different vertical scales to optimize peak visibility).

Experimental Details

General Considerations

All reactions were performed using standard Schlenk and N_2-atmosphere glovebox techniques. Glassware was stored in an oven at *ca.* 180 ºC. Solvents were dried by passing through a column of activated alumina and degassed with nitrogen.[40] d_8-Toluene was dried over Na/benzophenone, and vacuum transferred. NMR spectra were obtained in d_8-toluene at the specified temperature using a Bruker DRX 500 spectrometer. Temperature calibration was performed using changes in chemical shift separation of ethylene glycol at high temperature and methanol at low temperature. ^{1}H NMR chemical shifts (δ) were calibrated relative to residual solvent peak. UV-visible spectra were determined with a Varian Cary 50 UV-vis spectrophotometer using a 1 mm quartz cell. Mass spectral data (ESI-MS, positive mode) were obtained at the University of California, Berkeley Microanalytical Facility, using vacuum-dried samples dissolved in dry THF. X-ray crystal diffraction analyses were performed at the University of California, Berkeley CHEXRAY facility. Melting points were determined using sealed capillaries prepared under nitrogen and are uncorrected.

5,15-bis(2,4,6-trimethylphenyl)-10-(4-methoxyphenyl)corrole (Mes_2(*p*-OMePh) corroleH_3) and trilithium 5,15-bis(2,4,6-trimethylphenyl)-10-(4-methoxyphenyl)corrole hexakis (tetrahydrofuran) (Mes_2(*p*-OMePh)corroleLi_3·6THF) were prepared according to previously reported procedures.[27] 1,4,7-trimethyl-1,4,7-triazacyclononane ($TACNMe_3$) was obtained from Sigma Aldrich and purified by vacuum distillation from calcium hydride. La($(NSiMe_3)_2)_3$ was obtained from Alfa Aesar, Tb($(NSiMe_3)_2)_3$ was obtained from Gelest, and $GdCl_3$ was obtained from Strem and used as received.

Synthesis and Characterization of Complexes 3-1, 3-2 and 3-3

Lanthanum(III) 5,15-bis(2,4,6-trimethylphenyl)-10-(4-methoxyphenyl)corrole tetrakis-dimethoxyethane (3-1·4.5DME). Mes_2(*p*-OMePh)corroleH_3 (100 mg, 0.16 mmol) La($(NSiMe_3)_2)_3$ (107 mg, 1.1 equiv, 0.17 mmol) and 10 mL THF were combined in a vial in the glovebox. The solution was stirred overnight. The solvent was removed under vacuum and the solid was dissolved in a minimum amount of dimethoxyethane (~2 mL) and filtered. Crystals suitable for X-ray diffraction were grown by vapor diffusion of hexane into a concentrated solution of dimethoxyethane at room temperature (102 mg, 58 %). ^{1}H NMR (d_8-toluene, room temperature, note some peaks are partially coalesced at this temperature, see VT studies in SI. Assignments are based upon VT experiments): 8.50 (broad s, 1H, C_6H_3*H*OMe), 8.32 (s, 4H), 8.26 (s, 2H, β-*H*), 8.17 (s, 2H, β-*H*), 7.96 (s, 2H, β-*H*), 7.68 (s, 2H, β-*H*), 7.48 (s with shoulder, 3H, C_6HMe_3*H* and C_6H_3*H*OMe), 7.06 (s, masked), 6.84 (s, 2H), 6.49 (s, 2H), 6.42 (s, 2H), 5.68, (s, 1H, C_6H_3*H*OMe), 3.50 (s, 6H), 3.26 (s, 6H), 2.17 (s, 6H), 1.82 (s, 6H), 1.29 (masked), 1.25-1.10 (broad, masked). UV-vis (nm): 438, 545, 585, 619. ESI-MS (+) Calcd: 766.2025 for $C_{44}H_{37}N_4O_1La_1$, Observed: 776.2013. Mp: decomposition above 350 ºC.

Lanthanum(III) 5,15-bis(2,4,6-trimethylphenyl)-10-(4-methoxyphenyl) corrole·1,4,7-trimethyl-1,4,7-triazacyclononane (3-1·TACNMe$_3$) was prepared *in situ* from Mes_2(*p*-OMePh)corroleH_3 (25 mg, 0.039 mmol), La($(NSiMe_3)_2)_3$ (27 mg, 1.1 equiv, 0.043 mmol) and

$TACNMe_3$ (7.0 μL, 6.1 mg, 1.0 equiv, 0.043 mmol) in the same manner as **3-1·4DME** above for UV-visible characterization but was not isolated. UV-vis (nm): 423, 446, 588, 636.

Terbium(III) 5,15-bis(2,4,6-trimethylphenyl)-10-(4-methoxy phenyl) corrole·tetrakis-dimethoxyethane (**3-2·4DME**) was prepared from Mes_2(*p*-OMePh)corroleH_3 (50 mg, 0.078 mmol) and $Tb((NSiMe_3)_2)_3$ (55 mg, 1.1 equiv, 0.086 mmol) and crystals for X-ray diffraction grown in the same manner as **1·4DME** from (65 mg, 72 %). UV-vis (nm): 433, 541, 580, 611. ESI-MS (+) Calcd: 829.2192 for $C_{44}H_{38}N_4O_3Tb_1$ (corroleTbO_2H^+), 901.2767 for $C_{48}H_{46}N_4O_4Tb_1$ (corroleTbO_2H^+·THF), 973.3342 for $C_{52}H_{54}N_4O_5Tb_1$ (corroleTbO_2H^+·2THF) Observed: 829.2198, 901.2771, 973.3342. Mp: decomposition above 350 ºC.

Terbium(III) 5,15-bis(2,4,6-trimethylphenyl)-10-(4-methoxyphenyl) corrole·1,4,7-trimethyl-1,4,7-triazacyclononane (**3-2·TACNMe$_3$**) was prepared *in situ* from Mes_2(*p*-OMePh)corroleH_3 (10 mg, 0.016 mmol), $Tb((NSiMe_3)_2)_3$ (11 mg, 1.1 equiv, 0.017 mmol) and $TACNMe_3$ (2.8 μL, 2.4 mg, 1.0 equiv, 0.016 mmol) in the same manner as **3-1·4DME** for UV-visible characterization but was not isolated. UV-vis (nm): 433, 541, 580, 611.

Gadolinium(III) 5,15-bis(2,4,6-trimethylphenyl)-10-(4-methoxyphenyl) corrole·1,4,7-trimethyl-1,4,7-triazacyclononane (**3-3·TACNMe$_3$**). Mes_2(*p*-OMePh)corroleLi_3·6THF (75 mg, 0.069 mmol), gadolinium(III) trichloride (20 mg, 0.076 mmol), $TACNMe_3$ (12.2 μL, 10.8 mg, 0.069 mmol) and 10 mL THF were combined in a vial in the glovebox. The solution was stirred overnight. The solvent was removed under vacuum and the solid was dissolved in a minimum amount of toluene (~2 mL) and filtered. Crystals suitable for X-ray diffraction were grown by vapor diffusion of hexane into a concentrated solution of toluene at room temperature (53 mg, 73 %). UV-vis (nm): 423, 445, 586, 634. ESI-MS (+) Calcd: 967.4017 for $C_{53}H_{59}O_1N_7Gd_1$ (corroleGdTACNMe$_3$H$^+$) Observed: 967.4043. Mp: decomposition above 350 ºC.

Gadolinium(III) 5,15-bis(2,4,6-trimethylphenyl)-10-(4-methoxyphenyl) corrole·nTHF (**3-3·nTHF**) was prepared *in situ* from Mes_2(*p*-OMePh)corroleLi_3·6THF (8 mg, 0.007 mmol), and gadolinium(III) trichloride (3 mg, 0.008 mmol) in the same manner as **3-1·4DME** for UV-visible characterization but was not isolated. UV-vis (nm): 422, 633.

Variable Temperature NMR experiments

A J-Young NMR tube containing ~20 mg **3-1·4.5DME** in d_8-toluene was prepared in the glove box. ^{1}H NMR spectra were obtained at temperatures from 203 K to 323 K. Spectra for the aromatic region at temperatures from 203 K to 293 K are shown in Figure 3.4. Above this temperature peaks were too broad to provide useful information.

To this same tube was added a slight excess (~3.5 μL) of $TACNMe_3$). ^{1}H NMR spectra of the resulting solution were obtained at temperatures from 253 K to 373 K. ^{1}H NMR (d_8-toluene, room temperature): δ 8.53 (d, *J* = 3.8 Hz, 2H, β-*H*), 8.49 (d, *J* = 4.1 Hz, 2H, β-*H*), 8.30 (d, *J* = 4.1 Hz, 2H, β-*H*), 8.21 – 8.10 (br s, 1H, *becomes sharp at high T*), 8.07 (d, *J* = 3.7 Hz, 2H, β-*H*), 7.38 (s, 2H, C_6HMe_3*H*), 6.94 (s, 2H, C_6HMe_3*H*), 3.47 (s, 3H, C_6H_4OC*H*$_3$), 3.37 (broad s, *becomes sharp at high T*), 3.00 (s, 6H), 2.63 (s, 9H, TACNC*H*$_3$), 2.48 (s, 6H), 2.27 (s, 6H), 0.66

(s, 6H), 0.20 (s, 12H), 0.08 (s, 6H), 0.05 – -0.10 (m, 12H, $TACNMe_3$). Figure 3.5 shows spectra for the aromatic region from 253 K to 373 K.

Determination of molecular structure by single-crystal X-ray diffraction

X-ray structural determinations were performed on a Bruker APEX II Quazar diffractometer. The instrument is Kappa Geometry with DX. And is a 3-circle diffractometer that couples a CCD detector[41] with a sealed-tube source of monochromated Mo Kα radiation. A crystal of appropriate size was coated in Paratone-N oil and mounted on a Kaptan® loop. The loop was transfered to the diffractometer, centered in the beam, and cooled by a nitrogen flow low-temperature apparatus that had been previously calibrated by a thermocouple placed at the same position as the crystal. Preliminary orientation matrices and cell constants were determined by collection of 60 10 s frames, followed by spot integration and least-squares refinement. The reported cell dimensions were calculated from all reflections with $I > 10\ \sigma$. The data were corrected for Lorentz and polarization effects; no correction for crystal decay was applied. An empirical absorption correction based on comparison of redundant and equivalent reflections was applied using SADABS.[42] All software used for diffraction data processing and crystal-structure solution and refinement are contained in the APEX2 program suite (Bruker AXS, Madison, WI).[43] Thermal parameters for all non-hydrogen atoms were refined anisotropically. For all structures, $R_1 = \Sigma(|F_o| - |F_c|)/\Sigma(|F_o|)$; $wR_2 = [\Sigma\{w(F_o^2 - F_c^2)^2\}/\Sigma\{w(F_o^2)^2\}]^{1/2}$. ORTEP diagrams were created using the ORTEP-3 software package and POV-ray.[44]

Table 3.1 shows crystallographic data for corrole complexes **3-1·4.5DME**, **3-2·4DME**, and **3-3·TACNMe$_3$**. The formula given for **3-1·4.5DME** is in fact that of **3-1·3DME** because the residual 1.5 molecules of DME per formula unit were highly disordered and were solved using Squeeze[45] methodology in WinGX. **3-3·TACNMe$_3$** was solved as a twin.

Table 3.1. Crystallographic data for **3-1·4DME**, **3-2·4DME**, and **3-3·TACNMe$_3$**.

Compound	**3-1·4DME**	**3-2·4DME**	**3-3·TACNMe$_3$**
Formula	$C_{56}H_{67}La_1N_4O_7$	$C_{60}H_{57}N_4O_9Tb_1$	$C_{60}H_{66}GdN_7O_1$
Form. wt. (amu)	1047.05	1137.02	1058.45
Wavelength (Å)	0.71073	0.71073	0.71073
Space Group	P-1	P-1	$P2_1/c$
a (Å)	10.9588(9)	11.6378(8)	19.4694(10)
b (Å)	15.2867(13)	15.7546(10)	13.2999(7)
c (Å)	19.8423(15)	15.8507(11)	21.7953(12)
α (º)	68.450(3)	95.090(3)	90
β (º)	88.921(3)	101.785(3)	114.652(2)
γ (º)	83.803(3)	100.993(3)	90
V (Å^3)	3072.9(4)	2768.0(3)	5129.3(5)
Z	2	2	4
ρ_{calcd} (g/cm^3)	1.132	1.388	1.371
F_{000}	1088	1204	2188
μ (mm^{-1})	0.741	1.337	1.341
$\theta_{min}/\theta_{max}$	1.46/25.46	1.33/25.52	1.84/25.37
Refl'ns collected	35604	10176	15792
Indep. refl'ns	11189	10139	9415
R_{int}	0.0673	0.0498	0.0676
R_1, wR_2	0.0483/0.0982	0.0643/0.1520	0.0587/0.1322
R_1, (all data)	0.0715	0.0759	0.1067
GoF	1.015	1.072	1.099
Res. peak/hole (e$^-$/ Å^3)	1.132/-0.586	3.073/-2.057	2.159/-1.313

*Structure was solved as a twin

References

(1) Bünzli, J.-C. G. *Acc. Chem. Res.* **2006**, *39*, 53–61.
(2) Bünzli, J.-C. G. *Chem. Rev.* **2010**, *110*, 2729–2755.
(3) Parker, D.; Dickins, R.; Puschmann, H. *Chem. Rev.* **2002**, *102*, 1977–2010.
(4) Richardson, F. S. *Chem. Rev.* **1982**, *82*, 541–552.
(5) Moore, E. G.; Samuel, A. P. S.; Raymond, K. N. *Acc. Chem. Res.* **2009**, *42*, 542–552.
(6) Das, G. K.; Tan, T. T. T. *J. Phys. Chem. C* **2008**, *112*, 11211–11217.
(7) Alexander, V. *Chem. Rev.* **1995**, *95*, 273–342.
(8) Horrocks, W. D., J.; Wong, C. P. *J. Am. Chem. Soc.* **1976**, *98*, 7157–7162.
(9) Khalil, G. E.; Thompson, E. K.; Gouterman, M.; Callis, J. B.; Dalton, L. R.; Turro, N. J.; Jockusch, S. *Chem. Phys. Lett.* **2007**, *435*, 45–49.
(10) Jiang, J.; Ng, D. K. P. *Acc. Chem. Res.* **2009**, *42*, 79–88.
(11) Zhu, X.; Wong, W.-K.; Wong, W.-Y.; Yang, X. *Eur. J. Inorg. Chem.* **2011**, *2011*, 4651–4674.
(12) Moussavi, M.; De Cian, A.; Fischer, J.; Weiss, R. *Inorg. Chem.* **1986**, *25*, 2107–2108.
(13) Buchler, J. W.; Kapellmann, H.-G.; Knoff, M.; Lay, K.-L.; Pfeifer, S. *Z. Naturforsch. B* **1983**, *38*, 1339–1345.
(14) George, S.; Lipstman, S.; Goldberg, I. *Cryst. Growth Des.* **2006**, *6*, 2651–2654.
(15) Ishikawa, N.; Kaizu, Y. *Coord. Chem. Rev.* **2002**, *226*, 93–101.
(16) Gross, T.; Chevalier, F.; Lindsey, J. S. *Inorg. Chem.* **2001**, *40*, 4762–4774.
(17) Paolesse, R.; Mini, S.; Sagone, F.; Boschi, T.; Jaquinod, L.; Nurco, D. J.; Smith, K. M. *Chem. Commun.* **1999**, *2*, 1307–1308.
(18) Koszarna, B.; Gryko, D. T. *J. Org. Chem.* **2006**, *71*, 3707–3717.
(19) Gross, Z.; Galili, N.; Saltsman, I. *Angew. Chem. Int. Ed.* **1999**, *38*, 1427–1429.
(20) Aviv-Harel, I.; Gross, Z. *Coord. Chem. Rev.* **2010**, *255*, 717–736.
(21) Simkhovich, L.; Galili, N.; Saltsman, I.; Goldberg, I.; Gross, Z. *Inorg. Chem.* **2000**, *39*, 2704–2705.
(22) Luobeznova, I.; Simkhovich, L.; Goldberg, I.; Gross, Z. *Eur. J. Inorg. Chem.* **2004**, 1724–1732.
(23) Thomas, K. E.; Wasbotten, I. H.; Ghosh, A. *Inorg. Chem.* **2008**, *47*, 10469–10478.
(24) Aviv-Harel, I.; Gross, Z. *Chem. Eur. J.* **2009**, *15*, 8382–8394.
(25) Palmer, J. H. *Struct. Bond.* **2012**, *142*, 49–90.
(26) Thomas, K. E.; Alemayehu, A. B.; Conradie, J.; Beavers, C. M.; Ghosh, A. *Acc. Chem. Res.* **2012**, *45*, 1203–1214.
(27) Buckley, H. L.; Chomitz, W. A.; Koszarna, B.; Tasior, M.; Gryko, D. T.; Brothers, P. J.; Arnold, J. *Chem. Commun.* **2012**, *48*, 10766–10768.
(28) Palmer, J. H.; Durrell, A. C.; Gross, Z.; Winkler, J. R.; Gray, H. B. *J. Am. Chem. Soc.* **2010**, *132*, 9230–9231.
(29) Alemayehu, A. B.; Ghosh, A. *J. Porphyrins Phthalocyanines* **2011**, *15*, 106–110.
(30) Rabinovich, E.; Goldberg, I.; Gross, Z. *Chem. Eur. J.* **2011**, *17*, 12294–12301.
(31) Thomas, K. E.; Alemayehu, A. B.; Conradie, J.; Beavers, C.; Ghosh, A. *Inorg. Chem.* **2011**, *50*, 12844–12851.
(32) Schöfberger, W.; Lengwin, F.; Reith, L. M.; List, M.; Knör, G. *Inorg. Chem. Commun.* **2010**, *13*, 1187–1190.

(33) Reith, L. M.; Himmelsbach, M.; Schoefberger, W.; Knör, G. *J. Photochem. Photobiol., A* **2011**, *218*, 247–253.
(34) Reith, L. M.; Koenig, M.; Schwarzinger, C.; Schoefberger, W. *Eur. J. Inorg. Chem.* **2012**, *2012*, 4342–4349.
(35) Reith, L. M.; Stiftinger, M.; Monkowius, U.; Knör, G.; Schoefberger, W. *Inorg. Chem.* **2011**, *50*, 6788–6797.
(36) Vestfrid, J.; Botoshansky, M.; Palmer, J. H.; Durrell, A. C.; Gray, H. B.; Gross, Z. *J. Am. Chem. Soc.* **2011**, *133*, 12899–12901.
(37) Bendix, J.; Dmochowski, I. J.; Gray, H. B.; Mahammed, A.; Simkhovich, L.; Gross, Z. *Angew. Chem. Int. Ed.* **2000**, *39*, 4048–4051.
(38) Saltsman, I.; Goldberg, I.; Gross, Z. *Tetrahedron Lett.* **2003**, *44*, 5669–5673.
(39) Gryko, D. T.; Piechota, K. E. *J. Porphyrins Phthalocyanines* **2002**, *6*, 81–97.
(40) Alaimo, P. J.; Peters, D. W.; Arnold, J.; Bergman, R. G. *J. Chem. Ed.* **2001**, *78*, 64.
(41) SMART: Area Detector Software Package Bruker Analytic X-ray Systems I. Madison WI. SMART: Area Detector Software Package, Bruker Analytic X-ray Systems I. Madison, WI, 2003.
(42) SADABS: Bruker-Nonius Area Detector Scaling and Absorption V2.05 Bruker Analytical X-ray System, I. Madison, WI, 2003.
(43) Sheldrick, G. M. *Acta. Crystallogr. A.* **2008**, *64*, 112.
(44) Farrugia, L. J. *Appl. Crystallogr.* **1997**, *30*, 565.
(45) Van der Sluis, P.; Spek, A. L. *Acta Cryst.* **1990**, *A46*, 194–201.

Chapter 4: Corroles that "Click": Modular Synthesis of Azido- and Propargyl- Functionalized Metallocorrole Complexes and Convergent Synthesis of a Bis-Corrole Scaffold

Introduction

Interest in conjugated metallomacrocycles has rapidly increased in recent years, due to their close analogy to biological porphyrinoid systems and their potential application to real-world problems. Lanthanide phthalocyanines have exhibited single-molecule magnetism that may prove useful in molecular switches.[1–5] Porphyrins have been used recently as high quantum-yield sensitizers in solar cells,[6] in non-linear optics,[7] and molecular-scale electroluminescence,[8] among many other applications. While less studied than their 20-membered ring counterparts, metallocorrole complexes[9] have demonstrated excellent activity as oxygen reduction catalysts with potential applications in fuel cells,[10–13] as well as other catalytic activity for small molecule/ion activation[14,15] and detection of environmental toxins.[16,17] Additionally, iron corroles have been shown to catalytically lower cholesterol levels and may be used to prevent heart disease,[18] in addition to both gallium and phosphorus corroles being used as fluorescent reporters for tumor detection and treatment due to their high quantum yields.[19,20]

As potential applications of conjugated macrocycles and their metal complexes become increasingly prevalent, the question of how to practically incorporate these molecules into devices, drugs, and sensors is often what limits the next step in their development. Unattached small molecule catalysts are impractical in a fuel cell or battery and need to be affixed to an electrode; interest in the use of corrole as an oxygen reduction catalyst was an early motivator for this research.[11] Imaging agents and metal-based drugs are more effective if attached to a biomolecule that provides targeted delivery to the site of interest.[21] Methods for covalently attaching corroles to other substrates have been reported in the literature,[22] but none have seen widespread application.

Huisgen azide-alkyne cycloaddition,[23–25] or "click" chemistry, has demonstrated utility both in surface attachment of small molecules[26–31] and in targeted delivery in biological systems.[30,32–35] In particular, both surfaces and biomolecules are easily functionalized with azido groups, and so couplings with alkynyl-functionalized small molecules are of great utility.[36–40] The reaction takes place under mild conditions and is tolerant of a wide range of functional groups. This makes it ideal for attachment reactions of porphyrinoids, which are often fragile with regard to strongly oxidizing conditions. The fact that the "click" reaction, when optimized, occurs in quantitative yield is also an important attribute, considering both the possibility of unreacted starting materials compromising device functionality and the high value of porphyrinoids as a substrate. Indeed, several examples of azido- and alkynyl-functionalized porphyrins have been used for click reactions in the literature.[41–44] Further examples also exist where porphyrinoids have been attached to a surface by way of a "clicked" axial ligand.[42] One example of a corrole functionalized with an azido group was reported in 2005 as a synthetic intermediate;[45] this corrole has very recently been metallated with gallium and attached to a BODIPY dye by way of Huisgen azide-alkyne cycloaddition to demonstrate bidirectional fluorescence resonance energy transfer.[46] In addition, one example of a corrole functionalized with an alkynyl group has been reported;[47,48] while it was not used for "click" chemistry, this species was used for a cross coupling reaction between corrole and coumarin units in order to study the optical properties of the dyad.

One of the major advantages of the Gryko "A_2B" synthesis of corroles[49] is that it allows more straightforward access to conjugated macrocycles with a single *meso* substituent with unique properties. In contrast, porphyrins with one unique *meso* substituent[50] (*meso*-substituted A_3B porphyrins) are often prepared by statistical synthesis, and existing examples of alkynyl-substituted porphyrins have multiple alkynyl groups,[41] creating the potential for a complex mixture of molecular environments when these are attached to a surface.

Preparation of bisporphyrinoids is similarly challenged by the use of statistical syntheses, and is further plagued by compounding low yields. Although several groups have prepared interesting bis-corrole, bis-porphyrin, and porphyrin-corrole bimetallic complexes and demonstrated their activity as small molecule activation catalysts,[10,51,52] the reported yields are poor. In these unique cases the rigid backbone of these complexes is important to their reactivity and may not allow for the use of "click" chemistry. However, convergent synthesis where two corroles are assembled separately and then attached gives much better overall yields, as well as allowing for separate coordination of two different metals to produce a heterobimetallic complex.

Here we present the synthesis of two corrole ligands functionalized with propargyl and azido groups respectively. These corroles are metallated with copper and iron and then attached to small-molecule test substrates by Huisgen azide-alkyne cycloaddition as a proof-of concept. Finally, homobimetallic (Cu_2) and heterometallic (CuFe) bis-corrole molecules are prepared in good yields by the same "click" reaction.

Results and Discussion

Previous research has emphasized the importance of electron-withdrawing *meso*-substituents on corrole ligands.[53] These make the first oxidation potential more positive[54] and enhance the stability of the corrole towards light and oxygen.[55] For this reason, we chose 5-(pentafluorophenyl)dipyrromethane as a key substrate. Combination of two equivalents of 5-(pentafluorophenyl)dipyrromethane and one equivalent of 4-propargyloxybenzaldehyde in a mixture of methanol and acidic water at room temperature was followed by extraction with chloroform and the addition of DDQ.[49] After stirring overnight at room temperature, column chromatography and recrystallization gave 5,15-bis(pentafluorophenyl)-10-(4-propargyloxyphenyl)corrole ($((C_6F_5)_2$(*p*-O (CH_2CCH)Ph)corroleH_3) (**4-1**) as a purple crystalline solid in 23 % yield (Scheme 4.1a).

Following the same general procedure[49] 5,15-bis(pentafluorophenyl)-10-(3-bromomethylphenyl)corrole ($((C_6F_5)_2$(*m*CH_2Br)Ph)corroleH_3) (**4-2**) was prepared in 18 % yield. The bromomethyl group was then converted to an azidomethyl group by reaction with sodium azide in the presence of triethylbenzyl ammonium chloride (TEBA) as a phase transfer catalyst.[56] This reaction was stirred overnight at room temperature, and after aqueous extraction and column chromatography 5,15-bis(pentafluorophenyl)-10-(3-azidomethylphenyl)corrole ($((C_6F_5)_2$(*m*-CH_2N_3)Ph)corroleH_3) (**4-3**) was isolated as a purple crystalline solid in 69 % yield (Scheme 1b). Free-base corroles **4-1**, **4-2**, and **4-3** have been characterized by ^1H ^{13}C, and ^{19}F NMR spectroscopies, UV-visible spectroscopy and ESI mass spectrometry (See Experimental Details). To our knowledge, these species constitute only the second example in each case of of alkynyl-[47] (propargyl) and azido-[45,46] functionalized corrole ligands.

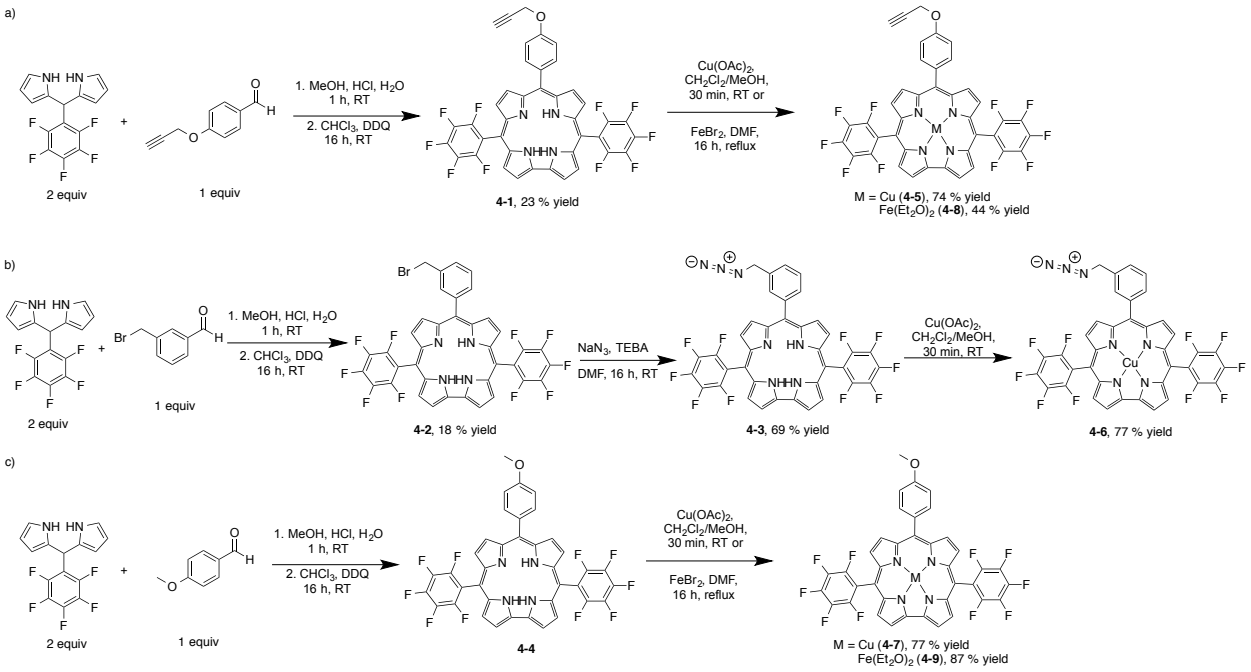

Scheme 4.1. Preparation of (a) propargyl- (b) azido- and (c) methoxy- functionalized metallocorroles.

Both **4-1** and **4-3**, in addition to the previously reported 5,15-bis(pentafluorophenyl)-10-(4-methoxyphenyl)corrole ($(C_6F_5)_2$(*p*-OMePh)corroleH$_3$) (**4-4**), reacted with copper(II) acetate to form **4-5** (74 % yield), **4-6** (77 % yield), and **4-7** (77 % yield) respectively (Scheme 4.1).[57] All three compounds have been characterized by ^{1}H and ^{19}F NMR spectroscopies, (**4-5** and **4-6** were also characterized by ^{13}C NMR spectroscopy), UV-visible spectroscopy and ESI mass spectrometry (See Experimental Details). **4-7** was prepared primarily as a reference compound for electrochemical characterization.

4-1 and **4-4** reacted with iron(II) bromide in refluxing dimethylformamide under Schlenk conditions to produce **4-8** (44 % yield) and **4-9** (87 % yield) respectively (Scheme 4.1).[58] Unlike for the analogous trisperfluorophenylcorrole complexes, these compounds were sensitive to oxidation to a bis-iron(IV) bridged μ-oxo species, and required either anhydrous, air-free workup (**4-9**) or column chromatography followed by reduction with hydrazine in diethyl ether (**4-8**) to cleanly produce the paramagnetic iron(III) corrole species. Both compounds have been characterized by ^{1}H and ^{19}F NMR spectroscopies (See Experimental Details), where their paramagnetically shifted peaks are diagnostic and match closely with those previously reported by Gross and coworkers for the paramagnetic high spin iron(III) trisperflouorophenyl corrole bis(diethylether).[58] Specifically, the broad signal at -95.3 ppm in the ^{19}F NMR spectrum of **4-8** (-100.5 ppm in **4-9**) can be assigned to the *ortho*-fluorine atoms, while that at -149.7 ppm (-149.5 ppm in **4-9**) can be assigned to the *para*-fluorine and that at -155.2 ppm (-155.7 ppm in **4-9**) to the *meta*-fluorine atoms. Differentiation of these compounds from the bis-iron(IV) bridged μ-oxo species is straightforward because the latter is displays five inequivalent diamagnetically shifted signals in the ^{19}F NMR spectrum. There are slight differences between the chemical shifts of these compounds in both the ^{1}H and ^{19}F NMR spectra; these differences correspond to a very slight difference in UV-visible absorption maxima between **4-8** (381 nm) and **4-9** (376 nm). As these compounds differ only by a remote substituent (propargyl- vs. methoxy-), the reasons for these differences are unclear, however they may relate to the slightly greater electronic donating nature of the methoxy group and subsequent inductive electron donation by the 10-phenyl *meso*-substitutent to the corrole ring. These compounds were also characterized by ESI mass spectrometry (See Experimental Details).

To test the reactivity of these species towards "click" chemistry and to ascertain that the presence of coordinated metals did not inhibit this reactivity, **4-5** reacted with 2-(2-azidoethoxy)ethan-1-ol and **4-5** and **4-8** each reacted with benzyl azide to produce **4-10** (49 % yield), **4-11** (72 % yield), and **4-12** (52 % yield) respectively (Scheme 4.2).

Similar to its precursor **4-8**, **4-12** reacted with hydrazine in diethyl ether to cleanly isolate the iron(III) corrole species. To a similar end, **4-6** reacted with propargyl alcohol to produce **4-13** (41 % yield) (Scheme 4.3). In all cases copper(I) acetate, recently published as an excellent catalyst for azide-alkyne cycloaddition,[59] was used as a heterogeneous catalyst for this reaction and the compounds were isolated by column chromatography. All three compounds were characterized by ^{1}H and ^{19}F NMR spectroscopies (and **4-10** by ^{13}C NMR spectroscopy), UV-visible spectroscopy and ESI mass spectrometry (See Experimental Details). The paramagnetic NMR spectra of **4-12** are consistent with those observed for **4-8** and with those reported in the literature.[58]

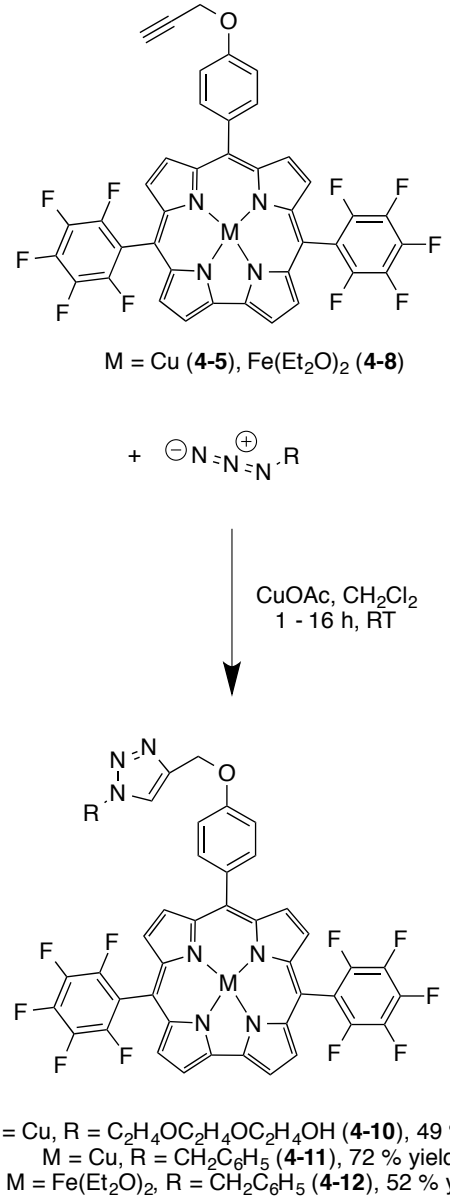

Scheme 4.2. Test reactions to confirm reactivity of propargyl-functionalized corroles **4-5** and **4-8** towards the "click" reaction with small substrates.

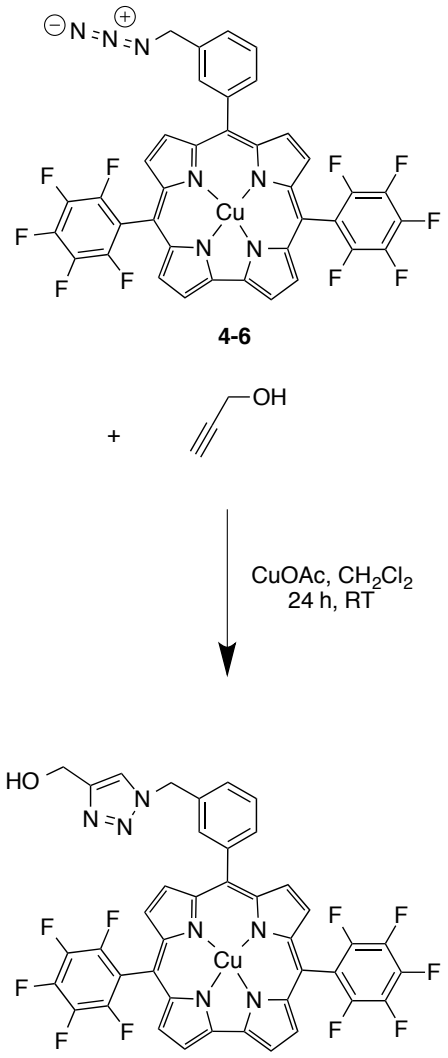

Scheme 4.3. Test reactions to confirm reactivity of azido-functionalized corrole **4-6** towards the "click" reaction with small substrates.

It should be noted that initial attempts were also made to react the free-base corrole **4-1** with benzyl azide. These resulted in very low yields of **4-5** and **4-11** among a mixture of species, suggesting metallation of the free base corrole by copper(I) acetate. However, there was no indication of substitution of iron with copper in reactions performed on **4-8**, indicating that metal exchange was not an issue in this case and that the presence of redox-active iron(III) and copper(III) species do not interfere with "click" reactivity.

Of greater interest than the ability to attach to small organic substrates was the question of whether azido- and alkynyl- derivatized corroles could be coupled with each other to produce biscorrole bimetallic species. To this end, **4-5** and **4-6** reacted in the presence of copper(I) acetate to produce bis-copper complex **4-14** in 84 % yield (Scheme 4.4). The identity of this compound as a single molecule (as opposed to a mixture of the two starting materials) was confirmed by ESI-MS (See Experimental Details). The ^{1}H and ^{19}F NMR spectra suggest that there is no significant interaction between the two corrole rings; unlike in several reported examples of "sandwich" species where the corroles are cofacial with metals and bridging ligands between them,[60–62] no unusual shifts of the β-pyrollic hydrogen atoms or the -C_6F_5 fluorine atoms are observed. If the two rings interacted, then non-equivalency of the *ortho* and *meta* fluorine atoms would be expected, and those on the inside of the cofacial "sandwich" would be shifted upfield due to shielding by added effects of two anisotropic corrole rings. The ^{19}F NMR spectrum is notable in that it is clearly a superposition of two sets of -C_6F_5 peaks in nearly identical chemical environments (Figure 4.1), consistent with two bis-perfluorinated copper(III) corroles that do not have any electronic communication. Figure 4.1 also shows enlarged regions (inset) for the *ortho*, *para*, and *meta* fluorine peaks for compounds **4-5**, **4-6**, and **4-14**. While the spectra cannot be overlaid directly due to differences in solvent and magnetic field strength, comparison of the complex peaks of **14** with those of its precursors shows that the spectrum is consistent with two corrole rings in diamagnetic environments. Additionally, the alkynyl proton observed in the ^{1}H NMR spectrum of **4-5** is not present in **4-14**, but an additional singlet that integrates to 1H is observed at 7.75 ppm in the aromatic region (which otherwise looks very much like a superposition of the spectra of **4-5** and **4-6**), consistent with formation of the triazole.

By a similar procedure, **4-8** and **4-6** reacted in the presence of copper(I) acetate to generate the heterobimetallic copper(III) iron(III) biscorrole complex **4-15** (54 % yield). Analogous to the iron(III) complex **4-12**, hydrazine was added to convert the product cleanly to an iron(III) species; in this case acetonitrile was used as the coordinating solvent due to limited solubility of the larger molecule in diethyl ether. ^{1}H and ^{19}F NMR spectroscopies again suggest that there is minimal interaction between the two metal centers, although broad peaks from the paramagnetic iron(III) corrole do overlap the peaks of the copper corrole in the ^{1}H NMR spectrum, precluding accurate integration of the sharp peaks. The paramagnetically shifted peaks of the iron corrole in both the ^{1}H and ^{19}F NMR spectra of **4-15** are again consistent with those previously reported for an iron(III) corrole species.[58] In the ^{19}F NMR five peaks are observed (δ -117.7 (*ortho-F*-Fe(corrole)), -140.5 (*ortho-F*-Cu(corrole)), -158.0 (possibly two peaks, *para-F*'s), -163.7 (*meta-F*), -165.2 (*meta-F*)); it is likely that two peaks are superimposed at -158 ppm due to slight broadening of this peak, however integration is inaccurate in the presence of a paramagnetic metal center. The meta-fluorine peaks cannot be distinguished without more advanced NMR spectroscopic studies.

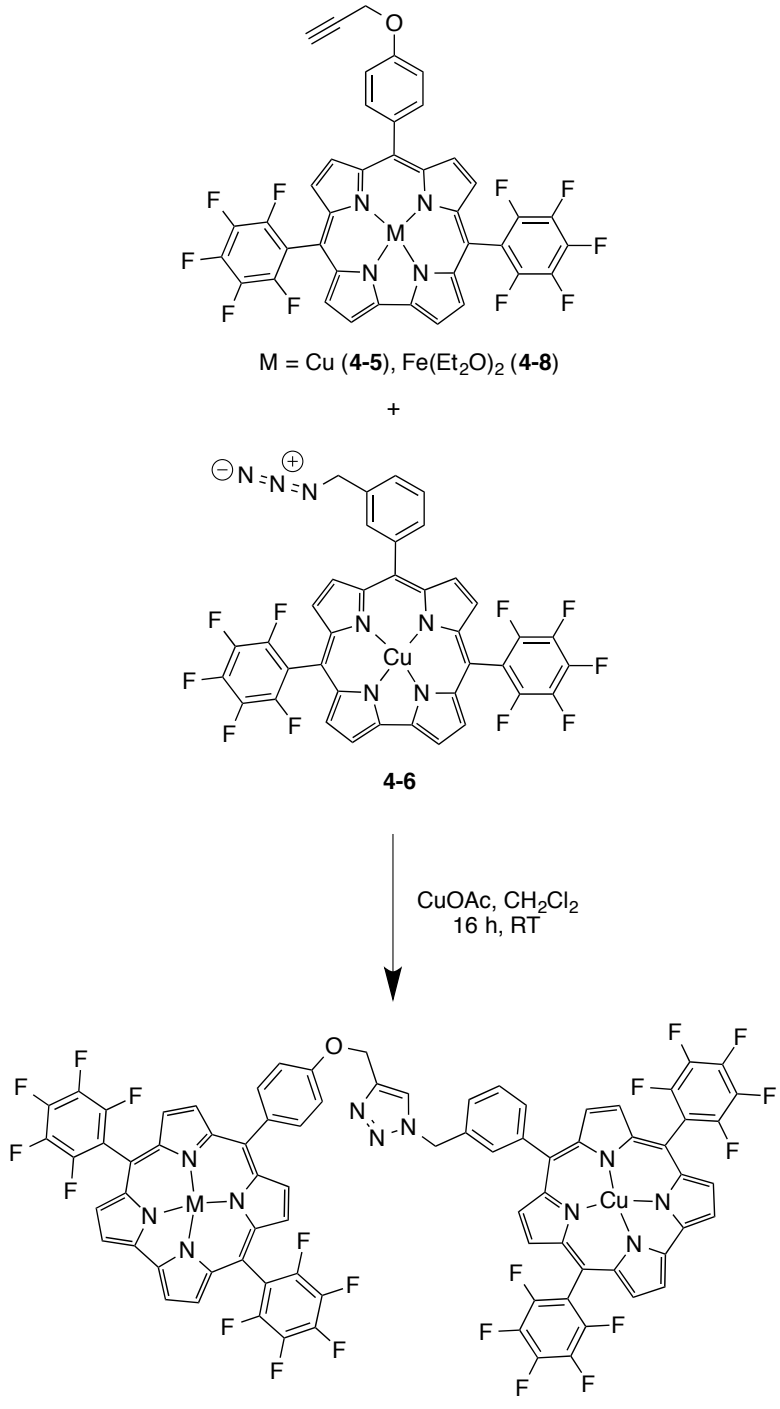

Scheme 4.4. Synthesis of homobimetallic (**4-14**) and heterobimetallic (**4-15**) biscorrole complexes by a "click" reaction.

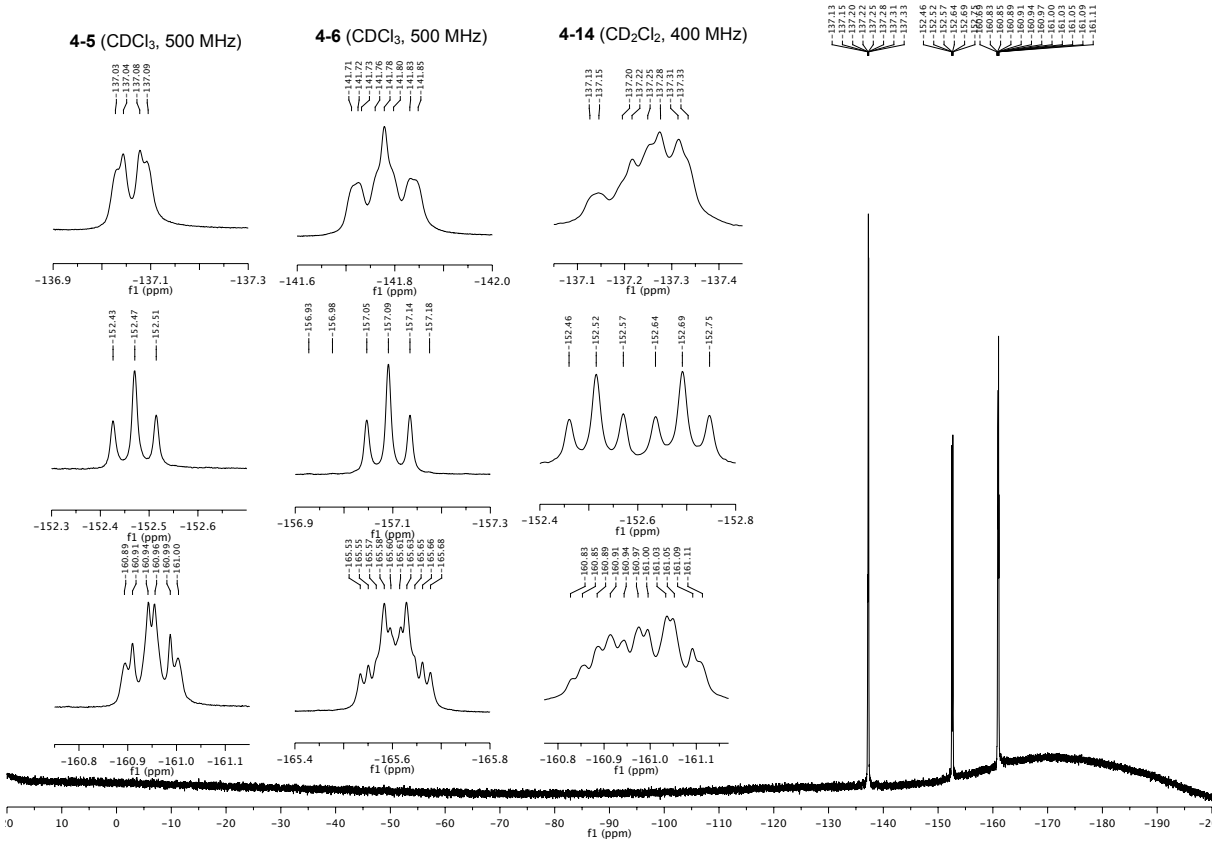

Figure 4.1. ^{19}F NMR spectrum of **4-14** (large spectrum), exhibiting typical chemical shifts for perfluorophenyl groups. Insets show *ortho*, *para*, and *meta* fluorine peaks for compounds **4-5**, **4-6**, and **4-14**.

Both **4-14** and **4-15** were characterized by cyclic voltammetry, as were **4-7** and **4-9** for comparison. **4-14** shows a single reversible peak at -0.21 V vs. Ag/Ag^+ in methylene chloride, corresponding to the Cu^{III}/Cu^{II} peaks of both copper centers (Figure 4.6, Table 4.1).[63] This peak is at essentially the same potential with double the current observed for **4-7** (-0.23 V vs. Ag/Ag^+) (Figure 4.3) and occurs at a potential 0.12 V more negative than the analogous peak in previously reported copper(III) tris(perfluorophenyl) corrole (Cu(tpfc)), and 0.33 V more positive than the previously reported copper(III) tris(*p*-methoxyphenyl) corrole. These numbers are consistent with the corresponding electron-withdrawing and electron-donating natures of the corrole ligands in **4-7**, Cu(tpfc), and Cu(*p*-OMePh)$_3$corrole (Cu(*p*-OMePh)$_3$corrole).[63] The voltammogram of **4-14** also shows a quasireversible peak at 0.74 V vs. Ag/Ag^+ with an oxidative shoulder at 0.64 V (0.1 V/s) that merges with the main peak at higher scan rates. These peaks correspond to oxidation of the ligand, and are again very similar to the corresponding ligand oxidation observed for **4-7** but with roughly double the current. The presence of a single peak for the Cu^{III}/Cu^{II} transition for **4-14** and the nearly identical ligand oxidations for both **4-14** and **4-7** suggest that there is no interaction or electronic communication between the two copper corroles in **4-14**, consistent with what is observed by NMR spectroscopy and consistent with the fact that a recently reported corrole-BODIPY dyad with click attachment exhibits only through-space and not through-bond fluorescence resonance energy transfer.[46]

Cyclic voltammetry of **4-15** in acetonitrile displays an oxidation and a reduction consistent with the presence of both copper and iron (Figures 4.7-4.10). The peak at -0.19 V vs. Ag/Ag^+ corresponds to the Cu^{III}/Cu^{II} couple, and that at 0.04 V corresponds to Fe^{III}/Fe^{IV};[58] these are essentially the same peaks observed for the two corresponding mononuclear species, **4-7** and **4-9** (Table 4.1). As is the case with the Cu^{III}/Cu^{II} peak, the Fe^{III}/Fe^{IV} couple occurs at a potential 0.40 V more negative than the analogous Fe^{III}/Fe^{IV} peak in Fe(tpfc).[58] It should be noted that the voltammograms of **4-14** and **4-15** were recorded in different solvents due to solubility limitations. Similarly to **4-14**, the voltammogram of **4-15** shows oxidative peaks corresponding to the oxidation of the ligand. Also analogous to **4-14**, there is no indication of interaction between the two metal centers, based on the fact that the metal oxidations and reductions are observed at essentially the same potentials as seen in the monometallic analogues.

Conclusion

In summary, we have demonstrated that bis-corroles possessing a flexible linker can be efficiently synthesized *via* Huisgen azide-alkyne cycloaddition chemistry. Our convergent strategy makes it possible to construct two building blocks independently and then to combine them in the final step. This methodology allows preparation of stable homo- and hetero-bimetallic complexes. Further studies are underway to demonstrate the utility of this reaction for attachment of corroles to larger substrates and surfaces.

Table 4.1. Assignment of peaks in cyclic voltammograms of **4-14** and **4-15** and comparison to reference compounds. All voltages calculated as E_{pf} - E_{pr}[a] at 0.1 V/s and reported in V vs. Ag/Ag^+,[b] unless otherwise indicated.

Corrole (Solvent)	*Reduction(s)*	*Cu^{III}/Cu^{II}*	*Fe^{III}/Fe^{IV}*	*Ligand oxidation(s)*
4-14 (CH_2Cl_2)		-0.21		0.74
4-15 (CH_3CN)[c]		-0.19	0.04	0.6[c], 0.9[c]
4-7 (CH_2Cl_2)		-0.23		0.73, 1.33[c], 1.53[c]
4-7 (CH_3CN)		-0.22		0.62, 1.43[d]
4-9 (CH_2Cl_2)	-0.69		-0.01	0.32, 1.00
4-9 (CH_3CN)	-0.76, -1.88		0.01	0.29, 0.84
Cu(tpfc) (CH_2Cl_2)[63]	-2.00	-0.09		0.82, 1.26
Cu(p-OMePh)$_3$corrole (CH_2Cl_2)[63]		-0.54		0.35, 1.01, 1.29
Fe(tpfc) (CH_2Cl_2)[58]	-1.08		0.44	(none reported)

[a]E_{pf} = peak potential in the forward direction, E_{pr} = peak potential in the reverse direction
[b]Voltages originally reported in SCE were converted to Ag/Ag^+ by subtracting 298 mV.[64]
[c]Data for **4-15** collected at 0.5 V/s due to low solubility. Ligand oxidations were poorly resolved; peak potentials estimated.
[d]Irreversible oxidations; reported as the oxidative peak potential

Experimental Details

General Considerations

Reactions were performed either using standard Schlenk and N_2-atmosphere glovebox techniques or under ambient conditions on the laboratory bench, as noted. As much as possible, flasks for synthesis were covered with aluminum foil to reduce exposure to light throughout the procedures. When required, solvents were dried by passing through a column of activated alumina and degassed with nitrogen[65] or using a Phoenix solvent drying system commercially available from JC Meyer Solvent Systems.

Purity of products was estimated by NMR spectroscopy, assuming that aliphatic impurities, when not identifiable, had a molecular weight of 100 and that a peak integrating to 1 in the ^{1}H NMR spectrum (relative to a corrole aromatic peak of area 2) had one equivalent of impurity to one equivalent of corrole. In general this will overestimate the concentration of impurity, and so the results given are conservative and represent a minimum limit on purity and yield. Aromatic impurities were compared to impurities observed in the ^{19}F NMR spectrum (where compounds were assumed to have a 1:1 mass ratio to the corrole product) and in this case were assumed to be redundant.

Instrumentation

All NMR spectra were obtained in at ambient temperature in deuterated solvents using Bruker AVB-400 or AVQ-400 spectrometers at the University of California, Berkeley or on 400, 500 or 600 MHz NMR instruments at the Organic Chemistry Institute, Polish Academy of Sciences. UV-visible spectra were determined with a Varian Cary 50 UV-Vis spectrophotometer using a 1 mm quartz cell. Mass spectral data (ESI-MS, positive mode) were obtained at the University of California, Berkeley Microanalytical Facility. Melting points were determined using sealed capillaries and are uncorrected.

5-Pentafluorophenyldipyrromethane[66] and 4-propargyloxybenzaldehyde[67] were prepared according to literature procedures. 5,15-bis(pentafluorophenyl)-10-(4-methoxyphenyl)corrole ($(C_6F_5)_2$(*p*-OMePh)corroleH$_3$) (**4-4**) was prepared according to a previously reported procedure.[49]

2,3-dichloro-5,6-dicyano-1,4-benzoquinone (DDQ), triethylbenzylammonium chloride (TEBA) and copper(I) acetate were purchased from TCI and used as received. Sodium azide was purchased from Acros and used as received. Copper(II) acetate, benzyl azide, and propargyl alcohol were purchased from Aldrich and used as received. 3-bromomethylbenzaldehyde, 2-(2-azidoethoxy)ethan-1-ol, and iron(II) bromide (bis(THF)) were obtained from commercial sources and used as received. Tetraethylammonium tetrafluoroborate ($TEABF_4$) was purchased from Fluka and used as received. Tetra-*n*-butylammonium tetrafluoroborate ($TBABF_4$) was purchased from Oakwood Products, Inc., and was purified by dissolving in ethyl acetate, precipitating with pentane, filtering, and drying *in vacuo* overnight.

Synthesis and characterization of compounds 4-1 to 4-15

5,15-bis(pentafluorophenyl)-10-(4-propargyloxyphenyl)corrole ($(C_6F_5)_2$(*p*-$O(CH_2CCH)Ph)corroleH_3$) (**4-1**) was prepared according to a modified literature procedure.[49] 5-Pentafluorophenyldipyrromethane (3.12 g, 10 mmol) and 4-propargyloxybenzaldehyde (0.80 g, 5 mmol) were dissolved in methanol (500 mL). Concentrated hydrochloric acid (36 %, 25 mL) was combined with 500 mL distilled water, and the acid solution was added to the methanol solution while stirring, immediately producing a peach-colored suspension. The mixture was stirred for one hour at room temperature and then extracted with chloroform. The organic extracts were combined, washed twice with water, dried over sodium sulfate, filtered, and diluted with chloroform to 1.25 L. DDQ (3.4 g, 15 mmol) was added and the reaction mixture was stirred overnight at room temperature. The solution was concentrated to 200 mL by rotary evaporation, then filtered through a short silica gel column (1:1 CH_2Cl_2:hexanes). The combined eluents were concentrated to dryness. Column chromatography on silica gel (1:1 CH_2Cl_2:hexanes, R_f = 0.62 in 1:1 CH_2Cl_2:hexanes) provided the corrole with a minor impurity, which appears as a yellow spot on the TLC plate. This impurity is removed by recrystallization of the solid from hexanes, which is repeated until the yellow spot disappears, yielding a purple solid (950 mg, 97 % est. purity, 23 % yield). ^{1}H NMR (500 MHz, $CDCl_3$): δ 9.09 (d , *J* = 4.5 Hz, 2H), 8.71 (t, *J* = 4.3 Hz, 4H), 8.56 (d, *J* = 3.0 Hz, 2H), 8.11 (d, *J* = 8.5 Hz, 2H), 7.37 (d, *J* = 5.5 Hz, 2H), 4.96 (d, *J* = 2.5 Hz, 2H, OC*H*$_2$CCH), 2.68 (t, *J* = 2.3 Hz, 1H, OCH_2CCH), -2.70 (br s, 3H, N*H*). ^{13}C{^{1}H} (125 MHz, $CDCl_3$): δ 197.7, 157.6, 147.1, 145.1, 140.7, 138.9, 136.9, 135.6, 134.6, 127.8, 125.3, 117.6, 114.0, 113.8, 112.9, 78.8, 75.9, 56.1. ^{19}F NMR (470 MHz, $CDCl_3$): δ -137.9 (d, *J* = 18.8 Hz), -152.9 (s), -161.8 (t, *J* = 17.9 Hz). UV-Vis (nm): 409, 561, 614. ESI-MS (+) Calcd: 761.13937 for $C_{40}H_{18}F_{10}O_1N_4H$, Observed: 761.14109. Mp: decomposition above 350 ºC.

5,15-bis(pentafluorophenyl)-10-(3-bromomethylphenyl)corrole
($(C_6F_5)_2$(*m*CH_2Br)Ph)corroleH$_3$) (**4-2**) was prepared according to a modified literature procedure.[49] 5-Pentafluorophenyldipyrromethane (1.56 g, 5 mmol) and 3-bromomethylbenzaldehyde (0.50 g, 2.5 mmol) were dissolved in methanol (250 mL). Concentrated hydrochloric acid (36 %, 12.5 mL) was combined with 250 mL distilled water, and the acid solution was added to the methanol solution while stirring, immediately producing a peach-colored suspension. The mixture was stirred for one hour at room temperature and then extracted with chloroform. The organic extracts were combined, washed twice with water, dried over sodium sulfate, filtered, and diluted with chloroform to 1 L. DDQ (1.7 g, 7.5 mmol) was added and the reaction mixture was stirred overnight at room temperature. The solution was concentrated to 200 mL by rotary evaporation, then filtered through a short silica gel column (1:1 CH_2Cl_2:hexanes). The combined eluents were concentrated to dryness. Column chromatography on silica gel (1:1 CH_2Cl_2:hexanes, R_f = 0.54 in 1:1 CH_2Cl_2:hexanes) and subsequent concentration of the combined fractions yielded the pure product as a purple microcrystalline solid (380 mg, 96 % est. purity, 18 % yield). ^{1}H NMR (500 MHz, $CDCl_3$): δ 9.12 (d, *J* = 4.2 Hz, 2H), 8.72 (dd, *J* = 18.4, 4.8 Hz, 4H), 8.58 (d, *J* = 4.7 Hz, 2H), 8.24 (m, 1H), 8.15 – 8.08 (m (dt, unresolved), 1H), 7.82 – 7.77 (m, 1H), 7.77 – 7.71 (m, 1H), 4.78 (s, 2H, C*H*$_2$N$_3$), -2.76 (br s, 3H, N*H*). ^{13}C{^{1}H} (125 MHz, $CDCl_3$): δ 147.1, 145.1, 142.8, 141.8, 140.7, 138.9, 137.0, 136.9, 135.1, 134.7, 128.4, 127.8, 125.8, 117.5, 114.0, 112.6, 33.5. ^{19}F NMR (470 MHz, $CDCl_3$): δ -137.1 (dd, *J* = 24.0, 8.0 Hz), -152.5 (t, *J* = 21.2 Hz), -160.95 (td, *J* = 22.8, 7.8 Hz). UV-Vis (nm): 409, 561, 612. ESI-MS (+) Calcd: 799.05497 for $C_{38}H_{17}Br_1F_{10}N_4$, Observed: 799.05352. Mp: decomposition above 350 ºC.

5,15-bis(pentafluorophenyl)-10-(3-azidomethylphenyl)corrole ($(C_6F_5)_2$(*m*-CH_2N_3)Ph)corroleH_3) (**4-3**). 5,15-bis(pentafluorophenyl)-10-(3-bromomethylphenyl)corrole (**4-2**) (150 mg, 0.188 mmol) was dissolved in dry dimethylformamide (30 mL) . Sodium azide (13.4 mg, 0.207 mmol) and triethylbenzyl ammonium chloride (TEBA) (4.3 mg, 0.019 mmol) were added and the reaction mixture was stirred overnight at room temperature.[56] The reaction was monitored by thin layer chromatography (silica gel, 1:1 CH_2Cl_2:hexanes). The reaction volume was diluted to 75 mL with chloroform. The organic phase was washed twice with water, dried over sodium sulfate, and the solvent removed by rotary evaporation. The solid was dissolved in 10 mL CH_2Cl_2 and the solvent again removed by rotary evaporation to ensure complete removal of the dimethyl formamide. Column chromatography on silica gel (1:1 CH_2Cl_2:hexanes, R_f = 0.49 in 1:1 CH_2Cl_2:hexanes) and subsequent concentration of the combined fractions yielded the pure product as a purple microcrystalline solid (106 mg, 92 % est. purity, 69 % yield). ^{1}H NMR (500 MHz, $CDCl_3$): δ 9.10 (d, *J* = 4.0 Hz, 2H), 8.71 (d, *J* = 4.0 Hz, 2H), 8.67 (d, *J* = 4.5 Hz, 2H), 8.56 (d, *J* = 2.5 Hz, 2H), 8.13 (m, 2H), 7.78 (m, 1H), 7.72 (m, 1H), 4.61 (s, 2H, C*H*$_2$N$_3$), -2.80 (br s, 3H, N*H*). ^{13}C{^{1}H} (125 MHz, $CDCl_3$): δ 162.3, 147.1, 145.1, 142.8, 141.9, 140.7, 136.9, 135.3, 134.5, 131.2, 128.8, 127.8, 125.8, 121.8, 117.6, 114.0, 112.6, 96.9, 54.8. ^{19}F NMR (470 MHz, $CDCl_3$): δ -137.9 (d, *J* = 18.8 Hz), -152.9 (s), -161.8 (t, *J* = 17.9 Hz). UV-Vis (nm): 409, 561, 613. ESI-MS (+) Calcd: 761.1313 for $C_{38}H_{17}F_{10}N_7$, Observed: 761.1307. Mp: decomposition above 350 ºC.

Copper(III) (5,15-bis(pentafluorophenyl)-10-(4-propargyloxyphenyl)corrole) ($(C_6F_5)_2$(*p*-O(CH_2CCH)Ph)corroleCu) (**4-5**) was prepared according to a modified literature procedure.[57] 5,15-bis(pentafluorophenyl)-10-(4-propargyloxyphenyl)corrole ($(C_6F_5)_2$(*p*-O(CH_2CCH)Ph) corroleH_3) (**4-1**) (50 mg, 0.066 mmol) was dissolved in CH_2Cl_2 (10 mL) under ambient conditions. Copper(II) acetate (36 mg, 0.197 mmol) was suspended in methanol (5 mL) and the suspension added to the corrole solution. An additional 5 mL of methanol was used in three portions to rinse residual copper(II) acetate into the reaction mixture. The reaction was allowed to stir 30 minutes at room temperature, and was monitored by thin-layer chromatography (silica gel, 1:1 CH_2Cl_2:hexanes). Upon completion, the solvent was removed by rotary evaporation and the resulting solid purified by column chromatography (silica gel, 1:4 CH_2Cl_2:hexanes, R_f = 0.75 in 1:1 CH_2Cl_2:hexanes). The product was isolated as a purple-brown solid (50 mg, 80 % est. purity, 74 % yield). ^{1}H NMR (500 MHz, $CDCl_3$): δ 7.95 (d, *J* = 4.0 Hz, 2H), 7.55 (d, *J* = 8.4 Hz, 2H), 7.42 (d, *J* = 4.2 Hz, 2H), 7.26 (d, *J* = 5.7 Hz, 2H), 7.21 (d, *J* = 4.4 Hz, 2H), 7.09 (d, *J* = 8.4 Hz, 2H), 4.80 (d, *J* = 2.4 Hz, 2H), 2.59 (t, *J* = 2.3 Hz, 1H). ^{13}C{^{1}H} (125 MHz, $CDCl_3$): δ 158.4, 150.4, 149.6, 146.1, 145.0, 144.1, 142.6, 140.9, 139.0, 136.8, 132.6, 132.1, 129.8, 122.8, 114.6, 112.0, 78.3, 75.9, 55.9,. ^{19}F NMR (470 MHz, $CDCl_3$): δ -137.1 (dd, *J* = 23.6, 7.9 Hz), -152.5 (t, *J* = 18.8 Hz), -161.0 (td, *J* = 22.6, 7.9 Hz). UV-Vis (nm): 399, 427, 548. ESI-MS (+) Calcd: 821.0455 for $C_{40}H_{15}Cu_1F_{10}N_4O_1H$, Observed: 821.0496. Mp: decomposition above 350 ºC.

Copper(III) (5,15-bis(pentafluorophenyl)-10-(3-azidomethylphenyl)corrole) ($(C_6F_5)_2$(*m*-CH_2N_3)Ph)corroleCu) (**4-6**) was prepared according to a modified literature procedure.[57] 5,15-bis(pentafluorophenyl)-10-(3-azidophenyl)corrole ($(C_6F_5)_2$(*m*-(CH_2N_3)Ph)corroleH_3) (**4-3**) (82 mg, 0.108 mmol) was dissolved in CH_2Cl_2 (12 mL) under ambient conditions. Copper(II) acetate (58 mg, 0.323 mmol) was suspended in methanol (6 mL) and the suspension added to the corrole solution. An additional 6 mL of methanol was used in three portions to rinse residual copper(II) acetate into the reaction mixture. The reaction was allowed to stir 30 minutes at room temperature and was monitored by thin-layer chromatography (silica gel, 1:1 CH_2Cl_2:hexanes).

Upon completion, the solvent was removed by rotary evaporation and the resulting solid was purified by column chromatography (silica gel, 1:1 CH_2Cl_2:hexanes, R_f = 0.70 in 1:1 CH_2Cl_2 :hexanes). The product was isolated as a brown solid (77 mg, 88 % est. purity, 77 % yield). ^{1}H NMR (500 MHz, $CDCl_3$): δ 7.97 (d, *J* = 4.0 Hz, 2H), 7.59 – 7.48 (m, 4H), 7.42 (d, *J* = 4.3 Hz, 2H), 7.24 – 7.16 (m, 4H), 4.44 (s, 2H). $^{13}C\{^1H\}$ (125 MHz, $CDCl_3$): δ 150.3, 149.5, 146.2, 144.9, 144.1, 142.6, 140.5, 138.8, 136.8, 135.6, 132.1, 130.3, 128.9, 126.6, 122.9, 111.7, 54.5. ^{19}F NMR (470 MHz, $CDCl_3$): δ -141.8 (ddd, *J* = 32.7, 23.3, 7.2 Hz), -157.1 (t, *J* = 21.2 Hz), -165.6 (tdd, *J* = 22.8, 15.3, 7.7 Hz). UV-Vis (nm): 406, 547. ESI-MS (+) Calcd: 821.0452 for $C_{38}H_{14}Cu_1F_{10}N_7$, Observed: 821.0460. Mp: decomposition above 350 ºC.

Copper(III) 5,15-bis(pentafluorophenyl)-10-(4-methoxyphenyl)corrole ($(C_6F_5)_2$(*p*-OMePh)corroleCu) (**4-7**) was prepared according to a modified literature procedure.[57] 5,15-bis(pentafluorophenyl)-10-(4-methoxyphenyl)corrole ($(C_6F_5)_2$(*p*-OMePh)corroleH$_3$) (**4-4**) (200 mg, 0.272 mmol) was dissolved in CH_2Cl_2 (50 mL) under ambient conditions. Copper(II) acetate (148 mg, 0.815 mmol) was suspended in methanol (20 mL) and the suspension added to the corrole solution. An additional 30 mL of methanol was used in three portions to rinse residual copper(II) acetate into the reaction mixture. The reaction was allowed to stir 30 minutes at room temperature, and was monitored by thin-layer chromatography (silica gel, 1:1 CH_2Cl_2:hexanes). Upon completion, the solvent was removed by rotary evaporation and the resultant solid was purified by column chromatography (silica gel, 1:1 CH_2Cl_2:hexanes). The product was isolated as a brown solid (203 mg, 82 % est. purity, 77 % yield). ^{1}H NMR (400 MHz, $CDCl_3$): δ 7.90 (br s, 2H) 7.52 (d, J = 8.0 Hz, 2H, $C_6H_2H_2$-OMe), 7.33 (br s, 2H), 7.06 (br s, 4H), 6.98 (d, J = 8.0 Hz, 2H, $C_6H_2H_2$-OMe), 3.88 (s, 3H, OCH_3). ^{19}F NMR (376 MHz, $CDCl_3$): δ -136.2 (d, *J* = 18.8 Hz, 4F), -151.6 (t, *J* = 20.7 Hz, 2F), -160.1 (quintet, *J* = 11.3 Hz, 4F). UV-Vis (nm): 399, 430, 549. ESI-MS (+) Calcd: 796.0377 for $C_{38}H_{15}Cu_1F_{10}O_1N_4$, Observed: 796.0379. Mp: decomposition above 350 ºC.

Iron(III) (5,15-bis(pentafluorophenyl)-10-(4-propargyloxyphenyl)corrole)bis (diethylether) ($(C_6F_5)_2$(*p*-O(CH_2CCH)Ph)corroleFe($Et_2O)_2$) (**4-8**) was prepared according to a modified literature procedure.[58] 5,15-bis(pentafluorophenyl)-10-(4-propargyloxyphenyl)corrole ($(C_6F_5)_2$(*p*-OMePh)corroleH$_3$) (**4-1**) (200 mg, 0.263 mmol) was dissolved in dry dimethylformamide (30 mL) under nitrogen on a Schlenk line. Iron(II) bromide(bis(THF)) (1.89 mg, 5.26 mmol) was placed in another nitrogen-filled Schlenk flask and the corrole solution transferred by cannula. The resulting mixture was refluxed overnight at 110 ºC and the reaction monitored by thin layer chromatography (silica gel, 1:1 CH_2Cl_2:hexanes). Dimethylformamide was removed under reduced pressure at 60 ºC and the resulting solid was triturated twice with diethyl ether, which was subsequently removed under reduced pressure to ensure complete removal of the dimethylformamide. The compound was purified by column chromatography (silica gel, 100 % diethyl ether) and the combined organic fractions were concentrated to 50 mL. Hydrazine (32 μL, 1.0 mmol) was added and the remaining solvent was removed under reduced pressure on a Schlenk line to give the product as a red-brown solid (130 mg, 84 % est. purity, 44 % yield). ^{1}H NMR (400 MHz, C_6D_6, 23 °C): 19.73 (br s), 7.49 (br s), 5.90 (br s), 3.27 (br), 1.11 (br s, Et_2O), 0.90 (br s), 0.16 (br s, Et_2O), -2.98 (br s), -58.78 (br s), -110.23 (br s). ^{19}F NMR (376 MHz, C_6D_6, 23 °C): δ -95.3 (br s, ortho-*F*), -149.7 (s, para-*F*), -155.2 (s, meta-*F*). UV-Vis (nm): 381, 551. ESI-MS (+) Calcd: 813.0430 for $C_{40}H_{15}F_{10}Fe_1N_4O_1$, Observed: 813.0457. Mp: decomposition above 350 ºC.

Iron(III) 5,15-bis(pentafluorophenyl)-10-(4-methoxyphenyl)corrole)bis(diethylether) $((C_6F_5)_2$(*p*-OMePh)corroleFe$(Et_2O)_2$) (**4-9**) was prepared according to a modified literature procedure.[58,68] 5,15-bis(pentafluorophenyl)-10-(4-methoxyphenyl)corrole $((C_6F_5)_2$(*p*-OMePh)corroleH_3) (**4-4**) (74 mg, 0.1 mmol) was dissolved in dry dimethylformamide (30 mL) under nitrogen on a Schlenk line. Iron(II) bromide (720 mg, 2.0 mmol) was placed in another flask under nitrogen and the corrole solution transferred by cannula. The resulting mixture was refluxed for six hours at 110 ºC and the reaction monitored by thin layer chromatography (silica gel, 1:1 CH_2Cl_2:hexanes). Dimethylformamide was removed under reduced pressure at 60 ºC and the resulting solid was triturated twice with diethyl ether, which was subsequently removed under reduced pressure to ensure complete removal of the dimethylformamide. The solid was extracted with diethyl ether and filtered by cannula, and the solvent was removed quickly under alternating nitrogen and vacuum to give a brown solid (82 mg, 93 % est. purity, 87 % yield). ^{1}H NMR (400 MHz, C_6D_6, 23 °C): δ 8.68 (s), 7.73 (s), 6.18 (br s), 3.73 (s), 2.37 (s), 1.89 (s), 0.30, (s), -0.97 (br s), -34.35 (br s), -46.23 (br s), -104.68 (br s). ^{19}F NMR (376 MHz, C_6D_6, 23 °C): δ -100.5 (br s, ortho-*F*), -149.5 (s, para-*F*), -155.7 (s, meta-*F*). UV-Vis (nm): 376. ESI-MS (+) Calcd: 789.0430 for $C_{38}H_{15}F_{10}Fe_1N_4O_1$, Observed: 789.0432. Mp: decomposition above 350 ºC.

Copper(III) (5,15-bis(pentafluorophenyl)-10-(4-oxymethyl-(1-ethoxyethanol-1,2,3-triazol-4-yl)phenyl)corrole) $((C_6F_5)_2$(*p*-O$(CH_2(C_2HN_3(CH_2CH_2OCH_2CH_2OH)))$ Ph)corroleCu) (**4-10**) was prepared as follows. Copper(III) (5,15-bis(pentafluorophenyl)-10-(4-propargyloxyphenyl)corrole) (**4-5**) (150 mg, 0.182 mmol) and 2-(2-azidoethoxy)ethan-1-ol (26 mg, 0.201 mmol) were placed in a dry 250 mL Schlenk flask. The flask was evacuated and filled with argon three times, and dry CH_2Cl_2 (50 mL) was added by cannula. Copper(I) acetate (catalytic, approximately 5 mg) was added and the suspension was stirred for 30 minutes at room temperature.[69] The reaction was monitored by thin layer chromatography (silica gel, 1:1 CH_2Cl_2:hexanes). The solution was extracted twice with water to remove excess azide. The combined extracts were dried over sodium sulfate, filtered, and the solvent removed by rotary evaporation. The resultant solid was purified by column chromatography (silica gel, 95:5 CH_2Cl_2:MeOH). The resulting solid was further purified by dry column vacuum chromatography (99:1 CH_2Cl_2:MeOH). The product was isolated as a brown solid (92 mg, 93 % est. purity, 49 % yield). ^{1}H NMR (600 MHz, $CDCl_3$): δ 7.94 (d, *J* = 4.0 Hz, 2H), 7.87 (s, 1H, N_3C_2H), 7.54 (d, *J* = 8.3 Hz, 2H), 7.42 (d, *J* = 4.3 Hz, 2H), 7.26 (d, *J* = 4.7 Hz, 2H), 7.21 (d, *J* = 4.5 Hz, 2H), 7.11 (d, *J* = 8.3 Hz, 2H), 5.31 (s, 2H, Ph-O-CH_2), 4.61 (t, *J* = 5.0 Hz, 2H), 3.96 – 3.91 (m, 2H), 3.75 – 3.68 (m, 2H), 3.61 – 3.56 (m, 2H), 1.26 (s, 1H). ^{13}C{^{1}H} (125 MHz, $CDCl_3$): δ 159.1, 149.6, 145.0, 144.1, 138.6, 136.9, 132.5, 132.1, 129.8, 124.0, 122.8, 114.5, 72.5, 69.3, 62.2, 61.7, 50.4. ^{19}F NMR (470 MHz, $CDCl_3$): δ -141.8 (dd, *J* = 24.0, 8.1 Hz), -157.2 (d, *J* = 23.5 Hz), -165.8 (td, *J* = 22.5, 7.7 Hz). UV-Vis (nm): 399, 429, 549. ESI-MS (+) Calcd: 951.1077 for $C_{44}H_{24}Cu_1F_{10}N_7O_1$, Observed: 951.1073. Mp: decomposition above 350 ºC.

Copper(III) (5,15-bis(pentafluorophenyl)-10-(4-oxymethyl-(1-benzyl-1,2,3-triazol-4-yl)phenyl)corrole) $((C_6F_5)_2$(*p*-O$(CH_2(C_2HN_3(CH_2C_6H_5)))$Ph)corroleCu) (**4-11**) was prepared as follows. Copper(III) (5,15-bis(pentafluorophenyl)-10-(4-propargyloxyphenyl)corrole) (**4-5**) (25 mg, 0.030 mmol) and benzyl azide (15 mg, 0.100 mmol) were placed in a dry 25 mL Schlenk flask. The flask was evacuated and filled with nitrogen three times, and dry CH_2Cl_2 (5 mL) was added by cannula. Copper(I) acetate (catalytic, approximately 1 mg) was added and the suspension was stirred for 30 minutes at room temperature.[69] The reaction was monitored by thin layer chromatography (silica gel, 1:1 CH_2Cl_2:hexanes). The solution was extracted twice with

water to remove excess azide. The combined extracts were dried over sodium sulfate, filtered, and the solvent removed by rotary evaporation. The product was purified by dry column vacuum chromatography (silica gel, 98:2 CH_2Cl_2:MeOH) and the solvent was removed under vacuum to give a brown microcrystalline solid (25 mg, 86 % est. purity, 72 % yield). ^{1}H NMR (400 MHz, $CDCl_3$): δ 7.93 (d, *J* = 4.4 Hz, 2H), 7.71 (dt, *J* = 7.4,3.7 Hz, 1H), 7.57-7.50 (m, 2H), 7.46-7.12 (m, 11H), 7.08 (d, *J* = 8.0 Hz, 2H), 5.56 (s, 2H), 5.30 (s, 2H). ^{19}F NMR (376 MHz, $CDCl_3$): δ -136.2 (dd, *J* = 24.0, 8.0 Hz), -151.6 (t, *J* = -22.6 Hz), -160.1 (td, *J* = 23.0, 7.9 Hz). UV-Vis (nm): 400, 430, 550. ESI-MS (+) Calcd: 954.1095 for $C_{47}H_{22}Cu_1F_{10}N_7O_1H$, Observed: 954.1107. Mp: decomposition above 350 ºC.

Iron(III) (5,15-bis(pentafluorophenyl)-10-(4-oxymethyl-(1-benzyl-1,2,3-triazol-4-yl)phenyl)corrole)bis(diethylether) ($(C_6F_5)_2$(*p*-O(CH_2(C_2HN_3($CH_2C_6H_5$)))Ph)corroleFe(Et_2O)$_2$) (**4-12**) was prepared as follows. Iron(III) (5,15-bis(pentafluorophenyl)-10-(4-propargyloxyphenyl)corrole) bis(diethylether) (**4-8**) (33 mg, 0.034 mmol) and benzyl azide (5 mg, 0.038 mmol) were placed in a dry 25 mL Schlenk flask. The flask was evacuated and filled with nitrogen three times, and dry CH_2Cl_2 (5 mL) was added by cannula. Copper(I) acetate (catalytic, approximately 1 mg) was added and the resulting suspension was stirred for 15 minutes at room temperature.[69] The reaction was monitored by thin layer chromatography (silica gel, 1:1 CH_2Cl_2:hexanes). The solution was extracted twice with water to remove excess azide. The combined extracts were dried over sodium sulfate, filtered, and the solvent removed by rotary evaporation. The solid was purified by dry column vacuum chromatography (silica gel, 1:1 diethyl ether:hexanes) The product was dissolved in diethyl ether and 5 μL of hydrazine was added. The solvent was removed by slow evaporation under a stream of nitrogen to isolate the compound as a brown solid (22 mg, 89 % est. purity, 52 % yield). ^{1}H NMR (400 MHz, C_6D_6, 23 °C): δ 10.65 (br s), 9.58 (br s), 9.23 (br s), 8.65 (br s), 5.48 (br s), 4.98 (br s), 3.85 (br s), 3.21 (br s), 1.35 (br s, Et_2O), 0.27 (br s), 0.05 (br s, Et_2O), -38.24 (br s), -50.08 (br s), -107.74 (br s). ^{19}F NMR (376 MHz, C_6D_6, 23 °C): δ -92.9 (br s, ortho-*F*), -150.2 (s, para-*F*), -155.5 (s, meta-*F*). UV-Vis (nm): 410, 561. ESI-MS (+) Calcd: 947.1148 for $C_{47}H_{22}F_{10}Fe_1N_4O_7H$, Observed: 947.1153. Mp: decomposition above 350 ºC.

Copper(III) (5,15-bis(pentafluorophenyl)-10-(3-methynyl-(4-methanol-1,2,3-triazol-1-yl)phenyl corrole ($(C_6F_5)_2$(*m*-$CH_2N_3C_2H$(CH_2OH))Ph)corroleCu) (**4-13**) was prepared as follows. Copper(III) (5,15-bis(pentafluorophenyl)-10-(3-azidomethylphenyl)corrole) (**4-6**) (30 mg, 0.037 mmol) and propargyl alcohol (2.5 mg, 0.045 mmol) were placed in a dry 25 mL Schlenk flask. The flask was evacuated and filled with argon three times, and dry CH_2Cl_2 (5 mL) was added by cannula. Copper(I) acetate (catalytic, approximately 1 mg) was added and the resulting suspension was stirred overnight at room temperature.[69] The reaction was monitored by thin layer chromatography (silica gel, 1:1 CH_2Cl_2:hexanes). After completion, the solvent was removed by rotary evaporation and the resulting solid was purified by column chromatography (silica gel, 98:2 CH_2Cl_2:MeOH, R_f = 0.32 in 98:2 CH_2Cl_2:MeOH) to yield a brown solid (14 mg, 94 % est. purity, 41 % yield). ^{1}H NMR (500 MHz, $CDCl_3$): δ 7.97 (d, *J* = 4.2 Hz, 2H), 7.60-7.40 (m, 6H), 7.23-2.10 (m, 5H), 5.60 (s, 2H), 4.79 (s, 2H), 2.22 (br s, 1H). ^{13}C{^{1}H} (125 MHz, $CDCl_3$): δ 149.6, 148.1, 146.2, 144.2, 142.6, 140.6, 138.8 136.8, 134.9, 131.9, 131.2, 130.4, 129.2, 127.0, 125.3, 123.0, 121.6, 111.6, 108.5, 56.7, 53.9. ^{19}F NMR (470 MHz, $CDCl_3$): δ -136.9 to -137.2 (m), -152.2 (t, *J* = 21.2 Hz), -160.8 (qd, *J* = 21.7, 8.0 Hz). UV-Vis (nm): 304, 548. LR-MS Calcd: 878.1 for $C_4H_{24}Cu_1F_{10}N_7O_1$, Observed: 878.1. Mp: decomposition above 350 ºC.

1-[(10-(3-methylene-phenyl))-5,15-bis(pentafluorophenyl)copper(III)corrole]-4-[(10-(4-oxymethylene))-5,15-bis(pentafluorophenyl)copper(III)corrole]triazole
(Cu(corrole((C_6F_5)$_2$(Ph))-*p*-O-(CH_2)(C_2HN_3)(CH_2)-*m*-(Ph(C_6F_5)$_2$corrole)Cu) (**4-14**) was prepared as follows. Copper(III) (5,15-bis(pentafluorophenyl)-10-(4-propargyloxyphenyl)corrole) (**4-5**) (25 mg, 0.030 mmol) and copper(III) (5,15-bis(pentafluorophenyl)-10-(3-azidomethylphenyl)corrole) (**4-6**) (25 mg, 0.030 mmol) were combined in a dry Schlenk flask under nitrogen. Dry CH_2Cl_2 (5 mL) and copper(I) acetate (catalytic, approximately 3 mg) were added and the reaction was stirred overnight at room temperature.[69] The reaction was monitored by thin layer chromatography (silica, 1:1 CH_2Cl_2:hexanes). The solvent was removed by rotary evaporation and the resulting solid was purified by column chromatography (silica gel, 1:1 CH_2Cl_2:hexanes, ramped to 100 % CH_2Cl_2, ramped to 95:5 CH_2Cl_2:MeOH) and the solvent was removed under vacuum to give a brown microcrystalline solid (45 mg, 93 % est. purity, 84 % yield). ^{1}H NMR (400 MHz, CD_2Cl_2): δ 8.04 (m, 4H), 7.75 (s, 1H), 7.62-7.40 (m, 10H), 7.24 (q, *J* = 5.1 Hz, 6H), 7.17 (d, *J* = 4.6 Hz, 2H), 7.08 (d, *J* – 8.3 Hz, 2H), 5.66 (s, 2H), 5.26 (s, 2H). ^{19}F NMR (376 MHz, CD_2Cl_2): δ -137.1 to -137.4 (m), -152.4 to -152.8 (m), -160.8 to -161.2 (m). UV-Vis (nm): 402, 550. ESI-MS (+) Calcd: 1664.0727 for $C_{78}H_{29}Cu_2F_{20}N_{11}O_1Na_1$, Observed: 1664.0732; Calcd: 1680.0466 for $C_{78}H_{29}Cu_2F_{20}N_{11}O_1K_1$, Observed: 1680.0468. Mp: decomposition above 350 ºC.

1-[(10-(3-methylene-phenyl))-5,15-bis(pentafluorophenyl)copper(III)corrole]-4-[(10-(4-oxymethylene))-5,15-bis(pentafluorophenyl)iron(III)corrole(bis(acetonitrile))]triazole
(Fe(CH_3CN)$_2$(corrole((C_6F_5)$_2$(Ph))-*p*-O-(CH_2)(C_2HN_3)(CH_2)-*m*-(Ph(C_6F_5)$_2$corrole)Cu) (**4-15**) was prepared as follows. Iron(III) (5,15-bis(pentafluorophenyl)-10-(4-propargyloxyphenyl)corrole) bis(diethylether) (**4-8**) (24 mg, 0.025 mmol) and copper(III) (5,15-bis(pentafluorophenyl)-10-(3-azidomethylphenyl)corrole) (**4-6**) (21 mg, 0.025 mmol) were combined in a dry Schlenk flask under nitrogen. Dry CH_2Cl_2 (5 mL) and copper(I) acetate (catalytic, approximately 3 mg) were added and the reaction was stirred overnight at room temperature.[69] The reaction was monitored by thin layer chromatography (silica, CH_2Cl_2:hexanes). The solvent was removed by rotary evaporation and the resultant solid was purified by column chromatography (silica gel, 1:1 CH_2Cl_2:hexanes, ramped to 100 % CH_2Cl_2, ramped to 95:5 CH_2Cl_2:MeOH). The solvent was removed under vacuum, the solid was dissolved in acetonitrile and 5 μL of hydrazine was added. The solvent was degassed with nitrogen and then removed under vacuum on the Schlenk line to produce a brown solid (26 mg, 90 % est. purity, 54 % yield). ^{1}H NMR (400 MHz, CD_3CN, 23 °C): δ 8.01-7.94 (m), 7.75 (d, *J* = 4 Hz), 7.65-7.40 (m), 7.1-4.6 (very br s), 5.81 (br s), 5.44 (s), 4.49 (s), 3.85 (s), 3.60 (s), 3.50 (s), 1.81 (s), 1.28 (s), -1.62 (br s), -12.20 (br s), -32.12 (br s), -83.08 (br s). ^{19}F NMR (376 MHz, CD_3CN, 23 °C): δ - 117.7, -140.5, -158.0, -163.7, -165.2. UV-Vis (nm): 403, 552. ESI-MS (+) Calcd: 1635.0955 for $C_{78}H_{30}Cu_1F_{20}Fe_1N_{11}O_1$, Observed: 1635.1101. Mp: decomposition above 350 ºC.

Cyclic voltammetry of compounds 4-7, 4-9, 4-14 and 4-15. Cyclic voltammetric measurements were performed with a Gamry Reference 600 potentiostat, using either 0.1 M tetraethylammonium tetrafluoroborate ($TEABF_4$) in acetonitrile or 0.1 M tetra-*n*-butylammonium tetrafluoroborate ($TBABF_4$) in CH_2Cl_2. A three-electrode cell was used, with a glassy carbon working electrode (3 mm diameter), a platinum mesh counter electrode, and a Ag/Ag^+ reference electrode. The reference electrode consisted of a silver wire in a solution of 0.01 M $AgNO_3$ and 0.1 M $TEABF_4$ in acetonitrile, separated from the bulk solution by a Vycor

frit. Electrolyte solutions were deoxygenated with nitrogen for at least 10 minutes before any compounds were added and were kept under a blanket of nitrogen during analysis. Between measurements, the working electrode was polished with 0.05 μm alumina and rinsed with distilled water and acetonitrile.

Figures 4.2-4.10 show the cyclic voltammograms of all compounds measured. All potentials are referenced to Ag/Ag^+ (0.01 M Ag^+). Potentials reproduced from other publications have been converted from SCE to Ag/Ag^+ by subtracting 298 mV.[64] All scans shown were taken at 100 mV/s, except for **4-15** (the Cu-Fe complex), which was not sufficiently soluble in acetonitrile (although solubility was better in acetonitrile than in CH_2Cl_2) and had to be measured at 500 mV/s to observe well-resolved peaks. Currents are reported as current densities, calculated using an electrode area of 0.071 cm^2. Arrows on the voltammograms indicate the direction of the first potential sweep.

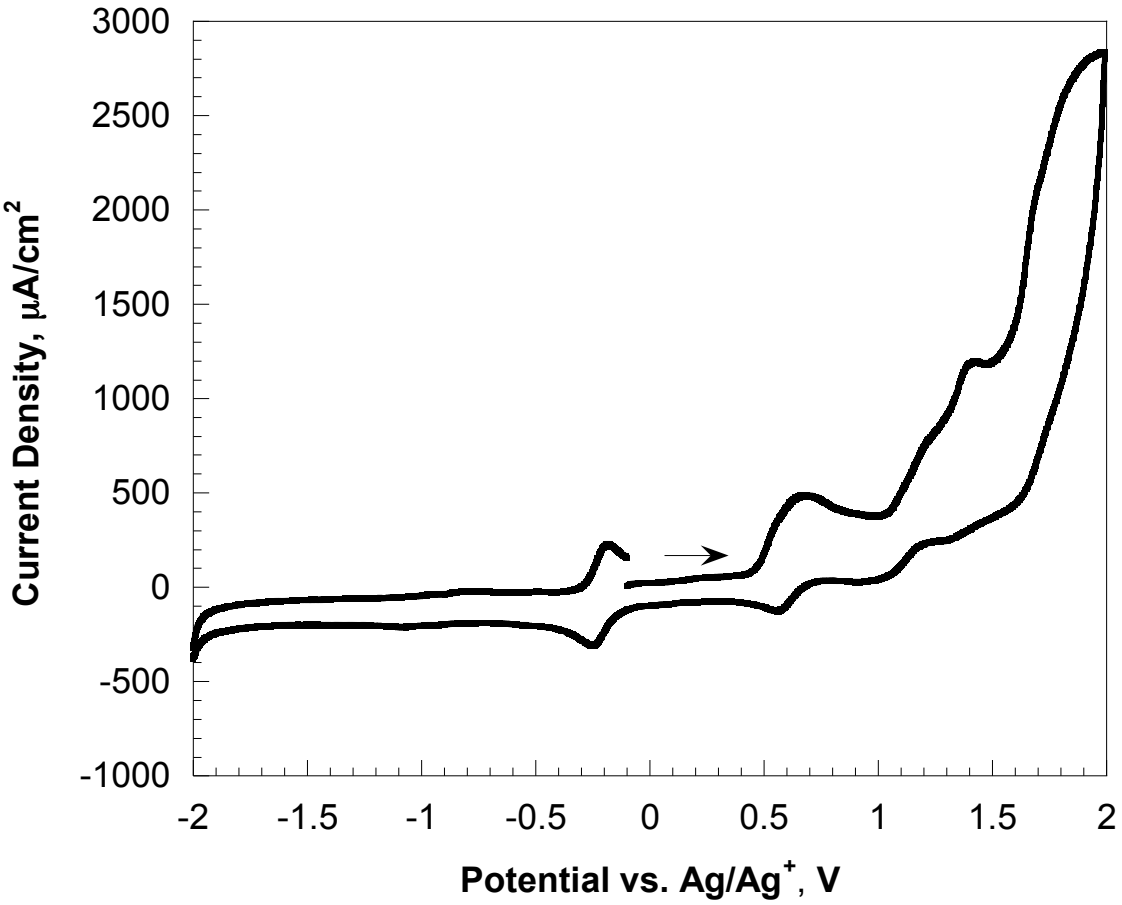

Figure 4.2. Cyclic voltammogram of 1 mM $(C_6F_5)_2$(*p*-OMePh)corroleCu (**4-7**) in acetonitrile, 100 mV/s.

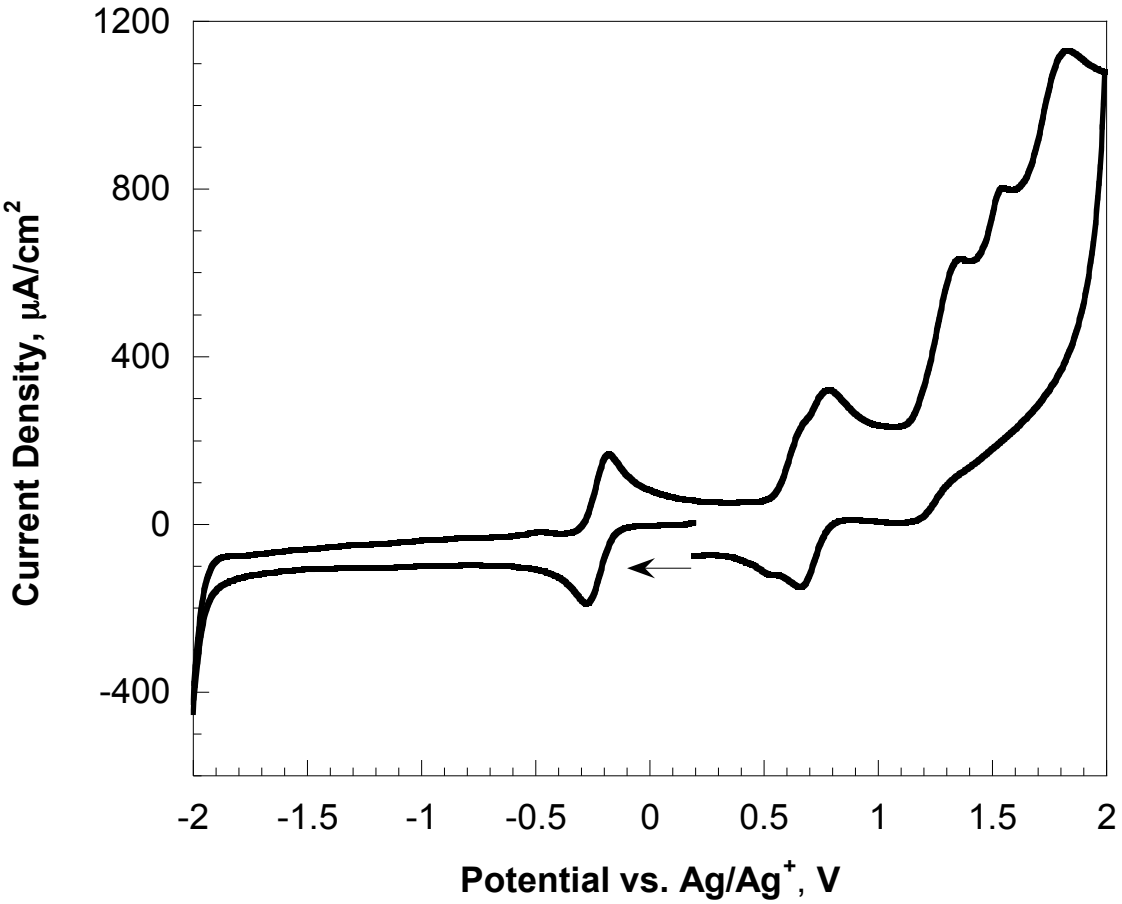

Figure 4.3. Cyclic voltammogram of 1 mM $(C_6F_5)_2$(*p*-OMePh)corroleCu (**4-7**) in CH_2Cl_2, 100 mV/s.

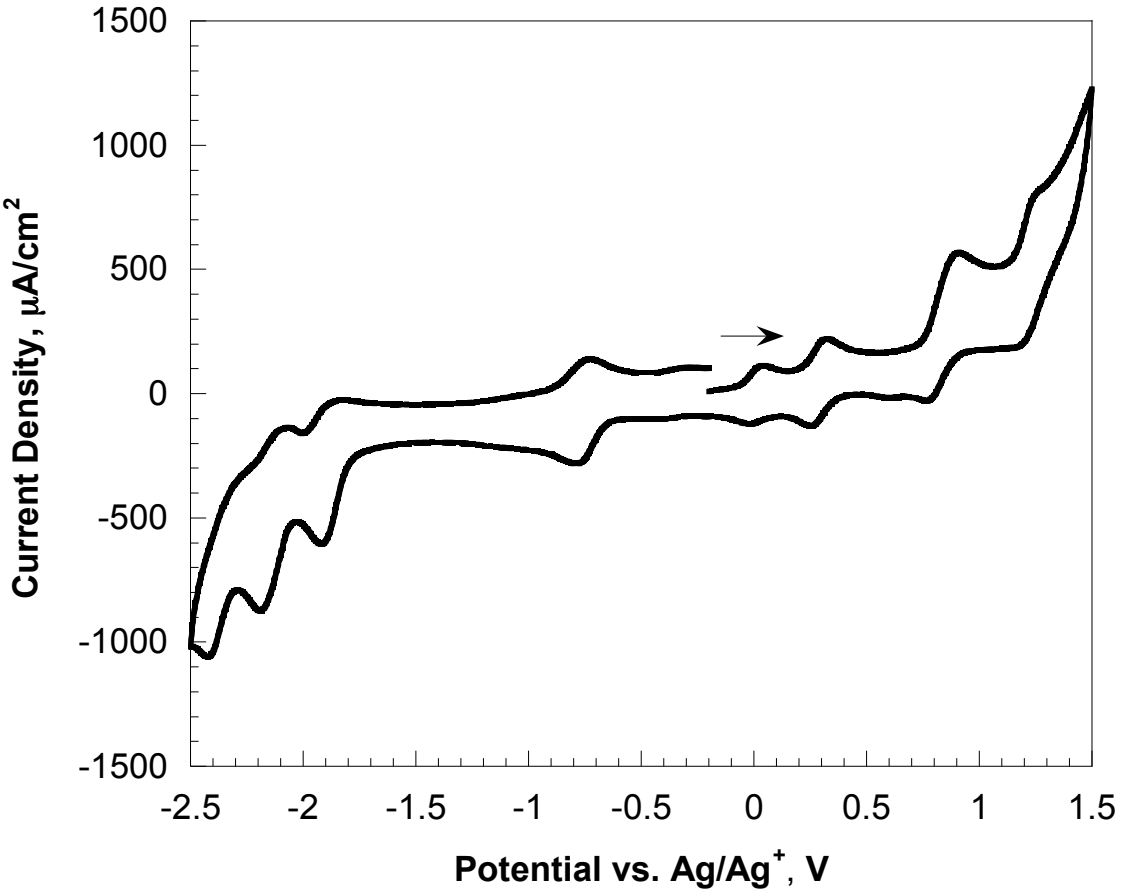

Figure 4.4. Cyclic voltammogram of 1 mM ($(C_6F_5)_2$(*p*-OMePh)corroleFe($Et_2O)_2$) (**4-9**) in acetonitrile, 100 mV/s.

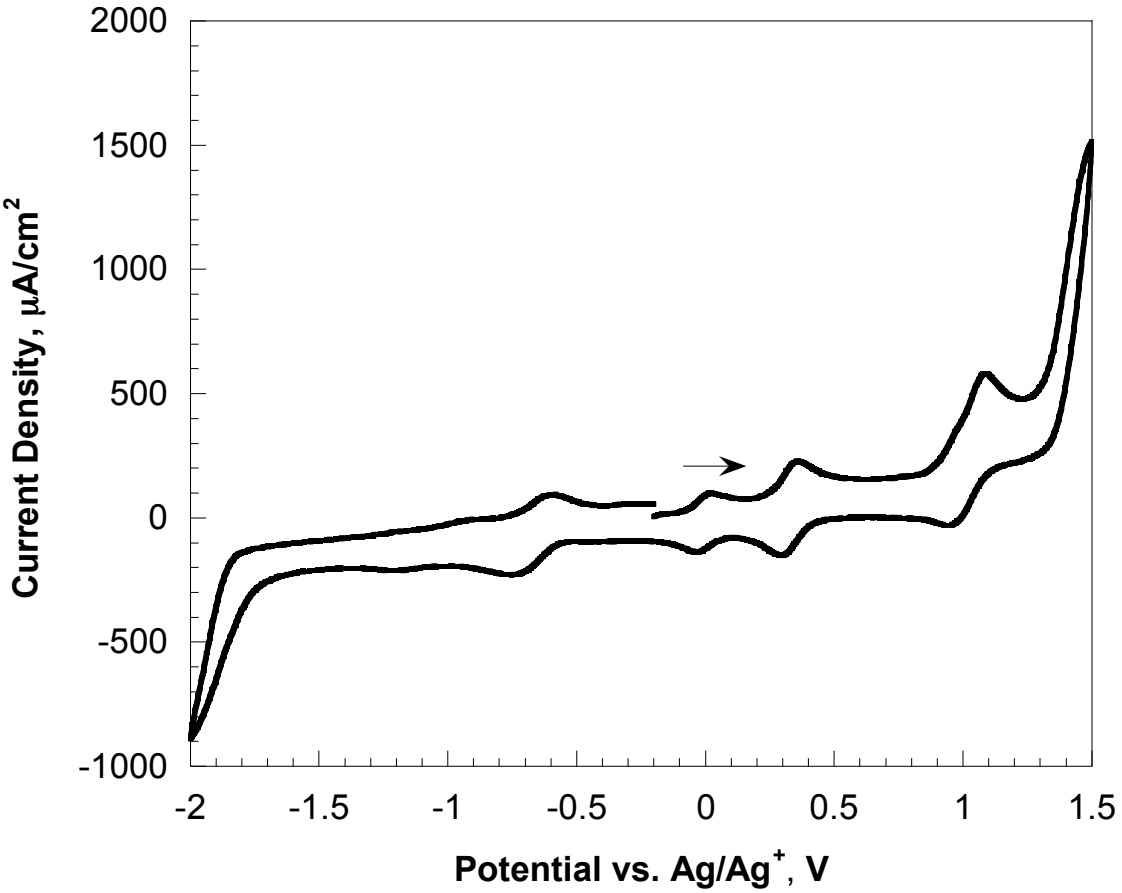

Figure 4.5. Cyclic voltammogram of 1 mM ($(C_6F_5)_2$(*p*-OMePh)corroleFe($Et_2O)_2$) (**4-9**) in CH_2Cl_2, 100 mV/s.

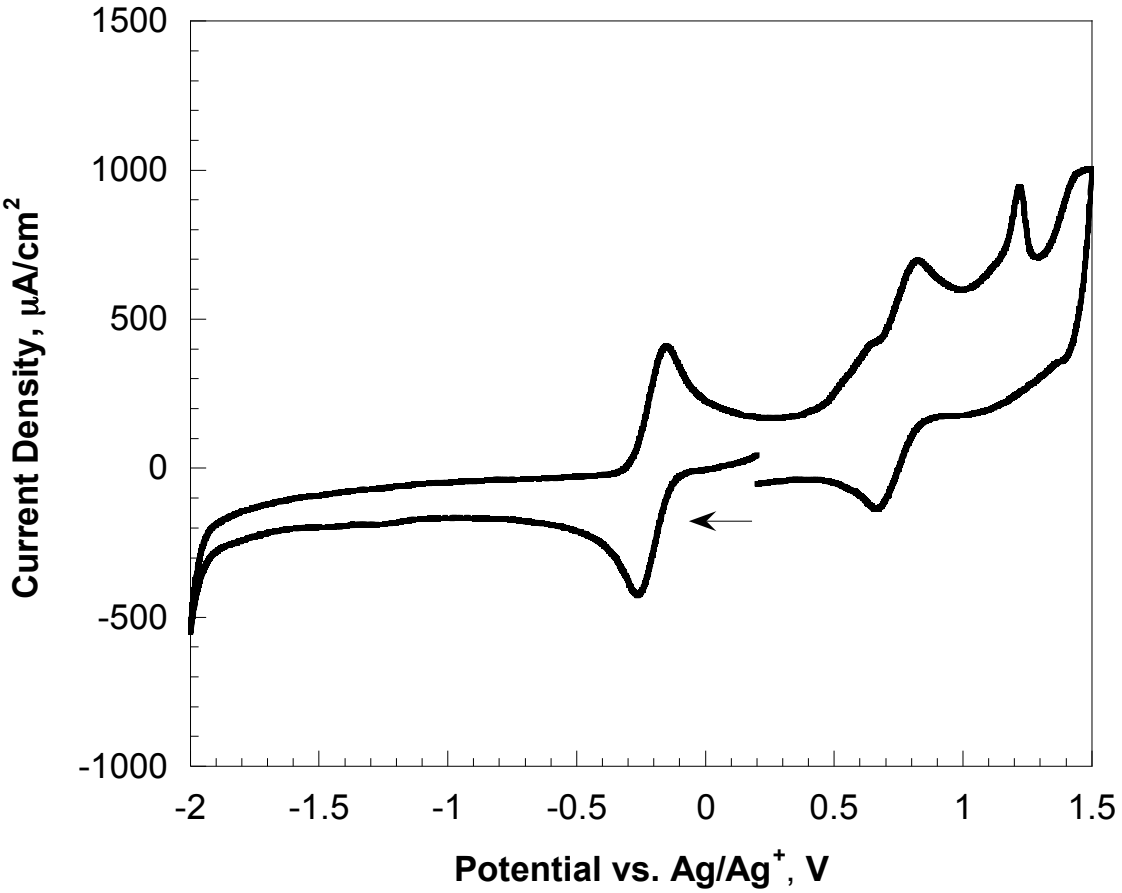

Figure 4.6. Cyclic voltammogram of 1 mM Cu(corrole((C_6F_5)$_2$(Ph))-*p*-O-(CH_2)(C_2HN_3)(CH_2)-*m*-(Ph(C_6F_5)$_2$corrole)Cu (**4-14**) corrole in CH_2Cl_2, 100 mV/s.

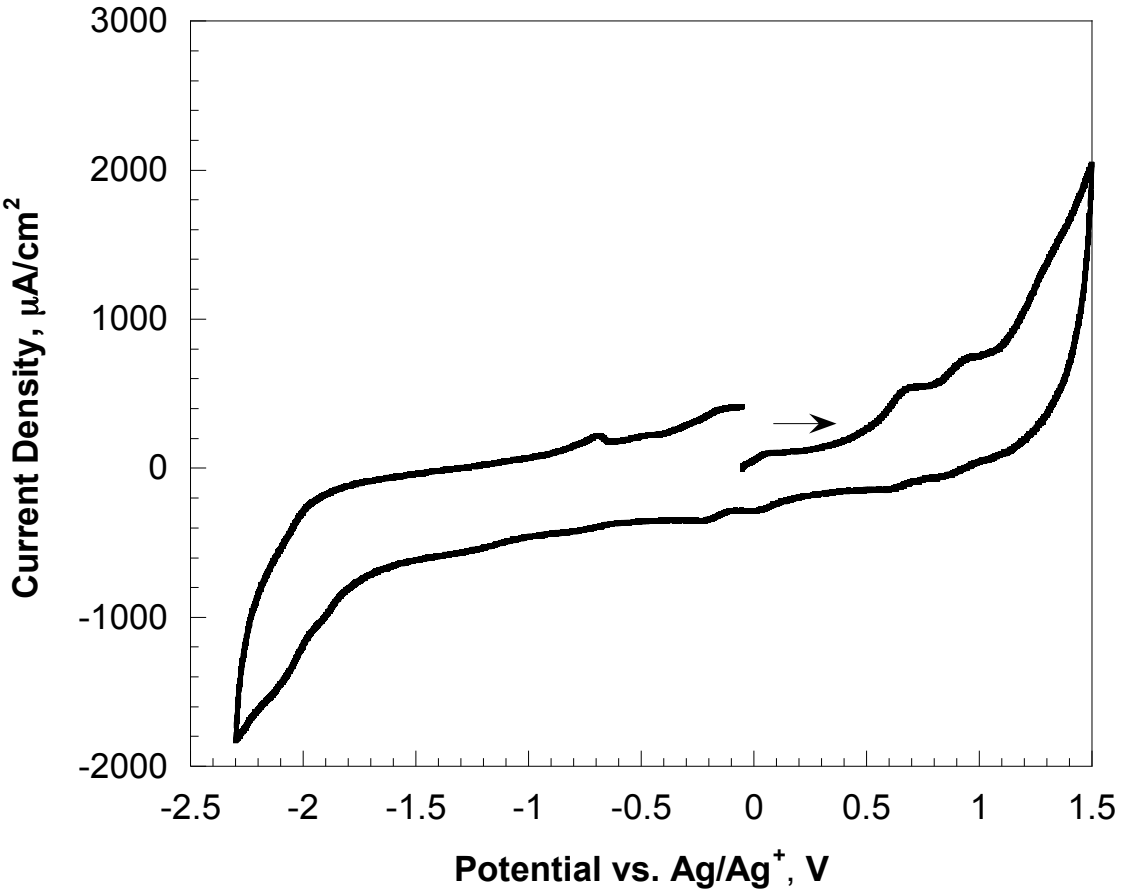

Figure 4.7. Cyclic voltammogram of <1 mM $Fe(CH_3CN)_2$(corrole((C_6F_5)$_2$(Ph))-*p*-O-(CH_2)(C_2HN_3)(CH_2)-*m*-(Ph(C_6F_5)$_2$corrole)Cu (**4-15**) in acetonitrile, 500 mV/s.

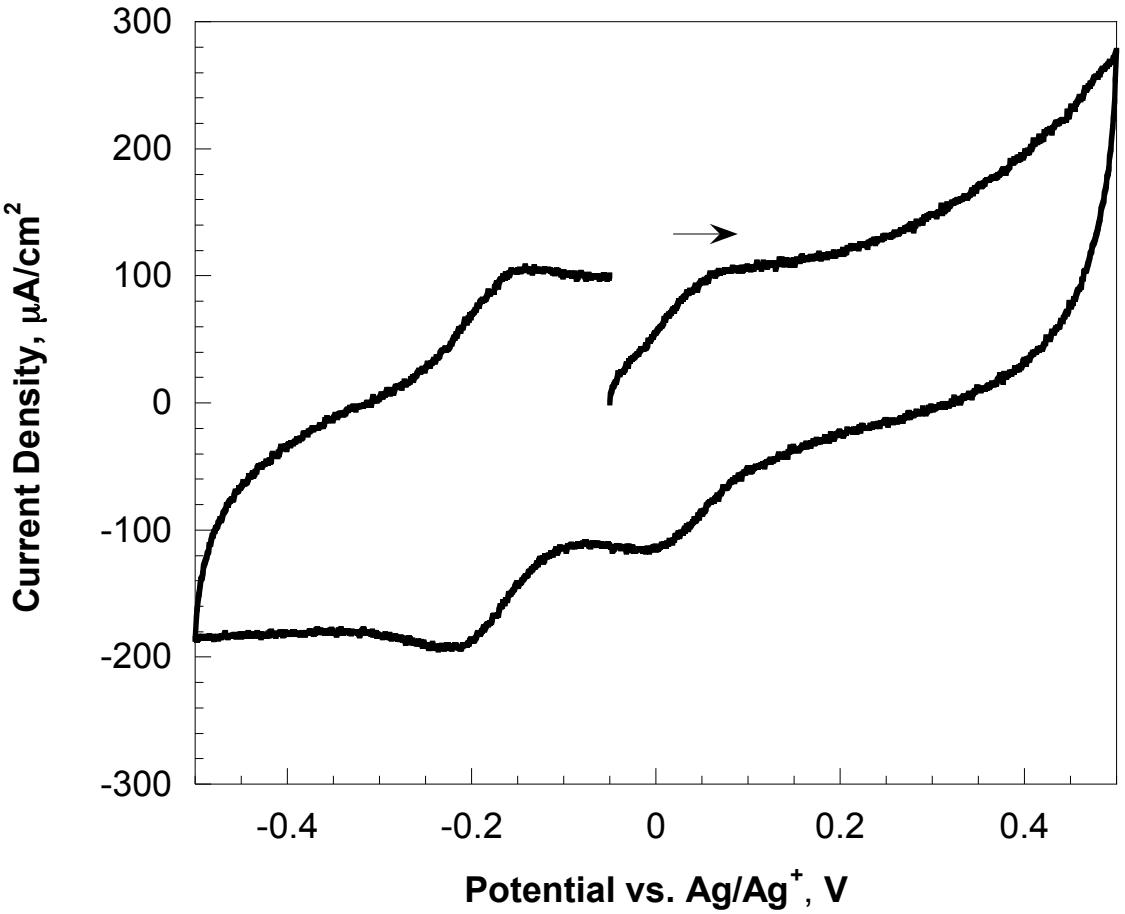

Figure 4.8. Cyclic voltammogram of <1 mM $Fe(CH_3CN)_2$(corrole((C_6F_5)$_2$(Ph))-*p*-O-(CH_2)(C_2HN_3)(CH_2)-*m*-(Ph(C_6F_5)$_2$corrole)Cu (**4-15**) in acetonitrile, focus on Cu and Fe peaks, 500 mV/s.

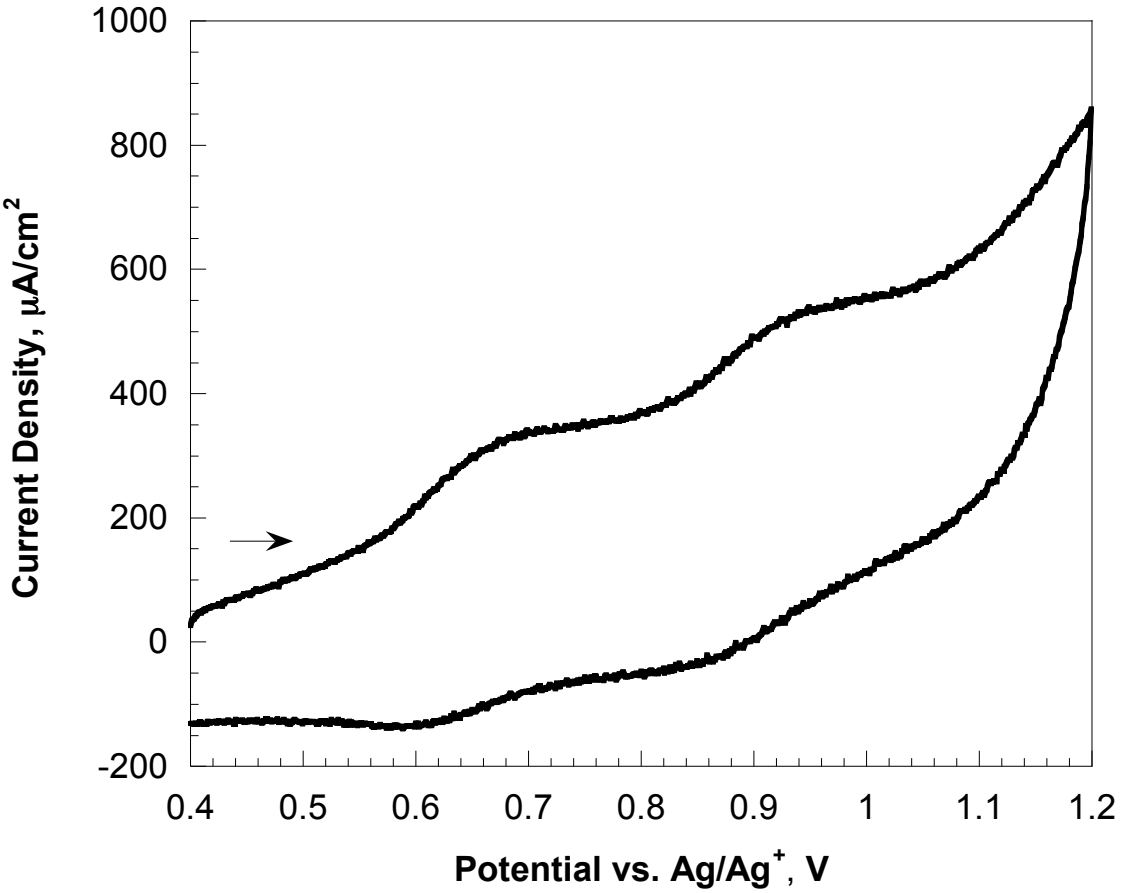

Figure 4.9. Cyclic voltammogram of <1 mM $Fe(CH_3CN)_2$(corrole((C_6F_5)$_2$(Ph))-*p*-O-(CH_2)(C_2HN_3)(CH_2)-*m*-(Ph(C_6F_5)$_2$corrole)Cu (**4-15**) in acetonitrile, focus on ligand oxidation, 500 mV/s.

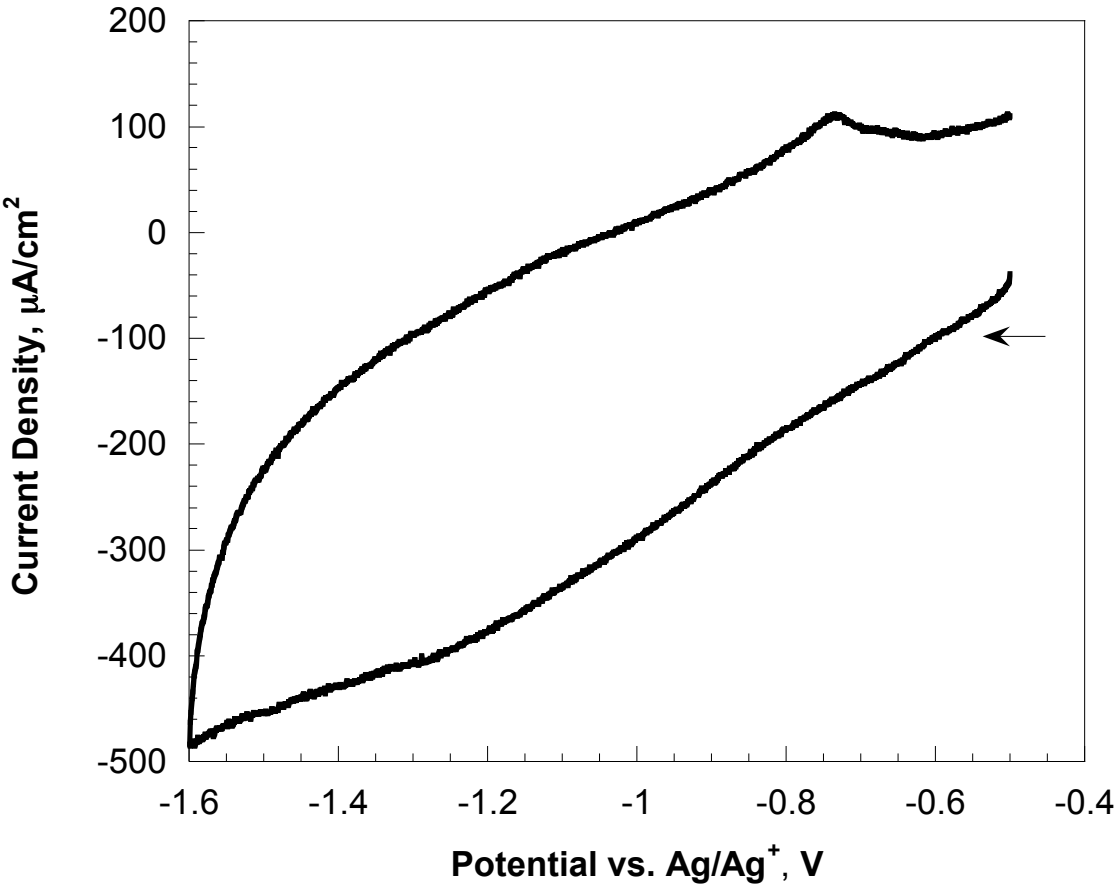

Figure 4.10. Cyclic voltammogram of <1 mM $Fe(CH_3CN)_2$(corrole((C_6F_5)$_2$(Ph))-*p*-O-(CH_2)(C_2HN_3)(CH_2)-*m*-(Ph(C_6F_5)$_2$corrole)Cu (**4-15**) in acetonitrile, focus on oxidative adsorption peak, 500 mV/s.

References

(1) Ishikawa, N.; Sugita, M.; Ishikawa, T.; Koshihara, S.-Y.; Kaizu, Y. *J. Am. Chem. Soc.* **2003**, *125*, 8694–8695.
(2) Woodruff, D. N.; Winpenny, R. E. P.; Layfield, R. A. *Chem. Rev.* **2013**.
(3) Layfield, R. A. *Organometallics* **2014**, *33*, 1084–1099.
(4) Katoh, K.; Asano, R.; Miura, A.; Horii, Y.; Morita, T.; Breedlove, B. K.; Yamashita, M. *Dalt. Trans.* **2014**, *43*, 7716–7725.
(5) Wang, K.; Qi, D.; Wang, H.; Cao, W.; Li, W.; Liu, T.; Duan, C.; Jiang, J. *Chem. Eur. J.* **2013**, *19*, 11162–11166.
(6) Zervaki, G. E.; Roy, M. S.; Panda, M. K.; Angaridis, P. A.; Chrissos, E.; Sharma, G. D.; Coutsolelos, A. G. *Inorg. Chem.* **2013**, *52*, 9813–9825.
(7) Wang, A.; Fang, Y.; Long, L.; Song, Y.; Yu, W.; Zhao, W.; Cifuentes, M. P.; Humphrey, M. G.; Zhang, C. *Chem. Eur. J.* **2013**, *19*, 14159–14170.
(8) Zhu, S.; Kuang, Y.; Geng, F.; Zhu, J.; Wang, C.; Yu, Y.; Luo, Y.; Xiao, Y.; Liu, K.; Meng, Q.; Zhang, L.; Jiang, S.; Zhang, Y.; Wang, G.; Dong, Z.; Hou, J. G. *J. Am. Chem. Soc.* **2013**, *135*, 15794–15800.
(9) Aviv-Harel, I.; Gross, Z. *Chem. Eur. J.* **2009**, *15*, 8382–8394.
(10) Kadish, K. M.; Frémond, L.; Ou, Z.; Shao, J.; Shi, C.; Anson, F. C.; Burdet, F.; Gros, C. P.; Barbe, J.-M.; Guilard, R. *J. Am. Chem. Soc.* **2005**, *127*, 5625–5631.
(11) Dogutan, D. K.; Stoian, S. A.; McGuire, R.; Schwalbe, M.; Teets, T. S.; Nocera, D. G. *J. Am. Chem. Soc.* **2011**, *133*, 131–140.
(12) Collman, J. P.; Kaplun, M.; Decréau, R. A. *Dalt. Trans.* **2006**, 554–559.
(13) Schechter, A.; Stanevsky, M.; Mahammed, A.; Gross, Z. *Inorg. Chem.* **2012**, *51*, 22–24.
(14) Aviv, I.; Gross, Z. *Chem. Commun.* **2006**, 4477–4479.
(15) Mahammed, A.; Mondal, B.; Rana, A.; Dey, A.; Gross, Z. *Chem. Commun.* **2014**, *50*, 2725–2727.
(16) Santos, C. I. M.; Oliveira, E.; Fernández-Lodeiro, J.; Barata, J. F. B.; Santos, S. M.; Faustino, A. F.; Cavaleiro, J. A. S.; Neves, M. G. P. M. S.; Lodeiro, C. *Inorg. Chem.* **2013**, *52*, 8564–8572.
(17) Santos, C. I. M.; Oliveira, E.; Barata, J. F. B.; Faustino, M. A. F.; Cavaleiro, J. a. S.; Neves, M. G. P. M. S.; Lodeiro, C. *Inorg. Chim. Acta* **2014**, *417*, 148–154.
(18) Adi Haber; Ali, A. A.-Y.; Aviram, M.; Gross, Z. *Chem. Commun.* **2013**, *49*, 10917–10919.
(19) Agadjanian, H.; Ma, J.; Rentsendorj, A.; Valluripalli, V.; Youn, J.; Mahammed, A.; Farkas, D. L.; Gray, H. B.; Gross, Z.; Medina-Kauwe, L. K. *PNAS* **2009**, *106*, 6105–6110.
(20) Liang, X.; Mack, J.; Zheng, L.; Shen, Z.; Kobayashi, N. *Inorg. Chem.* **2014**, *53*, 2797–2802.
(21) Zhang, X.; Zhang, Y. *Molecules* **2013**, *18*, 7145–7159.
(22) Blumenfeld, C. M.; Grubbs, R. H.; Moats, R. A.; Gray, H. B.; Sorasaenee, K. *Inorg. Chem.* **2013**, *52*, 4774–4776.
(23) Worrell, B. T.; Malik, J. A.; Fokin, V. V. *Science (80-.).* **2013**, *340*, 457–460.
(24) Kolb, H. C.; Finn, M. G.; Sharpless, K. B. *Angew. Chem. Int. Ed. Engl.* **2001**, *40*, 2004–2021.
(25) Huisgen, R. *J. Org. Chem.* **1976**, *41*, 403–419.

(26) Gomila, A.; Le Poul, N.; Cosquer, N.; Kerbaol, J.-M.; Noël, J.-M.; Reddy, M. T.; Jabin, I.; Reinaud, O.; Conan, F.; Le Mest, Y. *Dalt. Trans.* **2010**, *39*, 11516–11518.
(27) Jain, S.; Reiser, O. *ChemSusChem* **2008**, *1*, 534–541.
(28) Jee, J.-E.; Cheong, J. L.; Lim, J.; Chen, C.; Hong, S. H.; Lee, S. S. *J. Org. Chem.* **2013**, *78*, 3048–3056.
(29) Stenehjem, E. D.; Ziatdinov, V. R.; Stack, T. D. P.; Chidsey, C. E. D. *J. Am. Chem. Soc.* **2012**, *135*, 1110–1116.
(30) Prescher, J. A.; Dube, D. H.; Bertozzi, C. R. *Nature* **2004**, *430*, 873–877.
(31) Gobbo, P.; Mossman, Z.; Nazemi, A.; Niaux, A.; Biesinger, M. C.; Gillies, E. R.; Workentin, M. S. *J. Mater. Chem. B* **2014**, *2*, 1764–1769.
(32) Yu, M.; Price, J. R.; Jensen, P.; Lovitt, C. J.; Shelper, T.; Duffy, S.; Windus, L. C.; Avery, V. M.; Rutledge, P. J.; Todd, M. H. *Inorg. Chem.* **2011**, *50*, 12823–12835.
(33) Uttamapinant, C.; Tangpeerachaikul, A.; Grecian, S.; Clarke, S.; Singh, U.; Slade, P.; Gee, K. R.; Ting, A. Y. *Angew. Chem. Int. Ed.* **2012**, *51*, 5852–5856.
(34) Beahm, B. J.; Dehnert, K. W.; Derr, N. L.; Kuhn, J.; Eberhart, J. K.; Spillmann, D.; Amacher, S. L.; Bertozzi, C. R. *Angew. Chem. Int. Ed.* **2014**, *53*, 3347–3352.
(35) Gao, X.; Hannoush, R. N. *J. Am. Chem. Soc.* **2014**, *136*, 4544–4550.
(36) McCreery, R. L. *Chem. Rev.* **2008**, *108*, 2646–2687.
(37) Collman, J. P.; Devaraj, N. K.; Chidsey, C. E. D. *Langmuir* **2004**, *20*, 1051–1053.
(38) Devadoss, A.; Chidsey, C. E. D. *J. Am. Chem. Soc.* **2007**, *129*, 5370–5371.
(39) Lang, K.; Chin, J. W. *Chem. Rev.* **2014**, *114*, 4764–4806.
(40) Laughlin, S. T.; Agard, N. J.; Baskin, J. M.; Carrico, I. S.; Chang, P. V.; Ganguli, A. S.; Hangauer, M. J.; Lo, A.; Prescher, J. A.; Bertozzi, C. R. *Method Enzym.* **2006**, *415*, 230–250.
(41) Yao, S. A.; Ruther, R. E.; Zhang, L.; Franking, R. A.; Hamers, R. J.; Berry, J. F. *J. Am. Chem. Soc.* **2012**, *134*, 15632–15635.
(42) Coates, M.; Nyokong, T. *J. Electroanal. Chem.* **2012**, *687*, 111–116.
(43) Chromiński, M.; Zieleniewska, A.; Karczewski, M.; Gryko, D. *J. Porphyrins Phthalocyanines* **2014**, *18*, 1–15.
(44) Polevaya, Y. P.; Tyurin, V. S.; Beletskaya, I. P. *J. Porphyrins Phthalocyanines* **2014**, *18*, 20–34.
(45) Barbe, J.-M.; Canard, G.; Brandès, S.; Guilard, R. *Eur. J. Inorg. Chem.* **2005**, 4601–4611.
(46) Brizet, B.; Desbois, N.; Bonnot, A.; Langlois, A.; Dubois, A.; Barbe, J.-M.; Gros, C. P.; Goze, C.; Denat, F.; Harvey, P. D. *Inorg. Chem.* **2014**, *53*, 3392–3403.
(47) Tasior, M.; Voloshchuk, R.; Poronik, Y. M.; Rowicki, T.; Gryko, D. T. *J. Porphyrins Phthalocyanines* **2011**, *15*, 1011–1023.
(48) Tasior, M.; Gryko, D. T.; Pielacińska, D. J.; Zanelli, A.; Flamigni, L. *Chem. Asian J.* **2010**, *5*, 130–140.
(49) Koszarna, B.; Gryko, D. T. *J. Org. Chem.* **2006**, *71*, 3707–3717.
(50) Díaz-Moscoso, A.; Tizzard, G. J.; Coles, S. J.; Cammidge, A. N. *Angew. Chem. Int. Ed.* **2013**, *52*, 10784–10787.
(51) Chang, C. J.; Loh, Z.-H.; Shi, C.; Anson, F. C.; Nocera, D. G. *J. Am. Chem. Soc.* **2004**, *126*, 10013–10020.
(52) Gros, C. P.; Brisach, F.; Meristoudi, A.; Espinosa, E.; Guilard, R.; Harvey, P. D. *Inorg. Chem.* **2007**, *46*, 125–135.
(53) Gryko, D. T.; Koszarna, B. *Synthesis (Stuttg).* **2004**, *2004*, 2205–2209.

(54) Shen, J.; Shao, J.; Ou, Z.; E, W.; Koszarna, B.; Gryko, D. T.; Kadish, K. M. *Inorg. Chem.* **2006**, *45*, 2251–2265.
(55) Flamigni, L.; Gryko, D. T. *Chem. Soc. Rev.* **2009**, *38*, 1635–1646.
(56) Szeja, W. *Synthesis (Stuttg).* **1979**, *1979*, 822–823.
(57) Luobeznova, I.; Simkhovich, L.; Goldberg, I.; Gross, Z. *Eur. J. Inorg. Chem.* **2004**, 1724–1732.
(58) Simkhovich, L.; Mahammed, A.; Goldberg, I.; Gross, Z. *Chem. Eur. J.* **2001**, 1041–1055.
(59) Shao, C.; Cheng, G.; Su, D.; Xu, J.; Wang, X.; Hu, Y. *Adv. Synth. Catal.* **2010**, *352*, 1587–1592.
(60) Ward, A. L.; Buckley, H. L.; Lukens, W. W.; Arnold, J. *J. Am. Chem. Soc.* **2013**, *135*, 13965–13971.
(61) Padilla, R.; Buckley, H. L.; Ward, A. L.; Arnold, J. *Chem. Commun.* **2014**, *50*, 2922–2924.
(62) Nigel-Etinger, I.; Goldberg, I.; Gross, Z. *Inorg. Chem.* **2012**, *51*, 1983–1985.
(63) Ou, Z.; Shao, J.; Zhao, H.; Ohkubo, K.; Wasbotten, I. H.; Fukuzumi, S.; Ghosh, A.; Kadish, K. M. *J. Porphyrins Phthalocyanines* **2004**, *8*, 1236–1247.
(64) Pavlishchuk, V. V.; Addison, A. W. *Inorg. Chim. Acta* **2000**, *298*, 97–102.
(65) Alaimo, P. J.; Peters, D. W.; Arnold, J.; Bergman, R. G. *J. Chem. Ed.* **2001**, *78*, 64.
(66) Laha, J. K.; Dhanalekshmi, S.; Taniguchi, M.; Ambroise, A.; Lindsey, J. S. *Org. Proc. Res. Dev.* **2003**, *7*, 799–812.
(67) Hoogendoorn, S.; Blom, A. E. M.; Willems, L. I.; Van Der Marel, G. A.; Overkleeft, H. S. *Org. Lett.* **2011**, *13*, 5656–5659.
(68) Pan, Z.; Harischandra, D. N.; Newcomb, M. *J. Inorg. Biochem.* **2009**, *103*, 174–181.
(69) Shao, C.; Cheng, G.; Su, D.; Xu, J.; Wang, X.; Hu, Y. *Adv. Synth. Catal.* **2010**, *352*, 1587–1592.

Appendix A: Group 5 Imido and Oxo-Bridged Corrole Complexes

The first isolated group 5 corrole complexes were prepared; notably the niobium and tantalum complexes are also the first reported corrole complexes of these elements.

Results and Discussion

The tantalum(V) corrole imido complex (Mes_2(*p*-OMePh)corrole)TaN=*t*Bu (**A-2**) was prepared by the combination in toluene at room temperature of (Mes_2(*p*-OMePh)corrole)Li_3·6THF with 1.1 equivalents of Cl_3TaN=*t*Bu$(py)_2$ (py = pyridine) (Scheme A.1). Stirring overnight results in a deep red solution. Removal of the solvent and recrystallization of the solid by from pentane yields deep a red microcrystalline powder, which was characterized by ^{1}H NMR spectroscopy, UV-visible spectroscopy and ESI-MS (63 % yield).

Extensive attempts were made to grow crystals of suitable quality for X-ray diffraction studies including a range of solvents and the introduction of strongly coordinating ligands, but all attempts resulted in hydrolysis of the Ta=N bond and a concurrent color change from deep red to cherry red solution. This hydrolysis was also observed in the course of obtaining ESI-MS data on **A-2**. The use of silanized glassware prevented this reaction, indicating that terminal oxygen atoms on glassware and not improper technique were responsible for the observed hydrolysis; however under these conditions it was not possible to obtain X-ray quality crystals. This is consistent with difficulties encountered by other researchers in growing crystals of other low symmetry corrole complexes.[1]

Reacting **A-2** with a slight excess of potassium hydroxide in D_2O on a small scale led to the formation of hydrolysis product **A-3** (32 mg, 73 % yield). This compound was characterized by ^{1}H NMR spectroscopy, UV-visible spectroscopy and ESI-MS.

Despite the lack of success in obtaining X-ray diffraction data for **A-2**, X-ray quality crystals of **A-3** were obtained. This data confirmed that in the solid state, **A-3** is a bridged μ-oxo dimer with abbreviated chemical formula [(Mes_2(*p*-OMePh)corrole)Ta(μ-O)]$_2$, which is consistent with its greater stability and higher symmetry than **A-2** which allowed for growth of high quality crystals. The structure of **A-3** is shown in Figure A.1.; two oxygen atoms are disordered over the three bridging positions in the structure.

The niobium(V) imido corrole complex (Mes_2(*p*-OMePh)corrole)NbN=*t*Bu (**A-4**) was prepared by the same method as the tantalum corrole, and a deep red powder was characterized by ^{1}H NMR spectroscopy, UV-visible spectroscopy and ESI-MS (56 % yield). The *tert*-butyl group is again observed at -0.79 ppm in the ^{1}H NMR spectrum. **A-4** was also prepared from the free-base corrole (Mes_2(*p*-OMePh)corrole)H_3 and (benzyl)$_3$NbN=*t*Bu in 51 % yield. As is the case with the tantalum complex, the niobium(V) imido corrole eluded attempts at obtaining X-ray quality crystals. However, they hydrolysis product **A-5** was prepared (25 mg, 71 % yield) and characterized by ^{1}H NMR spectroscopy, UV-visible spectroscopy and ESI-MS. X-ray diffraction data was obtained for the bridged μ-oxo dimer **A-5**.

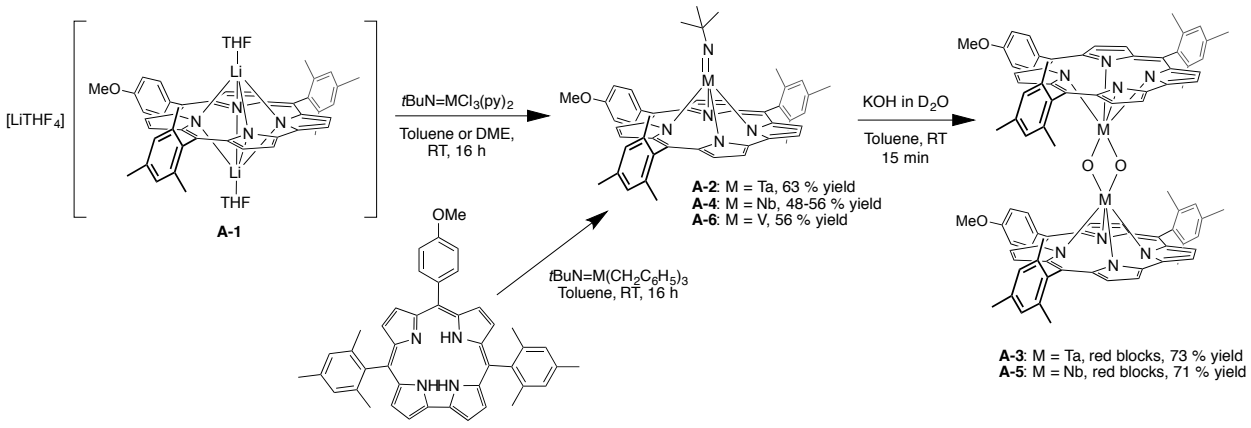

Scheme A.1: Synthesis of Ta, Nb, and V imido corroles **A-2**, **A-4**, and **A-6** and subsequent hydrolysis of **A-2** and **A-4** to bridged oxo species **A-3** and **A-5**.

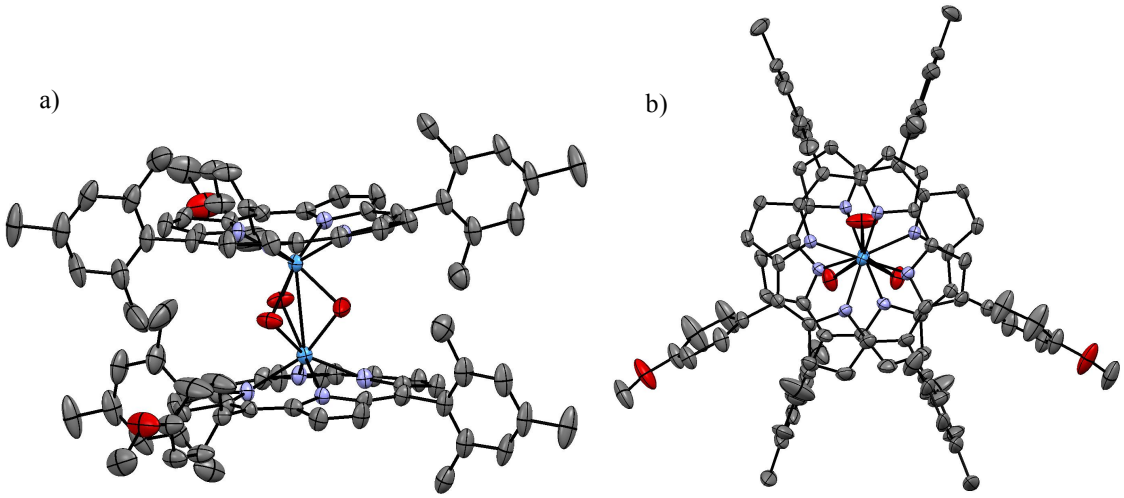

Figure A.1. Molecular structure of tantalum corrole μ-oxo dimer **A-3**, a) side view and b) top view, determined by single-crystal X-ray diffraction. H atoms omitted for clarity; thermal ellipsoids at 50 % probability level.

The vanadium(V) imido corrole complex (Mes_2(*p*-OMePh)corrole)NbN=*t*Bu (**A-6**) was also prepared by the same method as the tungsten corrole, and a deep red powder was characterized by ^{1}H NMR spectroscopy, UV-visible spectroscopy and ESI-MS (56 % yield). Although evidence of the hydrolysis product was observed by ESI-MS, it was not isolated for structural characterization.

The ^{1}H NMR spectra of all three imido complexes exhibit a characteristic signal corresponding to the *tert*-butyl protons. Due to the anisotropy of the corrole ring, the *tert*-butyl group is significantly shielded. As such, the tantalum and niobium complexes **A-2** and **A-4** exhibit this singlet at -0.80 and -0.79 ppm respectively. The similarity in chemical shift is consistent with the similar size and displacement of the two metals from the corrole ring (see analysis of X-ray structures below). The vanadium complex **A-6** exhibits the corresponding peak at -1.11 ppm, consistent with the smaller atomic radius of vanadium which would cause the metal and therefore the *tert*-butyl group to sit closer to the shielding of the corrole ring.

The structures of both the tantalum and niobium corrole are directly analogous to that of the tungsten corrole bridging oxo species recently reported by Gross and coworkers;[2] this similarity is highlighted by the disorder of the two oxygen atoms over three positions in both **A-3** and **A-5**. The niobium (Nb-N_4 plane distance = 0.987 Å) and tantalum (Ta-N_4 plane distance = 0.967 Å) sit slightly further from the N_4 plane of the corrole than does the reported tungsten compound (W-N_4 plane distance = 0.961-0.970 Å); this is consistent with hexavalent tungsten ion being smaller than the pentavalent niobium and tantalum. The structures of **A-3** and **A-5** are also similar to that of previously reported tris(μ-oxo)bis(tetraphenyl porphyrin niobium(V)).[3,4] The Nb-N_4 plane distance for the porphyrin (1.000 Å) is slightly longer than for the corrole complexes.

In summary, we have isolated and characterized the first examples of tanatalum, niobium, and vanadium corrole complexes as imido species, and confirmed the formation of tantalum and niobium corroles through the structural characterization of their bridged μ-oxo analogues. Studies are ongoing to determine reactivity of group 5 metallocorrole complexes.

Future Work

To determine conclusively the source of the oxygen in the rational syntheses of **A-3** and **A-5**, several experiments could be performed. Reaction of **A-2** or **A-4** with ^{18}O-labeled D_2O would allow characterization of **A-3**-^{18}O or **A-5**-^{18}O by mass spectrometry and possibly identification of the M-O stretches by infrared spectroscopy. Addition of an ^{18}O-labeled aldehyde or ketone (such as benzophenone) would allow identification of the same compounds, as well as of the benzophenone imine. Reaction with dry oxygen to determine the sensitivity of the imine group to the presence of O_2 will also be a useful gauge of the stability of this complex.

Experimental Details

General Considerations

Unless otherwise noted, all reactions were performed using standard Schlenk and N_2-atmosphere glovebox techniques. Glassware and cannulae were stored in an oven at *ca.* 180 ºC. Solvents were dried by passing through a column of activated alumina and degassed with nitrogen.[5] C_6D_6 was dried over Na/benzophenone, and vacuum transferred. All NMR spectra were obtained in C_7D_8 at ambient temperature using Bruker AVB-400, AVQ-400 or DRX-500 spectrometers. ^{1}H NMR chemical shifts (δ) were calibrated relative to residual solvent peak. UV-visible spectra were determined with a Varian Cary 50UV-vis spectrophotometer using a 1 mm quartz cell. Mass spectral data (ESI-MS, positive mode) were obtained at the University of California, Berkeley Microanalytical Facility, using vacuum-dried samples dissolved in dry THF. X-ray crystal diffraction analyses were performed at the University of California, Berkeley CHEXRAY facility. Melting points were determined using sealed capillaries prepared under nitrogen and are uncorrected. 5,15-bis(2,4,6-trimethylphenyl)-10-(4-methoxyphenyl)corrole (Mes_2(*p*-OMePh)corroleH$_3$) and trilithium 5,15-bis(2,4,6-trimethylphenyl)-10-(4-methoxyphenyl)corrole hexakis(tetrahydrofuran) (Mes_2(*p*-OMePh)corroleLi$_3$·6THF), Cl_3VN=*t*Bu, Cl_3NbN=*t*Bu(py)$_2$, Cl_3TaN=*t*Bu(py)$_2$, and Bn_3NbN=*t*Bu were prepared according to previously reported procedures.[6,7] Where indicated, glassware was silanized according to a previously reported procedure.[8]

Synthesis and characterization of free base corrole and of complexes A-2 to A-6

***Tert*-butyl imido tantalum(V) 5,15-bis(2,4,6-trimethylphenyl)-10-(4-methoxyphenyl) corrole** (*t*-BuN=TaMes$_2$(*p*-OMePh)corrole) (**A-2**). Mes$_2$(*p*-OMePh)corroleLi$_3$·6THF (100 mg, 0.092 mmol) and Cl_3TaN=*t*Bu(py)$_2$ (48 mg, 0.092 mmol) were combined in a silanized vial in the glovebox and 6 mL toluene was added. The solution was stirred overnight. The solvent was removed under vacuum and the resulting solid was extracted with pentane, filtered through silanized glass wool and concentrated. The solution was cooled to -40 ºC in a silanized vial to generate a deep red microcrystalline powder (52 mg, 63% yield). ^{1}H NMR (500 MHz, C_7D_8): δ 8.97 (d, *J* = 4.0 Hz, 2H, β-*H*), 8.79 (d, *J* = 4.1 Hz, 2H, β-*H*), 8.73 (d, *J* = 4.3 Hz, 2H, β-*H*), 8.55 (d, *J* = 4.0 Hz, 2H, β-*H*), 7.38 (d, *J* = 8.3 Hz, 1H, C_6H_3*H*-OMe), 7.35 (s, 2H, $C_6H_2Me_3$), 7.23 (s, 2H, $C_6H_2Me_3$), 7.10-7.05 (obscured multiplet, 2H, C_6H_3*H*-OMe), 6.86 (d, *J* = 8.3 Hz, 1H, C_6H_3*H*-OMe), 3.50 (s, 3H, OC*H*$_3$), 2.54 (s, 6H, $C_6H_2Me_2CH_3$), 2.47 (s, 6H, $C_6H_2Me_2CH_3$), 1.74 (s, 6H, $C_6H_2Me_2CH_3$), -0.80 (s, 9H, NC(C*H*$_3$)$_3$). UV-vis (nm): 415, 563. ESI-MS (+) Calcd: 889.3177 for $C_{48}H_{46}O_1N_5Ta_1$ Observed: 889.3182. Mp: decomposition above 350 ºC.

Tantalum(V) 5,15-bis(2,4,6-trimethylphenyl)-10-(4-methoxyphenyl) corrole μ-oxo dimer ([(μ-O)TaMes$_2$(*p*-OMePh)corrole]$_2$) (**A-3**). *t*-BuN=TaMes$_2$(*p*-OMePh)corrole (**A-2**) (48 mg, 0.054 mmol) was dissolved in 0.7 mL *d*$_8$-toluene in an NMR tube. Saturated KOH in D_2O (10 μL) was added, resulting in an immediate colour change from deep red to blood-red, and the resulting solution was shaken and allowed to stand for 15 minutes. Solvent was removed under vacuum and the resulting solid was extracted using a minimum volume of toluene to obtain a blood red powder (32 mg, 73 % yield). ^{1}H NMR (400 MHz, C_7D_8): δ 8.46 (s, 1H), 8.23 (s, 6H), 8.02 (d, *J* = 8.2 Hz, 1H, C_6H_3*H*-OMe), 7.30, (s, 2H), 7.16 (s, 1H), 6.86 (d, *J* = 8.1 Hz, 1H,

C_6H_3*H*-OMe), 6.69 (s, 4H), 3.54 (s, 3H, OCH_3), 2.48 (s, 6H, $C_6H_2Me_2CH_3$), 1.87-1.40 (m, 6H), 1.08 (s, 6H, $C_6H_2Me_2CH_3$). UV-vis (nm): 414, 563. ESI-MS (+) Calcd: 835.2475 for 1/2($C_{88}H_{74}O_4N_8Ta_2$)+2H^+ (full weight is greater than detection limit of ESI-MS – $M(2H)^{2+}$ ion detected) Observed: 835.2493. Mp: decomposition above 350 ºC.

***Tert*-butyl imido niobium(V) 5,15-bis(2,4,6-trimethylphenyl)-10-(4-methoxyphenyl) corrole** (*t*-BuN=NbMes$_2$(*p*-OMePh)corrole) (**A-4**). Procedure A: Mes$_2$(*p*-OMePh)corroleLi$_3$·6THF (100 mg, 0.092 mmol) and Cl_3NbN=*t*Bu(py)$_2$ (39 mg, 0.092 mmol) were combined in a silanized vial in the glovebox and 6 mL toluene was added. The solution was stirred overnight. The solvent was removed under vacuum and the resulting solid was extracted with hexane, filtered through silanized glass wool and concentrated. The solution was cooled to -40 ºC in a silanized vial to generate a deep red powder (41 mg, 56 % yield). Procedure B: Mes$_2$(*p*-OMePh)corroleH_3 (75 mg, 0.117 mmol) and $(C_6H_5CH_2)_3NbN$=*t*Bu (51 mg, 0.177 mmol) were combined in a vial in the glovebox and 8 mL toluene was added. The solution was stirred overnight. The solvent was removed under vacuum and the resulting solid was extracted with pentane, filtered and concentrated. The solution was cooled to -40 ºC to generate a deep red powder (48 mg, 51 % yield). ^{1}H NMR (500 MHz, C_7D_8): δ 8.97 (d, *J* = 4.0 Hz, 2H, β-*H*), 8.79 (d, *J* = 4.0 Hz, 2H, β-*H*), 8.73 (d, *J* = 4.3 Hz, 2H, β-*H*), 8.55 (d, *J* = 4.0 Hz, 2H, β-*H*), 7.39 (d, *J* = 7.7 Hz, 1H, C_6H_3*H*-OMe), 7.33 (s, 2H, $C_6H_2Me_3$), 7.23 (s, 2H, $C_6H_2Me_3$), 7.15-7.05 (obscured multiplet, 2H, C_6H_3*H*-OMe), 6.84 (d, *J* = 8.3 Hz, 1H, C_6H_3*H*-OMe), 3.49 (s, 3H, OCH_3), 2.54 (s, 6H, $C_6H_2Me_2CH_3$), 2.52 (s, 6H, $C_6H_2Me_2CH_3$), 1.74 (s, 6H, $C_6H_2Me_2CH_3$), -0.79 (s, 9H, NC(CH_3)$_3$). UV-vis (nm): 409, 565. ESI-MS (+) Calcd: 801.2761 for $C_{48}H_{46}O_1N_5Nb_1$ Observed: 801.2763. Mp: decomposition above 350 ºC.

Niobium(V) 5,15-bis(2,4,6-trimethylphenyl)-10-(4-methoxyphenyl) corrole μ-oxo dimer ([(μ-O)NbMes$_2$(*p*-OMePh)corrole]$_2$) (**A-5**). *t*-BuN=TaMes$_2$(*p*-OMePh)corrole (**A-3**) (38 mg, 0.048 mmol) was dissolved in 0.7 mL d_8-toluene in an NMR tube. Saturated KOH in D_2O (10 μL) was added, resulting in an immediate colour change from deep red to blood-red, and the resulting solution was shaken and allowed to stand for 15 minutes. Solvent was removed under vacuum and the resulting solid was extracted using a minimum volume of toluene to obtain a blood red powder (25 mg, 71 % yield). ^{1}H NMR (400 MHz, C_7D_8): δ 8.45-8.05 (m, 8H), 7.97 (d, *J* = 8.2 Hz, 1H, C_6H_3*H*-OMe), 7.28 (br s, 2H), 7.17 (d, *J* = 8.2 Hz, 1H, C_6H_3*H*-OMe), 6.84 (d, *J* = 7.0 Hz, 1H, C_6H_3*H*-OMe), 6.66 (br s, 3H), 3.52 (s, 3H, OCH_3), 2.46 (s, 6H, $C_6H_2Me_2CH_3$), 1.85-1.40 (m, 6H), 1.10 (s, 6H, $C_6H_2Me_2CH_3$). UV-vis (nm): 405, 546. ESI-MS (+) Calcd: 1492.3961 for $C_{88}H_{74}O_4N_8Nb_2$ Observed: 1492.4001. Mp: decomposition above 350 ºC.

***Tert*-butyl imido vanadium(V) 5,15-bis(2,4,6-trimethylphenyl)-10-(4-methoxyphenyl) corrole** (*t*-BuN=VMes$_2$(*p*-OMePh)corrole) (**A-6**). Mes$_2$(*p*-OMePh)corroleLi$_3$·6THF (84 mg, 0.078 mmol) and Cl_3VN=*t*Bu (18 mg, 0.078 mmol) were combined in a vial in the glovebox and 6 mL dimethoxyethane was added. The solution was stirred overnight. The solvent was removed under vacuum and the resulting solid was extracted with pentane, filtered and concentrated. The solution was cooled to -40 ºC to generate a deep red-brown microcrystals (33 mg, 56 % yield). ^{1}H NMR (500 MHz, C_7D_8): δ 8.68 (d, *J* = 4.4 Hz, 2H, β-*H*), 8.66-8.62 (m, 4H, β-*H*), 8.46 (d, *J* = 3.9 Hz, 2H, β-*H*), 8.04 (d, *J* = 7.5 Hz, 1H, C_6H_3*H*-OMe), 7.71 (d, *J* = 7.5 Hz, 1H, C_6H_3*H*-OMe), 7.29 (s, 2H, $C_6H_2Me_3$), 7.21 (s, 2H, $C_6H_2Me_3$), 7.13 (multiplet, 2H, C_6H_3*H*-OMe), 3.53 (s, 3H, OCH_3), 2.51 (s, 6H, $C_6H_2Me_2CH_3$), 2.40 (s, 6H, $C_6H_2Me_2CH_3$), 1.85 (s, 6H,

$C_6H_2Me_2CH_3$), -1.11 (s, 9H, $NC(CH_3)_3$). UV-vis (nm): 414, 554. ESI-MS (+) Calcd: 759.3137 for $C_{48}H_{46}O_1N_5V_1$ Observed: 759.3139. Mp: decomposition above 350 ºC.

Determination of molecular structure by single-crystal X-ray diffraction

X-ray structural determinations were performed on a Bruker APEX II Quazar diffractometer. It is Kappa Geometry with DX and is a 3-circle diffractometer that couples a CCD detector[9] with a sealed-tube source of monochromated Mo Kα radiation. A crystal of appropriate size was coated in Paratone-N oil and mounted on a Kaptan® loop. The loop was transfered to the diffractometer, centered in the beam, and cooled by a nitrogen flow low- temperature apparatus that had been previously calibrated by a thermocouple placed at the same position as the crystal. Preliminary orientation matrices and cell constants were determined by collection of 60 10 s frames, followed by spot integration and least-squares refinement. The reported cell dimensions were calculated from all reflections with $I > 10\ \sigma$. The data were corrected for Lorentz and polarization effects; no correction for crystal decay was applied. An empirical absorption correction based on comparison of redundant and equivalent reflections was applied using SADABS.[10] All software used for diffraction data processing and crystal-structure solution and refinement are contained in the APEX2 program suite (Bruker AXS, Madison, WI).[11] Thermal parameters for all non-hydrogen atoms were refined anisotropically. For all structures, $R_1 = \Sigma(|F_o| - |F_c|)/\Sigma(|F_o|)$; $wR_2 = [\Sigma\{w(F_o^2 - F_c^2)^2\}/\Sigma\{w(F_o^2)^2\}]^{1/2}$. ORTEP diagrams were created using the ORTEP-3 software package and POV-ray.[12]

Table A.1. Shows crystallographic data for corrole complexes **A-3** and **A-5**. Figure A.2. shows the molecular structure of **A-5**.

Table A.1. Crystallographic data for **A-3** and **A-5**.

Compound	**3**	**5**
Formula	$C_{44}H_{37}N_4O_{2.5}Ta$	$C_{44}H_{37}N_4NbO_{2.5}$
Form. wt. (amu)	842.73	754.69
Wavelength (Å)	0.70173	0.71073
Space Group	C2/c	C2/c
a (Å)	19.0850(16)	19.3283(8)
b (Å)	25.717(2)	25.4164(13)
c (Å)	18.508(2)	18.7112(10)
α (º)	90	90
β (º)	111.655(3)	112.710(2)
γ (º)	90	90
V (Å^3)	8442.9(14)	8479.3(7)
Z	8	8
ρ_{calcd} (g/cm^3)	1.326	1.182
F_{000}	3376	3120
μ (mm^{-1})	2.643	0.323
$\theta_{min}/\theta_{max}$	1.39/25.42	1.40/25.44
Refl'ns collected	73015	22516
Indep. refl'ns	7727	7785
R_{int}	0.0461	0.0416
R_1, wR_2	0.0465/0.1533	0.0675/0.1808
R_1, (all data)	0.0570	0.1047
GoF	1.101	1.035
Res. peak/hole (e$^-$/ Å^3)	2.249/-0.800	0.695/-0.566

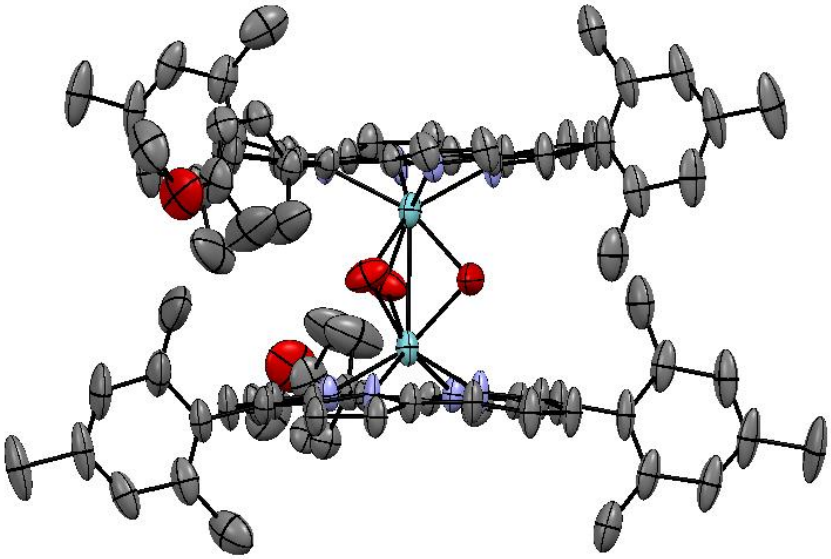

Figure A.2. Molecular structure of niobium corrole oxo dimer **A-5** determined by single-crystal X-ray diffraction. H atoms have been omitted for clarity; thermal ellipsoids at 50 % probability level.

References

(1) Albrett, A. M.; Thomas, K. E.; Maslek, S.; Młodzianowska, A.; Conradie, J.; Beavers, C. M.; Ghosh, A.; Brothers, P. J. *Inorg. Chem.* **2014**, *53*, 5486–5493.
(2) Nigel-Etinger, I.; Goldberg, I.; Gross, Z. *Inorg. Chem.* **2012**, *51*, 1983–1985.
(3) Johnson, J. F.; Scheidt, W. R. *Inorg. Chem.* **1978**, *17*, 1280–1287.
(4) Lecomte, C.; Protas, J.; Guilard, R.; Fliniaux, B.; Fournari, P. *J. Chem. Soc., Dalt. Trans.* **1979**, 1306–1313.
(5) Alaimo, P. J.; Peters, D. W.; Arnold, J.; Bergman, R. G. *J. Chem. Ed.* **2001**, *78*, 64.
(6) Anderson, L. L.; Schmidt, J. A. R.; Arnold, J.; Bergman, R. G. *Organometallics* **2006**, *25*, 3394–3406.
(7) Buckley, H. L.; Chomitz, W. A.; Koszarna, B.; Tasior, M.; Gryko, D. T.; Brothers, P. J.; Arnold, J. *Chem. Commun.* **2012**, *48*, 10766–10768.
(8) Hastings, C. J.; Pluth, M. D.; Bergman, R. G.; Raymond, K. N. *J. Am. Chem. Soc.* **2010**, *132*, 6938–6940.
(9) SMART: Area Detector Software Package, Bruker Analytic X-ray Systems I. Madison, WI, 2003.
(10) SADABS: Bruker-Nonius Area Detector Scaling and Absorption V2.05 Bruker Analytical X-ray System, I. Madison, WI, 2003.
(11) Sheldrick, G. M. *Acta. Crystallogr. A.* **2008**, *64*, 112.
(12) Farrugia, L. J. *Appl. Crystallogr.* **1997**, *30*, 565.

Appendix B: Preparation of Late Transition Metal 1,3-Salphen Complexes

In the interest of exploring changes to the geometry of salen-type ligands around late first-row transition metals, 1,3-salphen complexes of nickel(II) and cobalt(II) were prepared. Reactions with cobalt(II) acetate tetrahydrate and nickel(II) acetate tetrahydrate generated compounds **B-1** and **B-2** (Scheme B.1).

Results and Discussion

The nickel(II) 1,3-salphen complex (**B-1**) was characterized by NMR spectroscopy, IR spectroscopy, mass spectrometry, and X-ray crystallography. The ^{1}H and ^{13}C NMR spectra both show paramagnetically shifted peaks. This is consistent with a tetrahedral rather than square-planar d^8 complex – this is likely due to paramagnetism of the nickel(II) centre, which suggests that the nickel centre is tetrahedral rather than square planar. Consistent with this, the magnetic susceptibility is calculated to be μ = 2.6 BM,[1] consistent with two unpaired electrons per Ni centre. The ^{1}H NMR spectrum shows seven peaks while eight peaks are expected – one may be buried in a broader peak. The ^{13}C NMR spectrum contains nine peaks as expected. The infrared indicates an imine C=N stretch at 2953 cm^{-1} and no evidence of an O-H stretch. ESI-MS(+) of **B-1** shows a major peak at 1193.5889, which suggests a $M_2(ligand)_2$ complex that is protonated in the ESI (exact mass of this dimer is expected to be 1192.5826).

X-ray crystallography of **B-1** confirms that the complex does indeed have a dimeric structure (Figure B.1). The nickel(II) centres are distorted tetrahedra with N/O-Ni-N/O angles ranging from 91.78(8)º to 131.64(9)º. The distance between the two nickel(II) centres in **B-1** is 7.216 Å.

The cobalt(II) 1,3-salphen complex (**B-2**) was characterized by IR spectroscopy, elemental analysis, mass spectrometry and X-ray crystallography. Elemental analysis is consistent with a 1:1 ligand: metal ratio and no additional ligands. ESI-MS (+) is again consistent with a dimeric structure. A dimeric structure is also observed by X-ray crystallography where both the unit cell and the structure are nearly identical to that recorded for **B-1**. The magnetic susceptibility for **B-2** was calculated to be μ = 3.9 BM,[1] consistent with three unpaired electrons per Co centre.

While monomeric species were originally anticipated as the products of these reactions, a previously reported zinc complex of the 1,3-salphen ligand does not include structural characterization or mass spectrometry to confirm that the reported species is monomeric.[2] The much longer M-N and M-O bond distances that would be required to maintain a square planar monomeric structure make it unsurprising that a bridged dimeric structure is preferred for **B-1** and **B-2**. **B-2** is, however, an interesting "textbook example" of the differences between the expected square planar d^8 nickel(II) complex and the observed tetrahedral complex (Figure B.2). While no other interesting chemistry was observed with this molecule, the synthesis of **B-2** is quite straightforward and it could be used in a teaching laboratory setting.

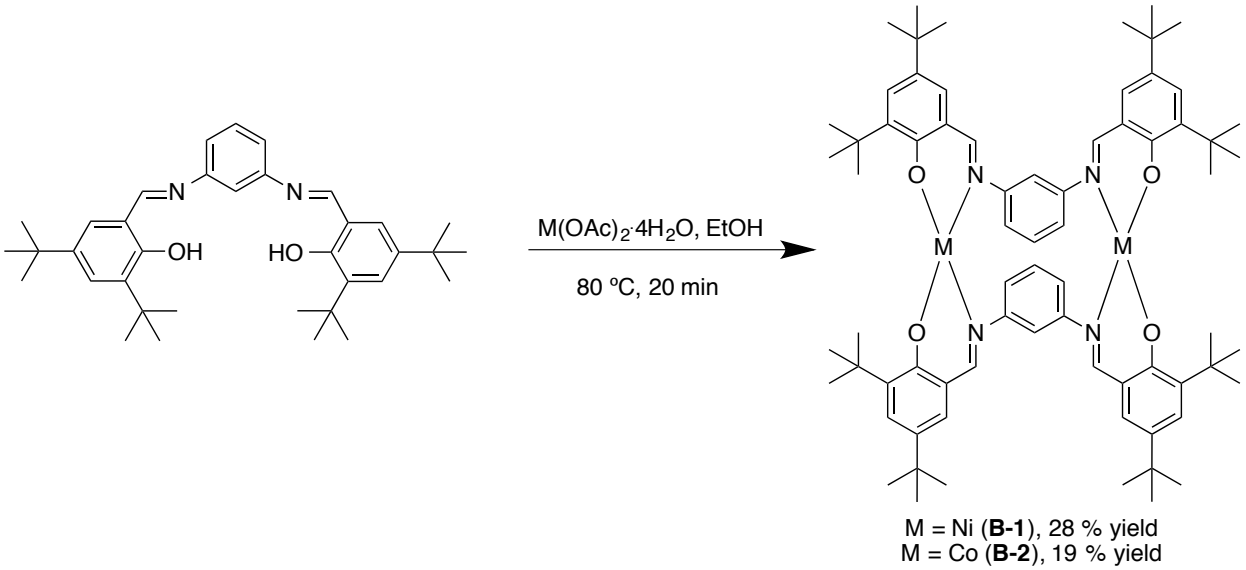

Scheme B.1. Preparation of 1,3-salphen complexes of Ni (**B-1**) and Co (**B-2**).

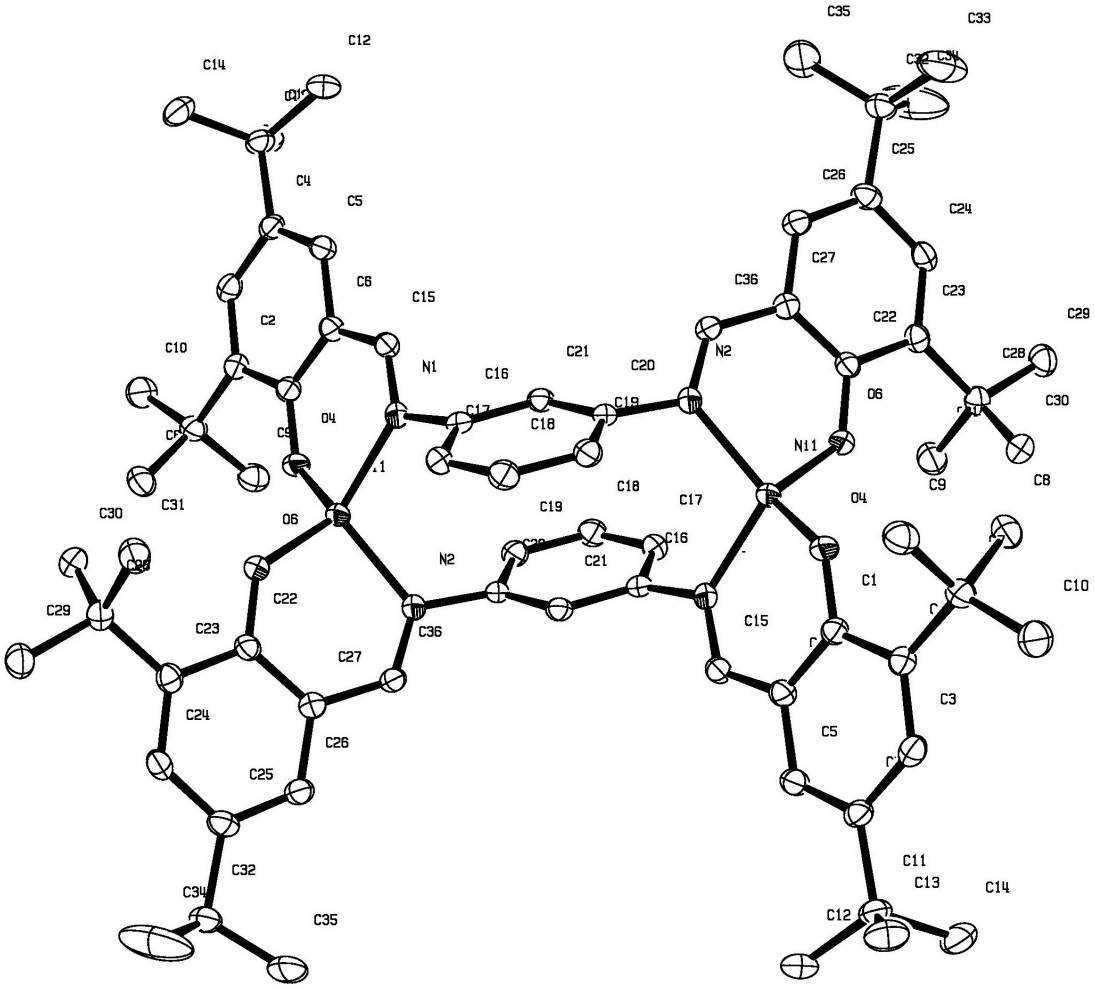

Figure B.1. Thermal Ellipsoid (50%) Plot of Nickel(II) Complex **B-1**. Hydrogen atoms and solvent molecules have been omitted for clarity.

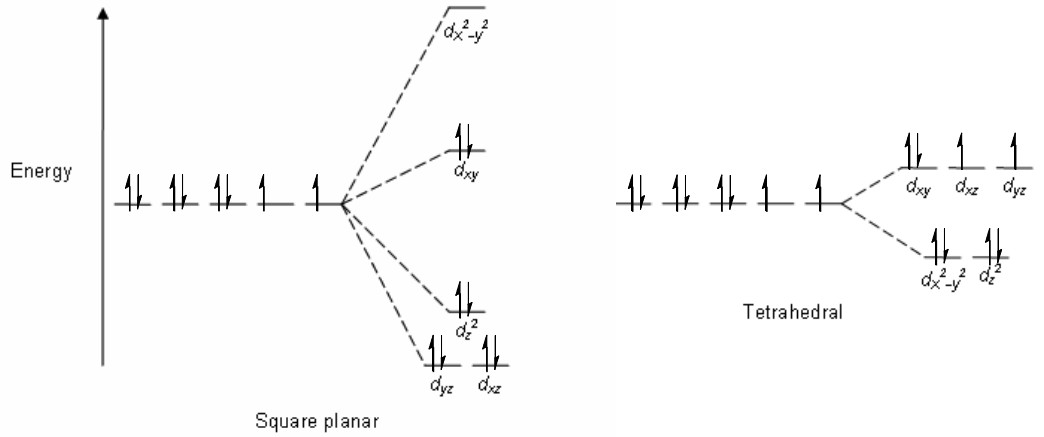

Figure B.2. Square Planar vs. Tetrahedral orbital occupation for a d^8 complex

Experimental Details

Reactions were performed under standard laboratory conditions or under air free conditions on a Schlenk line. All NMR spectra were obtained in $CDCl_3$ at room temperature using a Bruker AVQ-400 spectrometer. ^1H NMR chemical shifts (δ) were calibrated relative to residual solvent peak. Infrared (IR) spectra were recorded with a Thermo Scientific NicoletS10 either as a Nujol mull between KBr plates in the case of air sensitive compounds, or directly on the SmartITR platform. Melting points were determined under laboratory conditions and are uncorrected. Elemental analyses and mass spectral data (ESI-MS) were obtained at the University of California, Berkeley Microanalytical Facility. Magnetic susceptibilities were determined using Evans' method.[1] X-ray crystal diffraction analysis was performed at the University of California, Berkeley CHEXRAY facility using the MicroSTAR-H APEXII diffractometer.

The 1,3-salphen ligand was synthesized according to a literature procedure.[2] Nickel(II) acetate tetrahydrate and cobalt(II) acetate tetrahydrate were obtained from commercial sources and used as received.

Bis-nickel(II) bis-1,3-salphen complex **B-1** was prepared as follows. Nickel(II) acetate tetrahydrate (0.187 g, 0.753 mmol), and 1,3-salphen ligand (0.188 g, 0.753 mmol) were dissolved in ethanol (50 mL). The solution was refluxed at 80 ºC for 20 min. The mixture was cooled to room temperature, and the solvent was then removed by cannula filtration. The solid was washed with hexanes, followed by ether, and the remaining solid was recrystallized from a concentrated solution in methylene chloride layered with ethanol and allowed to stand at room temperature for several days (0.125 g, 28 % yield). ^1H NMR ($CDCl_3$): δ 39.29 (s, 2H), 29.01 (s, 1H), 15.03 (s, 2H), 8.55 (s, 18H), -1.09 (s, 18H), -4.95 (brs, 2H), -30.25 (brs, 1H). See Figure S3. Note broad field means that integrations are estimates. $^{13}C\{^1H\}$ NMR ($CDCl_3$): δ 56.76, 53.66, 43.66, 31.70, 29.92, 29.64, -19.40, -19.87, -66.05. IR (cm^{-1}): 2953.26 (m), 2904.85 (w), 2866.78 (w), 1577.69 (s), 1527.11 (s), 1421.54 (s), 1251.85 (m) 1166.93 (m). See Figure S5. No melting or decomposition observed up to 300 ºC. ESI MS Calc'd for $C_{72}H_{92}Ni_2N_4O_2$ 1192.5826, found 1193.5889.

Bis-cobalt(II) bis-1,3-salphen complex **B-2** was prepared by the same method from cobalt(II) acetate tetrahydrate (0.450 g, 0.753 mmol) using dry, degassed solvents under an atmosphere of dry nitrogen. The red solid was taken up into a saturated solution in methylene chloride that upon slow cooling to -80 ºC gave fine red crystals (0.085 g, 19% yield). IR (cm^{-1}): 2952.05 (m), 2905.53 (w), 2867.80 (w), 1574.88 (s), 1524.34 (s), 1250.76 (m) 1165.26 (m). No melting or decomposition observed up to 300 ºC. EA: Anal. Calc'd for $C_{72}H_{92}Co_2N_4O_2$ C, 72.34; H, 7.76; N, 4.69. Found: C, 72.25; H, 7.67; N, 4.91. ESI MS Calc'd for $C_{72}H_{92}Co_2N_4O_2$ 1194.5783, found 1195.5836.

X-ray Diffraction Data Collection and Refinement

Single crystals of **B-1** and **B-2** were coated in Paratone N-oil, mounted on a Kaptan loop and cooled under a controlled temperature stream of liquid nitrogen boil-off during data collection. X-ray crystal diffraction analysis was performed at the University of California, Berkeley CHEXRAY facility using the MicroSTAR-H APEXII diffractometer with Cu K_α radiation. All

data were integrated by the program SAINT.[3] The data were corrected for Lorentz and polarization effects. Data were analyzed for agreement and possible absorption using XPREP,[4] and an empirical absorption correction was applied in SADABS.[5] Equivalent reflections were merged without an applied decay correction. The structures were solved using SHELXS[6] and refined on all data by full-matrix-least-squares by SHELXL-97.[7] Thermal parameters for all non-hydrogen atoms were refined anisotropically.

References

(1) Piguet, C. *J. Chem. Ed.* **1997**, *74*, 815–816.
(2) Morris, G. A.; Zhou, H.; Stern, C. L.; Nguyen, S. T. *Inorg. Chem.* **2001**, *40*, 3222–3227.
(3) SAINT: SAX Area-Detector Integration Program; V.6.40 ed.; Bruker Analytical X-ray Systems, Inc.: Madison, WI, 2003.
(4) XPREP: Part of SHELXTL Crystal Structure Determination Package; V.6.12 ed.; Bruker Analytical X-ray Systems, Inc.: Madison, WI, 2001.
(5) SADABS: Bruker-Nonius Area Detector Scaling and Absorption V2.05 Bruker Analytical X-ray System, I. Madison, WI, 2003.
(6) SHELXS: Program for the Refinement of X-ray Crystal Structures - Part of the SHELXTL Crystal Structure Determination Package; Bruker Analytical X-ray Systems Inc.: Madison, WI,, 1999.
(7) SHELXL: Program for the Refinement of X-ray Crystal Structures - Part of the SHELXT Crystal Structure Determinatino Package; Bruker Analytical Systems Inc.: Madison, WI, 1999.